Developing Reference Materials for VOC, Formaldehyde and SVOC Emissions Testing

Zhe Liu

Dissertation submitted to the faculty of the Virginia Polytechnic Institute and State University in partial fulfillment of the requirements for the degree of

Doctor of Philosophy
In
Civil Engineering

John C. Little
Linsey C. Marr
Peter J. Vikesland
Eva Marand

April 24, 2012
Blacksburg, VA

Keywords: emissions; reference material; volatile organic compounds; formaldehyde; semi-volatile organic compounds

Developing Reference Materials for VOC, Formaldehyde and SVOC Emissions Testing

Zhe Liu

ABSTRACT

Volatile organic compounds (VOCs) and semi-volatile organic compounds (SVOCs) constitute important classes of indoor contaminants. Emissions of VOCs and SVOCs from myriad building materials and consumer products cause high indoor concentrations with health risks that may be orders-of-magnitude greater than outdoors. The need to control VOC and SVOC emissions from interior materials and thereby reduce indoor concentrations is made more urgent by the prevailing drive for air-tight, energy efficient buildings. To develop low-emission products, emission rates are usually measured in emission chambers. However, there are three significant problems associated with chamber tests: (1) VOC emissions testing procedures of individual laboratories are frequently subject to error and uncertainty; (2) SVOC emissions testing in chambers is extremely difficult and time-consuming, and also subject to error and uncertainty; and (3) chamber tests provide little insight into the mechanisms controlling emissions.

This research aimed to solve these problems by developing reference materials for VOC and SVOC emissions testing. Formaldehyde was studied separately from other VOCs because of its unusual properties. Emission mechanisms, and the related modeling approaches for predicting emissions, were investigated by reviewing the literature and performing chamber studies. Based on the internally controlled VOC and formaldehyde emission mechanisms, diffusion-controlled reference materials, which mimic real sources, were created for VOCs and formaldehyde. Approaches for developing externally controlled reference materials for SVOC emissions testing were also explored. Appropriate mechanistic models can predict the true emission rates of the reference materials and therefore provide reference values to validate emissions testing results and certify procedures of individual laboratories. The potential of a solid phase microextraction (SPME) method was also evaluated and found to be a promising technique that can be used in chamber tests to simplify and improve sampling and analytical procedures.

This research elucidates the mass-transfer mechanisms of VOC and SVOC emissions and provides practical approaches for developing reference materials for emissions testing. The fundamental understanding and methodological advances will enhance indoor air quality science, improve the emissions testing industry, and provide a sound basis on which to develop standards and regulations.

Acknowledgements

I am extremely grateful to Dr. John Little, my advisor and the chair of my committee. His guidance, support, enthusiasm, encouragement and understanding have always been strong driving forces in my research. I am very thankful for my committee members, Dr. Linsey Marr, Dr. Peter Vikesland and Dr. Eva Marand, who have provided valuable comments and advice on my research.

I would like to express sincere appreciation to Dr. Cynthia Howard-Reed at the National Institute of Standards and Technology, Dr. Xiaoyu Liu at the US Environmental Protection Agency, and Dr. Steven Cox in our research group. Without their cooperation and valuable assistance, I could never have reached the heights in this research. I thank Dr. Ying Xu at the University of Texas at Austin for her unflagging encouragement and warm help and serving as a role model for me. I also extend my gratitude to Dr. Jennifer Benning at the South Dakota School of Mines and Technology, Dr. Per Clausen at the Denmark National Research Centre for the Working Environment, and Dr. Yinping Zhang and his research group at Tsinghua University for helpful discussion and constructive suggestions.

I also thank all the staff members and colleagues in the Environmental and Water Resources Engineering program for their help and support in the past few years. Particularly, I want to thank the Air VT group where I have acquired a lot of inspiration and encouragement, and Julie Petruska and Jody Smiley, who have been of considerable help in my laboratory work.

My very special thanks go to all my friends in the US, China and other parts of the world for accompanying me through this journey and being sources of support, comfort and joy.

Finally, I want to dedicate this work to my beloved family, whose unwavering faith and unconditional support has shaped me to be the person I am today. Thank you for everything – I hope I make you proud.

Attributions

Several colleagues contributed to the research presented in this dissertation. A brief description of their background and contributions is included here. Mr. Zhe Liu (doctoral candidate, Department of Civil and Environmental Engineering, Virginia Tech) performed the primary research work and writing for every chapter under the guidance of Dr. John C. Little (Professor, Department of Civil and Environmental Engineering, Virginia Tech; Advisor and Committee Chair) and their specific contributions will not be discussed in detail.

Chapters 3 and 4: Dr. Cynthia Howard-Reed (Research scientist, the National Institute of Standards and Technology (NIST)) helped develop the research intellectually, performed all the emission chamber tests at NIST, contributed to the coordination of the inter-laboratory studies, and reviewed the document. Dr. Steven S. Cox (Visiting assistant professor, Department of Civil and Environmental Engineering, Virginia Tech) helped to develop the research intellectually and to build the experimental infrastructure.

Chapter 6: Dr. Xiaoyu Liu (Research scientist, the US Environmental Protection Agency (EPA)) performed the emission chamber tests at EPA and reviewed the document.

Chapter 7: Dr. Ying Xu (Assistant professor, Department of Civil, Architectural and Environmental Engineering, University of Texas at Austin) contributed to the experimental design and data analysis. Dr. Jennifer L. Benning (Assistant professor, Department of Civil and Environmental Engineering, South Dakota School of Mines and Technology) helped with the experimental design and provided instructions on the experimental techniques.

Table of Contents

List of Figures

List of Tables

Chapter 1 – Executive Summary: Developing Reference Materials for VOC, Formaldehyde and SVOC Emissions Testing

1.1 Research background

In modern societies, people typically spend most of their time indoors. Although this alone may not necessarily lead to greater exposure to pollutants, many contaminants have higher concentrations in indoor air than outdoor air. Therefore, indoor air quality (IAQ) has been recognized as a compelling environmental problem in the last few decades. Degradation of IAQ may cause adverse comfort and health effects and reduce worker productivity in different ways, including toxic effects, irritant effects, infectious diseases, allergic disorders, and psychological effects (Chang and Gershwin, 2004; Jones, 1999). The reduction of worker productivity and the medical costs caused by IAQ problems give rise to substantial economic loss (Fisk and Rosenfeld, 1997; Haymore and Odom, 1993). It has been estimated that the overall health and productivity gains that could be achieved by improving the indoor environment are worth as much as $200 billion per year in the US alone (Fisk, 2000). For a commercial office building, the economic value of a 5% improvement in productivity over a single year may exceed the entire cost of the building (Fanger, 2000). The IAQ problem will only get worse as efforts to conserve energy lead to increasingly air-tight, energy-efficient buildings (NSTC, 2008).

Among all the causes of IAQ degradation, including biological pollutants (for example, mold, bacteria, and viruses), chemical pollutants (for example, carbon monoxide, sulfur oxides, nitrogen oxides, radon, asbestos, volatile organic compounds, and particulate matter), and other mass or energy stressors, volatile organic compounds (VOCs) have been recognized as one of the most important classes of indoor air pollutants (Weschler, 2009). VOCs are a large group of organic chemicals that have low boiling points and high vapor pressures allowing them to vaporize into air. Although outdoor VOC is defined by the US Environmental Protection Agency (EPA) based on photochemical reactivity as “any compound of carbon, excluding carbon monoxide, carbon dioxide, carbonic acid, metallic carbides or carbonates, and ammonium carbonate, which participates in atmospheric photochemical reactions”, when discussing indoor environments, VOCs are generally defined based on their volatility. For example, the European Commission Directive 1999/13/EC defines VOC as any organic compound having a vapor

pressure of 10 Pa or more at 20 ºC. Common VOCs occurring in the indoor environment include formaldehyde, benzene, toluene, xylene, styrene, acetaldehyde, naphthalene, limonene, and hexanal, with major sources including adhesives, caulks, sealants, paints, solvents, wood stain, floor wax, carpets, textiles, wallboard, treated wood, urethane coatings, pressed-wood products, and floorings. Indoor VOC concentrations generally far exceed outdoor levels. Exposure to VOCs may cause reduced worker productivity (Fanger, 2006), acute health effects (for example, eye and respiratory irritations, headaches, fatigue, and asthmatic symptoms) (Wolkoff and Nielsen, 2001), and even cancers (Boeglin et al., 2006; Rennix et al., 2005; Sax et al., 2006). The health effect of individual VOCs may vary greatly. For example, benzene is a "known human carcinogen" (NTP, 2011) while toluene is much less toxic although it shares a similar molecular structure. However, the clinical effects are generally complicated by the coexistence of a wide range of VOCs in indoor air.

Formaldehyde is one of the most common VOCs and a notorious indoor pollutant. Sharing common features of VOCs, it also possesses distinct physicochemical properties, such as an especially low boiling point (it is a gas at room temperature) and high polarity and reactivity. Therefore, it is quite often thought of as being distinct from VOCs and tends to be listed in parallel with VOCs by the indoor air scientific community. This may also be due to the priority associated with its significant industrial use, widespread occurrence in indoor air and highly-toxic nature. Global industrial production of formaldehyde is currently more than 20 million tonnes per annum (Bizzari, 2000), mainly being used for producing synthetic resins, other industrial chemicals, and preservation and disinfection agents. Due to high emission rates from many indoor sources and relatively slow indoor removal rates, formaldehyde concentration in indoor air is usually much higher than outdoors, ranging from 10 to 4000 $\mu g/m^3$ (IARC, 2006). Although people may be exposed to formaldehyde through other sources, such as food, indoor air is the most substantial source for the general population. Exposure to formaldehyde can cause eye and upper respiratory system irritation and it has also been concluded that chronic formaldehyde exposure can cause nasopharyngeal cancer (IARC, 2006).

Less volatile than VOCs, semi-volatile organic compounds (SVOCs) generally have vapor pressures in the range of 10^{-9} to 10 Pa. In recent years, SVOCs such as phthalate plasticizers,

brominated flame retardants, and organophosphate pesticides have been recognized as important indoor pollutants due to their increased occurrence in the indoor environment and the discovery of their potential endocrine disrupting effects (Rudel and Perovich, 2009; Weschler, 2009; Weschler and Nazaroff, 2008). Sources of SVOCs include a vast array of building materials and consumer products, including polyvinyl chloride (PVC) products, lotions, nail polish, cling film, shampoo, computers, televisions, foams, and shower curtains, because SVOCs are extensively used as additives or solvents in these materials. Due to their low volatility, SVOCs tend to emit slowly from these sources and then sorb strongly to interior surfaces, including airborne particles and dust. In contrast to VOCs, which are primarily present in the gas phase after being emitted, the high concentrations of SVOCs in the sorbed phase lead to significant human exposure through inhalation of particles, ingestion of dust, and absorption through skin in addition to breathing of air (Xu et al., 2009). Adverse health effects are associated with many SVOCs. For example, polybrominated diphenyl ethers (PBDEs, which are common flame retardants) may interfere with thyroid hormone function and adversely impact neurodevelopment (Darras, 2008; McDonald, 2005). Exposure to phthalate esters (used as plasticizers in PVC products and solvents in personal care products) may result in profound and irreversible changes in the development of the reproductive tract, especially in males (Heudorf et al., 2007; Latini et al., 2004; Matsumoto et al., 2008). The health risks associated with SVOCs are of special concern because SVOCs may be emitted over decades. Even after the original source is removed, the indoor environment will retain significant amount of SVOCs in the sorbed phase for periods of years (Weschler and Nazaroff, 2008).

To understand the source-to-dose continuum for risk assessment and management and to develop low-emission products, emission rates of VOCs and SVOCs from various materials and products need to be characterized. This is primarily achieved by emission chamber tests, measuring the gas-phase chamber concentrations (and thus inferring the emission rates) of the volatile pollutants released from the test materials. Based on the emission chamber test results, mechanisms controlling emissions can be evaluated and mathematical models predicting emissions can be developed, which in turn facilitates emission characterizations. However, accurately measuring VOC and SVOC emissions in chamber tests is still rather challenging. Although subject to extensive practice and standardization for years (ASTM, 2001; ASTM,

2010a; ASTM, 2010b; ASTM, 2011; BSI, 2004; ISO 2006; ISO, 2007; ISO, 2011), the measurements of VOC and formaldehyde emissions by laboratories still have many unidentified errors and variations which decrease the credibility of test results (Huxham and Thomas, 2000). For example, VOC emission rates from the same material measured by different laboratories have coefficients of variation on the order of 50% and as large as 300% (De Bortoli et al., 1999; Howard-Reed and Nabinger, 2006). In the case of formaldehyde, the measurement is further complicated because the major analytical methods for VOCs (gas chromatography (GC) with flame ionization detector (FID) or mass spectrometry detector (MS)) cannot be used and derivatization pretreatments are needed (Salthammer et al., 2010). In addition, there are various standards which specify different methods for formaldehyde emissions testing, causing additional variability (Risholm-Sundman et al., 2007). Even more difficult to measure than VOCs due to the greater analytical challenges, ubiquitous laboratory contamination, and long testing time required, emissions of SVOCs have not been widely tested in chambers. Only a few papers have examined SVOC emissions in chambers with most of the data sets subject to substantial uncertainties. As emphasized by the National Science and Technology Council (NSTC, 2008), "reliable test methods to measure emission rates" are needed and methods to validate the emission chamber test procedures and test results of individual laboratories are urgently required.

1.2 Research significance

The most straightforward and comprehensive way to calibrate an apparatus and assess a measurement method is by testing a standard reference. A reference material is defined as a "material, sufficiently homogenous and stable with respect to one or more specified properties, which has been established to be fit for its intended use in a measurement process" (ISO, 2008). In the case of emissions testing, the reference material should have consistent emission rates under specified emissions testing configurations and the reference value of the emission rate (the best estimate of the true emission rate and associated uncertainties) should be known. Therefore, individual laboratories can test such reference materials and compare their measured emission rates to the reference values. Although evaluating chamber performance of VOC emissions testing has been carried out using simple standard sources such as permeation tubes, the validity and usefulness of these simple procedures are far from satisfactory and emissions testing

laboratories still have to resort to costly and sometimes misleading inter-laboratory studies (ILS) for performance checking. In this research, we developed reference materials for VOC, formaldehyde and SVOC emissions testing. The uniqueness and innovation of this research is that the reference material development was based upon a thorough and consistent understanding of the fundamental emission mechanisms. By understanding the controlling mechanisms for emissions of VOCs, formaldehyde and SVOCs respectively, we were able to create reference materials which mimic real test materials. Such reference materials can be tested by emissions testing laboratories in chambers following the exact same procedure they regularly use for real materials. The laboratories can therefore check every aspect of the test procedure which can impact results, including specimen preparation, chamber operation, sampling strategy, and analytical techniques. Also by understanding the emission mechanisms, we were able to predict their true emissions (both chamber concentration development profiles and emission rates) under various emissions testing configurations using proper mechanistic emission models, which serve as the reference values.

1.3 Research scope and objectives

This doctoral research aimed to develop reference materials for VOC, formaldehyde and SVOC emissions testing guided by a clear understanding of the emission mechanisms. We focused on emissions from dry and solid materials because most test materials fall within this domain and the approaches are also applicable for wet materials such as paints and adhesives. As the basis for developing reference materials which can mimic real test materials, we investigated the mechanisms of VOC and SVOC emissions from various sources and reviewed/developed mechanistic models for predicting emissions. Then we applied the approach to develop VOC reference materials in collaboration with the National Institute of Standards and Technology (NIST) and formaldehyde reference materials in collaboration with EPA. Recognizing the vulnerability of the conventional sampling and analytical procedures to environmental and human-induced errors and the associated variability in emission chamber tests, we also studied the potential of a solid phase microextraction (SPME) method as an alternative for eliminating complicated sampling and analytical procedures. Due to the current lack of understanding of SVOC emissions and a well-developed emissions testing method, we performed SVOC emission

tests in a specially-designed chamber which elucidated the emission mechanisms and allowed us to explore the feasibility of developing SVOC reference materials.

Specific objectives of this research were to:

(1) Review the current state-of-knowledge of VOC and SVOC emissions from various materials and the modeling approaches for predicting emissions (Chapter 2);
(2) Develop a prototype reference material for VOC emissions testing and evaluate the validity and usefulness in extensive chamber tests and inter-laboratory studies (Chapter 3);
(3) Examine the impact of temperature and humidity on the performance of the VOC reference material (Chapter 4);
(4) Evaluate the potential of the SPME method as an alternative for measuring VOC concentrations in indoor air (Chapter 5);
(5) Develop and validate a prototype reference material for formaldehyde emissions testing (Chapter 6);
(6) Characterize phthalate emissions in a specially-designed chamber, develop a SVOC emission model, and explore the feasibility of developing SVOC reference materials (Chapter 7).

1.4 Conclusions

The results from this research provide important scientific, methodological and practical contributions to IAQ science, benefit the emissions testing field, facilitate low-emission product development and emission labeling programs, and support regulatory measures. The review of the current understanding about VOC and SVOC emission mechanisms and available emission models revealed that VOC and SVOC emissions can be modeled within a consistent mass-transfer framework, with VOC emissions from dry solid materials largely controlled by internal diffusion and SVOC emissions controlled externally (Chapter 2). We therefore created a diffusion-controlled reference material for VOC emissions testing by loading a representative VOC into a thin polymer film, whose subsequent emission rate can be accurately predicted by a mechanistic model. The capability of the reference material in assessing VOC emissions testing performance has been clearly demonstrated in a series of inter-laboratory studies (Chapter 3). We

also showed that emission from the VOC reference material depends substantially on temperature, but that humidity makes no significant difference. Overall, the reference material performs well at different temperature and relative humidity levels, allowing its use over a range of environmental conditions (Chapter 4). Concerning the errors and variability associated with the sorbent trapping sampling method which is commonly used in VOC emission chamber tests, we evaluated the sorption equilibrium and kinetics of the emerging SPME sampling method. It was found to be a promising alternative for VOC sampling, being simple, accurate, sensitive and cost and time efficient (Chapter 5). Given the success of the VOC reference material, we then applied the same approach to create a formaldehyde reference material. Although formaldehyde was found to have more complicated mass-transfer mechanisms than VOCs, our preliminary results suggest that it is indeed possible to create a reference material for formaldehyde emissions testing (Chapter 6). Finally, by carefully testing phthalate emissions in a specially-designed chamber, we elucidated the mechanisms controlling SVOC emissions and developed a SVOC emission model, concluding that a very simple externally controlled reference material can be used to evaluate SVOC emissions testing performance.

Overall, with the mass-transfer principles and the approaches for developing reference materials presented in this research, it is possible to produce validated reference materials for VOC, formaldehyde and SVOC emissions testing in an effective and economical manner. Large scale production (either centralized or distributed) of such reference materials can be adopted by regulatory agencies to certify emissions testing laboratories. The reference materials can also be independently used by individual laboratories to calibrate their chamber test apparatus and procedures. Reference materials hold great potential to eliminate the need for costly inter-laboratory studies, instill confidence and consensus in emissions testing, and level the playing field for emissions testing laboratories and product manufacturers.

1.5 References

ASTM (2001) *ASTM D6670-01, Standard Practice for Full-scale Chamber Determination of Volatile Organic Emissions from Indoor Materials/Products*, ASTM International, West Conshohocken, PA.

ASTM (2010a) *ASTM D5116-10, Standard Guide for Small-scale Environmental Chamber Determinations of Organic Emissions from Indoor Materials/Products*, ASTM International, West Conshohocken, PA.

ASTM (2010b) *ASTM E1333-10, Standard Test Method for Determining Formaldehyde Concentrations in Air and Emission Rates from Wood Products Using a Large Chamber*, ASTM International, West Conshohocken, PA.

ASTM (2011) *ASTM D7143-11, Standard Practice for Emission Cells for the Determination of Volatile Organic Emissions from Indoor Materials/Products*, ASTM International, West Conshohocken, PA.

Bizzari, S.N. (2000) *CEH Marketing Research Report: Formaldehyde*, SRI International, Palo Alto, CA.

Boeglin, M.L., Wessels, D. and Henshel, D. (2006) An investigation of the relationship between air emissions of volatile organic compounds and the incidence of cancer in Indiana counties, *Environmental Research*, **100**, 242-254.

BSI (2004) *BS EN 717-1, Wood-based Panels - Determination of Formaldehyde Release- Part 1: Formaldehyde Emission by the Chamber Method*, British Standards Institution, London, United Kingdom.

Chang, C. and Gershwin, M.E. (2004) Indoor air quality and human health: Truth vs mass hysteria, *Clinical Reviews in Allergy and Immunology*, **27**, 219-239.

Darras, V.M. (2008) Endocrine disrupting polyhalogenated organic pollutants interfere with thyroid hormone signaling in the developing brain, *Cerebellum*, **7**, 26-37.

De Bortoli, M., Kephalopoulos, S., Kirchner, S., Schauenburg, H. and Vissers, H. (1999) State-of-the-art in the measurement of volatile organic compounds emitted from building products: results of European interlaboratory comparison, *Indoor Air*, **9**, 103-116.

Fanger, P.O. (2000) Indoor air quality in the 21st century: search for excellence, *Indoor Air*, **10**, 68-73.

Fanger, P.O. (2006) What is IAQ? *Indoor Air*, **16**, 328-334.

Fisk, W.J. (2000) Health and productivity gains from better indoor environments and their relationship with building energy efficiency, *Annual Reviews Energy and Environment*, **25**, 537-566.

Fisk, W.J. and Rosenfeld, A.H. (1997) Estimates of improved productivity and health from better indoor environments, *Indoor Air*, **7**, 158-172.

Haymore, C. and Odom, R. (1993) Economic effects of poor IAQ, *EPA Journal*, **19**, 28-29.

Heudorf, U., Mersch-Sundermann, V. and Angerer, J. (2007) Phthalates: toxicology and exposure, *International Journal of Hygiene and Environmental Health*, **210**, 623-634.

Howard-Reed, C. and Nabinger, S.J. (2006) 'Developing a standard reference material for VOC emissions testing' In: *Proceedings of the Indoor Environmental Quality: Problems, Research and Solutions Conference*, Research Triangle Park, NC, EPA/AWMA conference.

Huxham, M. and Thomas, C.L.P. (2000) Sampling procedures for intrinsically valid volatile organic compound measurements, *Analyst*, **125**, 825-832.

IARC (2006) *IARC monographs on the evaluation of carcinogenic risks to humans. Vol 88. Formaldehyde, 2-Butoxyethanol and 1-tert-Butoxypropan-2-ol*, International Agency for Research on Cancer, Lyon, France.

ISO (2006) *ISO 16000-9, Indoor air - Part 9: Determination of The Emission of Volatile Organic Compounds from Building Products and Furnishing – Emission Test Chamber Method*, International Organization for Standardization, Geneva, Switzerland.

ISO (2007) *ISO 12460-1, Wood-based Panels – Determination of Formaldehyde Release – Part 1: Formaldehyde Emission by the 1-cubic-metre Chamber Method*, International Organization for Standardization, Geneva, Switzerland.

ISO (2008) *ISO Guide 30: 1992/Amd 1:2008, Revision of Definitions for Reference Material and Certified Reference Material*, International Organization for Standardization, Geneva, Switzerland.

ISO (2011) *ISO 16000-6, Indoor air - Part 6: Determination of Volatile Organic Compounds in Indoor and Test Chamber Air by Active Sampling on Tenax TA Sorbent, Thermal Desorption and Gas Chromatography Using MS or MS/FID*, International Organization for Standardization, Geneva, Switzerland.

Jones, A.P. (1999) Indoor air quality and health, *Atmospheric Environment*, **33**, 4535-4565.

Latini, G., De Felice, C. and Verrotti, A. (2004) Plasticizers, infant nutrition and reproductive health, *Reproductive Toxicology*, **19**, 27-33.

Matsumoto, M., Hirata-Koizumi, M. and Ema, M. (2008) Potential adverse effects of phthalic acid esters on human health: a review of recent studies on reproduction, *Regulatory Toxicology and Pharmacology*, **50**, 37-49.

McDonald, T.A. (2005) Polybrominated diphenylether levels among United States resident: daily intake and risk of harm to the developing brain and reproductive organs, *Integrated Environmental Assessment and Management*, **1**, 343-354.

NSTC (2008) *Federal Research and Development Agenda for Net-Zero Energy, High-Performance Green Buildings, Report of the Subcommittee on Buildings Technology Research and Development*, National Science and Technology Council, Committee on Technology.

NTP (2011) *Report on Carcinogens, Twelfth Edition*, U.S. Department of Health and Human Services, National Toxicology Program.

Rennix, C.P., Quinn, M.M., Amoroso, P.J., Eisen, E.A. and Wegman, D.H. (2005) Risk of breast cancer among enlisted army women occupationally exposed to volatile organic compounds, *American Journal of Industrial Medicine*, **48**, 157-167.

Risholm-Sundman, M., Larsen, A., Vestin, E. and Weibull, A. (2007) Formaldehyde emission-comparison of different standard methods, *Atmospheric Environment*, **41**, 3193-3202.

Salthammer, T., Mentese, S. and Marutzky, R. (2010) Formaldehyde in the indoor environment, *Chemical Reviews*, **110**, 2536-2572.

Sax, S.N., Bennett, D.H., Chillrud, S.N., Ross, J., Kinney, P.L. and Spengler, J.D. (2006) A cancer risk assessment of inner-city teenagers living in New York City and Los Angeles, *Environmental Health Perspectives*, **114**, 1558-1566.

Weschler, C.J. (2009) Changes in indoor pollutants since the 1950s, *Atmospheric Environment*, **43**, 153-169.

Weschler, C.J. and Nazaroff, W.W. (2008) Semivolatile organic compounds in indoor environments, *Atmospheric Environment*, **42**, 9018-9040.

Wolkoff, P. and Nielsen, G.D. (2001) Organic compounds in indoor air-their relevance for perceived indoor air quality? *Atmospheric Environment*, **35**, 4407-4417.

Xu, Y., Cohen Hubal, E.A, Clausen, P.A. and Little, J.C. (2009) Predicting residential exposure to phthalate plasticizer emitted from vinyl flooring: A mechanistic analysis, *Environmental Science and Technology*, **43**, 2374-2380.

Chapter 2 – Predicting Emissions of Volatile and Semi-volatile Organic Compounds from Building Materials and Consumer Products: A Review

Zhe Liu and John C. Little

Department of Civil and Environmental Engineering, Virginia Tech, Blacksburg, VA 24061

2.1 Abstract

Volatile organic compounds (VOCs) and semi-volatile organic compounds (SVOCs) constitute important classes of indoor air contaminants and characterizing their emissions from building materials and consumer products is of great interest for risk assessment and the development of environmentally benign products. Compared with emission chamber studies, emission models provide a more cost efficient and powerful way to examine the emission behaviors of VOCs and SVOCs. The objective of this paper is to review existing mechanistic models for predicting VOC and SVOC emissions from various sources, investigate their differences and similarities, and discuss the mass-transfer mechanisms on which the models are based. Because the usefulness of the emission models largely depends on the availability and reliability of model parameters, techniques for determining key model parameters are also reviewed. The models covered in this review fall into three categories: models for VOC emissions from "dry" materials (dry/VOC); models for VOC emissions from "wet" materials (wet/VOC); and models for SVOC emissions from "dry" materials (dry/SVOC). It is shown that VOC and SVOC emissions can be modeled within a very consistent mass-transfer framework with the three model categories being intimately related. While substantial advances have been made in developing the predictive models and understanding the emission mechanisms, large knowledge gaps still exist and further research is needed. The mechanisms controlling VOC and SVOC emissions reviewed in this paper constitute the theoretical basis for developing reference materials which can mimic real sources with the models providing reference values of emission rates.

2.2 Introduction

Modern living exposes people to a vast array of building materials and consumer products, many of which release volatile organic compounds (VOCs) and semi-volatile organic compounds

(SVOCs) and contribute substantially to the degradation of indoor air quality (Weschler, 2009; Weschler and Nazaroff, 2008). Examples of VOCs include formaldehyde, benzene, hexanal, and phenol, with major indoor sources including adhesives, caulks, sealants, paints, solvents, wood stain, floor wax, carpets, textiles, wallboard, treated wood, urethane coatings, pressed-wood products, and vinyl flooring (Bluyssen et al., 1996; Missia et al., 2010). Short-term exposure to VOCs may reduce worker productivity (Bako-Biro et al., 2004; Fanger, 2006) and cause acute health effects such as eye and respiratory irritations, headaches, fatigue, and asthmatic symptoms (Billionnet et al., 2011; Jie et al., 2011; Mølhave, 1989; Wolkoff and Nielsen, 2001). Long-term exposure may even cause cancers (Boeglin et al., 2006; Rennix et al., 2005; Sax et al., 2006) with benzene and formaldehyde documented as "known human carcinogens" (NTP, 2011). SVOCs, such as plasticizers, flame retardants, and biocides, are added to many materials and products to enhance performance. For example, phthalate plasticizers are found in vinyl flooring, wallpaper, electrical insulation, food packaging, and toys; flame retardants are found in computers, electronics, cables, televisions, textiles, foam furniture, and insulating foams; and biocides are found in shower curtains. In the past few decades, there has been growing awareness about the health risks associated with many SVOCs especially their endocrine disrupting effects. Exposure to SVOCs during development (*in utero*, infants and children) is of special concern because developing tissues are exquisitely sensitive to endocrine signals and disruption of these signaling pathways can result in permanent alterations in tissue structure and function (Rudel and Perovich, 2009). For example, recent reviews (Heudorf et al., 2007; Jaakkola and Knight, 2008; Latini et al., 2004; Matsumoto et al., 2008; McKee et al., 2004; Ritter and Arbuckle, 2007) collectively show that exposure to phthalate esters may result in profound and irreversible changes in the development of the reproductive tract, especially in males. Effects such as increases in prenatal mortality, reduced growth and birth weight, and skeletal, visceral, and external malformations are also associated with exposure to phthalates. In addition, epidemiologic studies in children suggest associations between phthalate exposure in the home and the risk of asthma and allergies.

To characterize VOC and SVOC emissions from building materials and consumer products for risk assessment and for the development of low-emission products, emission chamber tests are often conducted. Although valuable results for the specific test conditions can be obtained via

direct measurements, they are generally not applicable to other conditions. In addition, experiments are often expensive, time-consuming and difficult, especially for SVOCs. For example, chamber tests for phthalates may take several months (Clausen et al., 2007; Clausen et al., 2010). Therefore, substantial effort has been devoted to understanding the behavior of various emission sources and to developing models for predicting VOC and SVOC emissions. Generally, predictive models can be categorized into two groups (Zhang and Xu, 2003). The first group consists of empirical models which are constructed upon statistical analysis of emission chamber test data (Guo, 2002a). Although simple to derive and use, empirical models lack a physical basis, provide little insight into the controlling mechanisms, and therefore cannot be easily scaled from the test conditions to other conditions. In contrast, the second group of models is based on valid mass-transfer mechanisms with model parameters having clear physical meaning, and therefore can predict emissions for various conditions if the requisite model parameters are known.

An important issue for the validation and application of mass-transfer models is the estimation of model parameters. Model parameters can be obtained by fitting the models to emission chamber test data, which is quite common during the early stages of model development. However, it is more rigorous to obtain the model parameters by experimental approaches that are completely independent of the emission data used to validate the models. The availability of independently measureable model parameters is essential for predictive models and the usefulness of a model is largely determined by whether the parameters can be readily obtained (Guo, 2002b).

Several reviews of existing VOC emission models and the methods to estimate required model parameters have been published (Blondeau et al., 2008; Guo, 2002a; Guo, 2002b; Haghighat et al., 2002; Haghighat et al., 2005). The present review focuses on the physically-based mass-transfer models for predicting VOC and SVOCs emissions, and discusses the difference and inner links among them to illustrate the evolution of the emissions modeling field and the understanding of the mass-transfer mechanisms. The methods available to estimate key model parameters are also described. In the present review, models are classified into three categories: models for VOC emissions from “dry” materials (dry/VOC); models for VOC emissions from “wet” materials (wet/VOC); and models for SVOC emissions from “dry” materials (dry/SVOC).

Providing mass-transfer models are adequately validated, they can provide a more cost efficient and powerful way to characterize emissions from a wide range of building materials and consumer products. The mechanisms governing VOC and SVOC emissions discussed in this review provide theoretical guidance for developing VOC and SVOC reference materials that mimic real sources and the predictive models can be used to obtain reference values for their true emission rates.

2.3 Review of mass-transfer emission models

2.3.1 Dry/VOC models

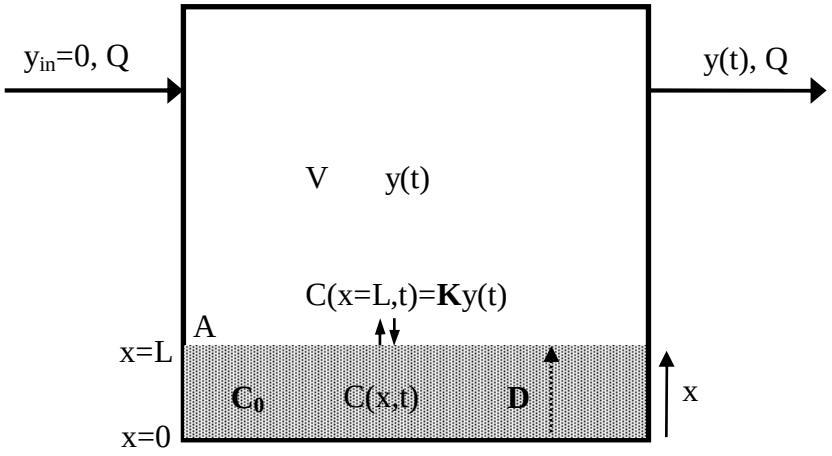

Figure 2.1 Schematic representation of VOC emission from a homogeneous solid material with external convective mass-transfer resistance ignored.

Most early mass-transfer models (Chang and Guo, 1992; Clausen et al., 1991; Dunn and Tichenor, 1988; Silberstein et al., 1988; Tichenor et al., 1991) examined surface effects and ignored internal diffusion, which limits their application since VOCs emitted from building materials and consumer products generally originate inside the materials and internal diffusion plays a significant role in the emission process. An early diffusion model developed in the mid-1990s (Little et al., 1994) forms the basis of a widely accepted framework for later development of VOC and SVOC emissions modeling.

Figure 2.1 shows the schematic representation of VOC emission from a slab of a homogeneous solid material (Little, et al., 1994). With reference to Figure 2.1, the transient diffusion equation within the material is given by Fick's second law, or

$$\frac{\partial C(x,t)}{\partial t} = D\frac{\partial^2 C(x,t)}{\partial x^2} \tag{2.1}$$

where C(x,t) is the concentration of a VOC in the material, D is the material-phase diffusion coefficient, t is time and x is the distance from the bottom of the slab. The boundary condition at the bottom of the material assumes zero mass flux, or

$$\left.\frac{\partial C(x,t)}{\partial x}\right|_{x=0} = 0 \tag{2.2}$$

while the boundary condition at the exposed surface is imposed by a mass balance on the VOC in the chamber air assuming that the chamber is well-mixed and that the influent concentration is zero, or

$$V\frac{dy(t)}{dt} = -D\cdot A\left.\frac{\partial C(x,t)}{\partial x}\right|_{x=L} - Q\cdot y(t) \tag{2.3}$$

where y(t) is the VOC concentration in the well-mixed chamber air, Q is the air flow rate through the chamber, V is the chamber volume, A is the exposed surface area, and L is the thickness of the material. A linear and instantaneously reversible equilibrium relationship is assumed to exist between the material surface and the chamber air, or

$$K = \frac{C(x,t)|_{x=L}}{y(t)} \tag{2.4}$$

where K is the partition coefficient between the material and air for the VOC. Equation (2.4) implies that the external convective mass-transfer resistance is ignored so that there is no concentration difference between the bulk chamber air and the air adjacent to the material surface (air in the boundary layer). Assuming D and K are independent of concentration and that the initial material-phase concentration (C_0) is uniform, the solution to governing Equation (2.1) together with auxiliary Equations (2.2)-(2.4) is given by (Little et al., 1994)

$$C(x,t) = 2C_0\sum_{n=1}^{\infty}\left\{\frac{\exp\left(-Dq_n^2 t\right)\left(h-kq_n^2\right)\cos(q_n x)}{\left[L\left(h-kq_n^2\right)^2 + q_n^2(L+k)+h\right]\cos(q_n L)}\right\} \tag{2.5}$$

where

$$h = \frac{Q/A}{D \cdot K} \tag{2.6}$$

$$k = \frac{V/A}{K} \tag{2.7}$$

and the q_ns are the positive roots of

$$q_n \tan(q_n L) = h - kq_n^2 \tag{2.8}$$

Equation (2.5) gives the full analytical solution by which the VOC concentration in the material can be obtained given the distance from the bottom of the material and time. Knowing the material-phase concentration at the surface of the material (x=L), Equation (2.4) can be used to calculate the concentration in the chamber air at any time. In obtaining the analytical solution, D and K are assumed independent of material-phase concentration within low concentration range, which is validated by subsequent studies (Cox et al., 2001a). If D and K do depend on concentration, Equations (2.1)-(2.4) are still valid although a simple analytical solution may not be achievable.

Within this mass-transfer framework, research to develop a comprehensive mass-transfer model without neglecting the external mass-transfer resistance continued. One example is a numerical model employing 3-D convection-diffusion equations to calculate the external mass transfer in the chamber air while the internal diffusion and partition at the material/air interface were calculated using the 1-D approach as in Equations (2.1) and (2.4) (Yang et al., 2001a). In addition, the model considered the case of composite materials with two or more layers of homogeneous materials. Although this comprehensive model can provide detailed knowledge of air flow and VOC concentration profiles in the chamber, the numerical computation of the 3-D convection-diffusion equations, which is essentially computational fluid dynamics (CFD) approach, is quite complicated.

Fortunately, external convective mass transfer was soon incorporated into emission models in a simple mathematical form. Figure 2.2 shows the emission mechanisms adopted in several models (Deng and Kim, 2004; Huang and Haghighat, 2002; Xu and Zhang, 2003). The difference between Figure 2.2 and Figure 2.1 is the introduction of external convective mass transfer via a

convective mass-transfer coefficient, h_m. With the diffusion-governing Equation (2.1) and boundary condition at the bottom, Equation (2.2), still valid, the boundary condition at the exposed surface, Equations (2.3) and (2.4) are replaced by

$$-D\cdot\left.\frac{\partial C(x,t)}{\partial x}\right|_{x=L}=h_m\left(y_0(t)-y(t)\right) \tag{2.9}$$

$$V\frac{dy(t)}{dt}=A\cdot h_m\left(y_0(t)-y(t)\right)-Q\cdot y(t) \tag{2.10}$$

$$K=\frac{C(x,t)\big|_{x=L}}{y_0(t)} \tag{2.11}$$

Equation (2.9) shows how external convective mass transfer is taken into account. The diffusion flux at the material surface is equal to the convective mass transfer through the boundary layer, where $y_0(t)$ is the VOC concentration in the air adjacent to the material surface and y(t) is the bulk air concentration. Equation (2.10) is the transient mass balance in the chamber air, assuming the influent concentration is zero. Similar to Equation (2.4), Equation (2.11) assumes an instantaneous reversible partition equilibrium at the material/air interface.

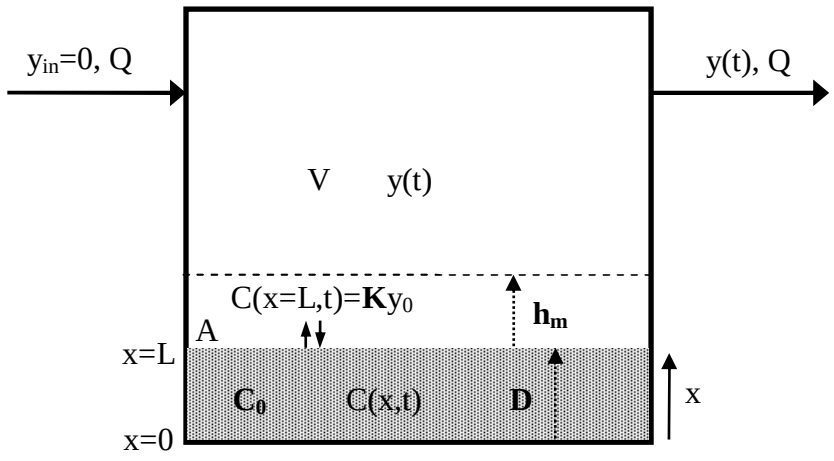

Figure 2.2 Schematic representation of VOC emission from a homogeneous solid material considering external convective mass-transfer resistance.

Huang and Haghighat (2002) solved Equations (2.1), (2.2), (2.9), (2.10) and (2.11) with a uniform initial material-phase concentration (C_0) by a finite difference method. By assuming y is much smaller than y_0, they also derived an approximate analytical solution. Xu and Zhang (2003)

developed a semi-analytical solution for this set of equations, which still requires finite difference methods and computation from the initial condition. Using Laplace transforms, Deng and Kim (2004) obtained a full analytical solution as

$$C(x,t) = 2C_0 \sum_{n=1}^{\infty} \frac{(\alpha - q_n^2)}{A_n} \cos\left(\frac{x}{L} q_n\right) e^{-DL^{-2} q_n^2 t} \tag{2.12}$$

$$y(t) = 2C_0 \beta \sum_{n=1}^{\infty} \frac{q_n \sin q_n}{A_n} e^{-DL^{-2} q_n^2 t} \tag{2.13}$$

with

$$A_n = [K\beta + (\alpha - q_n^2) KBi_m^{-1} + 2] q_n^2 \cos q_n + q_n \sin q_n [K\beta + (\alpha - 3q_n^2) KBi_m^{-1} + \alpha - q_n^2] \tag{2.14}$$

$$Bi_m = h_m L / D \tag{2.15}$$

$$\alpha = QL^2 / (DV) \tag{2.16}$$

$$\beta = AL / V \tag{2.17}$$

and q_ns are positive roots of

$$q_n \tan q_n = \frac{\alpha - q_n^2}{K\beta + (\alpha - q_n^2) KBi_m^{-1}} \tag{2.18}$$

Equations (2.12) and (2.13) can directly calculate the material-phase concentration and bulk air concentration at any time point. Due to the introduction of h_m, the analytical solution is more complicated than Equations (2.5)-(2.8). When the external convective mass-transfer resistance is ignored, or h_m becomes infinite so that y_0 is equal to y, the analytical solution simplifies to Equations (2.5)-(2.8). This comprehensive model with a full analytical solution provides a useful approach to predict VOC emissions from a homogeneous single-layer material. When a nonzero influent concentration needs to be considered, the finite difference methods (Huang and Haghighat, 2002; Xu and Zhang, 2003) or a recently developed state-space method (Yan et al., 2009) can be used.

These mass-transfer models provide tools for prediction, as well as clear insights into the emission mechanisms. The mechanisms governing emissions of VOCs from a solid dry material include internal diffusion of VOCs within the material (characterized by diffusion coefficient D), partition between the material and the chamber air at the material/air interface (characterized by partition coefficient K), and external convective mass transfer through the boundary layer near

the material/air interface (characterized by convective mass-transfer coefficient, h_m). These three parameters together with the initial material-phase concentration, C_0, collectively and exclusively determine the emission profile for a given chamber configuration (V, Q, L and A). Since partition at the material/air interface is instantaneous, the emission experiences two mass-transfer resistances: the first within the solid material (due to internal diffusion), and the second in the boundary layer at the exposed surface (due to external convection). Using the heat and mass transfer analogy, Bi_m/K is found to be a measure of the relative significance of internal mass-transfer resistance versus external convective mass-transfer resistance. When Bi_m/K is much larger than 1, internal diffusion largely determines the emission rate while external mass-transfer resistance can be neglected; in contrast, Bi_m/K values that are close to or smaller than 1 indicate that external convective mass transfer plays a substantial or primary role. For common VOCs present in indoor dry materials, h_m is on the order of 0.05 cm/s to 0.1 cm/s; L may range from 1 mm to 1 cm; D is generally smaller than 10^{-11} m^2/s; and K is generally in the range of 500-10000. The resulting Bi_m/K values are much larger than 1 and VOC emissions from typical dry materials are thus mostly controlled by internal diffusion. In addition, convective mass transfer mainly influences the initial period of emissions (Deng and Kim, 2004; Xu and Zhang, 2003; Xu and Zhang, 2004). The model developed by Little et al. (1994) ignoring the external mass-transfer resistance is therefore a reasonable simplification for internal-diffusion controlled cases, but may overestimate the early stage emissions in some situations.

Further development of mechanistic models has progressed rapidly within this well-established mass-transfer framework, with three main advances: (1) sink behavior of single-layer materials, (2) more complicated emission scenarios for single-layer materials, and (3) integrated prediction of multiple materials. With regard to the sink behavior of materials, Little and Hodgson (1996) suggested the need for mathematical models to predict sorption of VOCs by different building materials because sorption is closely related to re-emission and significantly affects gas-phase concentrations. They also derived an extended version of the source model (Little et al., 1994) based on the same principles shown in Figure 2.1 but focusing on the sink effect. The sink model was later employed to evaluate the sink effect of indoor materials and predict the transient VOC concentration in indoor air in response to several time-varying sources (Zhao et al., 2002). However, external mass transfer was also ignored in this model. Yang et al. (2001b) developed a

model to predict the VOC sorption rate into materials, which can be used as a "wall function" in combination with CFD models. The model, however, is inherently complicated due to the CFD approach they used to calculate external mass transfer. In fact, a rather simple sink model could be constructed based on the principles shown in Figure 2.2, using h_m to account for external mass transfer. It can be expressed by the same set of equations as the source model with different boundary and initial conditions, and can therefore be combined with the source model into a generalized sink/source model, as discussed later. As suggested by the concentration profile of 2,2,4-trimethyl-1,3-pentanediol monoisobutyrate (TMPD-MIB) in a vinyl flooring sample (Cox et al., 2002), the initial VOC concentration in building materials may not be uniform. Also, the influent air concentration may be nonzero and time-dependent for real indoor environments (Zhao et al., 2002). Therefore, improved models were developed to accommodate these more complicated emission scenarios. Kumar and Little (2003a) developed a full analytical single-layer model to predict the source/sink behavior of building materials and they considered the time-dependent influent concentration as well as a non-uniform initial material-phase concentration. However, they only considered diffusion-controlled materials and ignored external convective mass transfer. Taking the external convective mass transfer into account as well as a non-uniform initial material-phase concentration, Xu and Zhang (2004) developed a semi-analytical model focusing on emission behavior of building materials, which is an extension of their previous work (Xu and Zhang, 2003). Many building materials have composite structures comprised of two or more layers of homogeneous materials and are not compatible with the single-layer source and sink models. Although the above-mentioned comprehensive CFD model is applicable for multi-layer materials (Yang et al., 2001a), the model remains complicated. Employing the same mass transfer principles as for the single-layer models (Figure 2.1 or 2.2), several multi-layer emission models have therefore been developed (Deng et al., 2010; Haghighat and Huang, 2003; Hu et al., 2007; Kumar and Little, 2003b; Yuan et al., 2007a). Kumar and Little (2003b) considered the diffusion-controlled emission from a double-layer composite material and the external convective mass transfer was again ignored. They also considered non-uniform initial material-phase concentrations in the two layers and a transient influent concentration and derived an analytical solution. Haghighat and Huang (2003) included the external convective mass transfer into their numerical multi-layer model and Deng et al. (2010) presented a similar multi-layer model solved by Laplace transforms. One obstacle to a

numerical solution for multi-layer composite materials arises from the difficulty in solving sharply discontinuous concentration profiles at the interface of two adjacent materials. Therefore, Yuan et al. (2007a) developed a fugacity model to predict emissions from multi-layer materials, which has the advantage that the fugacity is continuous at the material interface so that the numerical computation is easier. Considering the external convective mass transfer as well as a non-uniform initial material-phase concentration in each layer, Hu et al. (2007) developed a semi-analytical multi-layer model, which is however very complicated. Furthermore, numerical models considering simultaneous source and sink behavior of several multi-layer composite materials, such as flooring, wall and ceiling in a room, have been developed, which come closer to the real indoor environment (Li and Niu, 2007; Zhang and Niu, 2004).

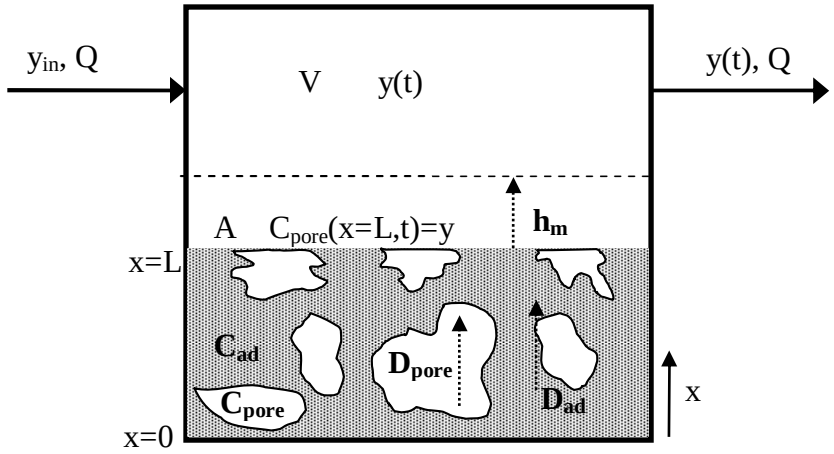

Figure 2.3 Schematic representation of VOC emission from a porous material.

An important application in modeling VOC emissions from dry materials and understanding the mass-transfer principles was achieved by considering mass transfer within porous materials (Blondeau et al., 2008; Haghighat et al., 2005; Lee et al., 2005; Lee et al., 2006; Marion et al., 2011). This so-called multi-phase model describes VOC transport in a porous material, which consists of pores and solid parts, as shown in Figure 2.3. VOC molecules are present in pores (gas phase) and solid parts (adsorbed phase) and undergo mass transfer via gas-phase diffusion in pores and surface diffusion in the adsorbed phase while diffusion through the solid is negligible compared with the much faster diffusion through pores. The governing equation of one-dimensional diffusion within the porous material can therefore be given by

$$\varepsilon \frac{\partial C_{pore}}{\partial t} + \frac{\partial C_{ad}}{\partial t} = D_{pore} \frac{\partial^2 C_{pore}}{\partial x^2} + D_{ad} \frac{\partial^2 C_{ad}}{\partial x^2} \tag{2.19}$$

where ε is the porosity, C_{pore} is the gas-phase VOC concentration in pores, C_{ad} is the adsorbed-phase VOC concentration in solid parts, D_{pore} is the effective diffusion coefficient for gas-phase diffusion and D_{ad} is the effective diffusion coefficient for surface diffusion in the adsorbed phase. An instantaneous partition equilibrium characterized by a partition coefficient between the air in the pores and the solid parts (K_{pore}) can be assumed so that the relation between C_{ad} and C_{pore} is given by

$$K_{pore} = \frac{C_{ad}}{C_{pore}} \tag{2.20}$$

Substituting (2.20) into (2.19) and introducing an overall effective diffusion coefficient of the porous material (D_s), the governing Equation (2.19) becomes

$$\frac{\partial C_{pore}}{\partial t} = \frac{D_{pore} + K_{pore} D_{ad}}{\varepsilon + K_{pore}} \frac{\partial^2 C_{pore}}{\partial x^2} = \frac{D_s}{\varepsilon + K_{pore}} \frac{\partial^2 C_{pore}}{\partial x^2} \tag{2.21}$$

The same boundary condition at the bottom surface as Equation (2.2) can be obtained by assuming the bottom surface to be impermeable, or

$$\left. \frac{\partial C_{pore}}{\partial x} \right|_{x=0} = 0 \tag{2.22}$$

A third type boundary condition the same as Equation (2.9) can be used to describe the external convective mass transfer. Assuming the VOC concentration in pores and in air is continuous at the material surface, the boundary condition at the exposed surface is given by

$$-D_s \left. \frac{\partial C_{pore}}{\partial x} \right|_{x=L} = h_m \left(\left. C_{pore} \right|_{x=L} - y \right) \tag{2.23}$$

In addition, a transient mass balance of the VOC in the chamber air, as in Equation (2.10), is required to supplement the upper boundary condition. Given the initial VOC concentration in the porous material, Equations (2.19) - (2.23) and the mass balance equation can be solved to obtain concentrations in the porous material and in the bulk chamber air as a function of time. The partition isotherm given by Equation (2.20) can be substituted by other forms determined from experiments (Marion et al., 2011; Tiffonnet et al., 2002). Including secondary source and sink behavior within the porous material, a semi-analytical solution was developed (Lee et al., 2005). Conjugated with CFD analysis of the chamber air concentration instead of using Equation (2.23)

as the upper boundary condition, the porous emission model can be extended to a more detailed numerical model (Lee et al., 2006), which is analogous to the work of Yang et al. (2001a; 2001b). It is clear that the set of equations for the porous material is analogous to that previously described for the homogeneous solid materials. Although some additional parameters are needed for the porous material models, it has been shown that the porous material models and the solid material models can be transformed from one to the other and that their model parameters are interrelated (Blondeau et al., 2008; Haghighat et al., 2005; Xu et al., 2009). Therefore, emissions from porous materials can be investigated either by treating the material with multi-phase models and considering the effect of porosity, or by lumping pores and solid parts of the porous material into a representative homogeneous solid material and using the single-phase solid models. The second approach is obviously easier. As suggested in a detailed analysis of the impact of porosity (Haghighat et al., 2005), ignoring porosity and using the single-phase solid models is generally safe.

2.3.2 Wet/VOC models

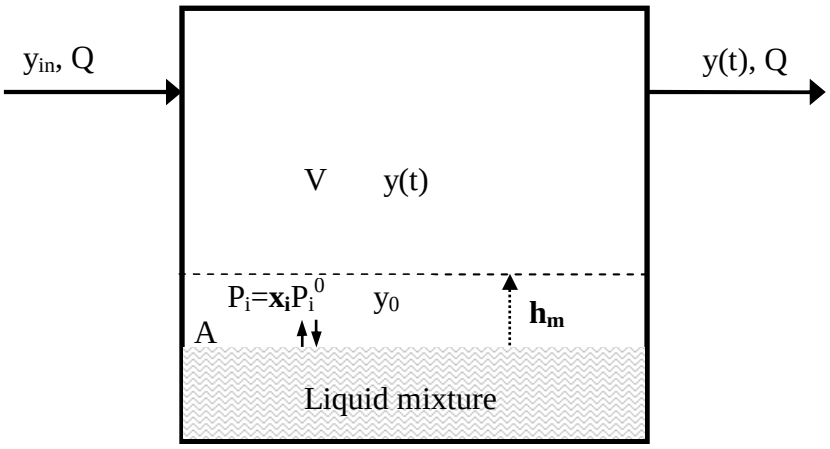

Figure 2.4 Schematic representation of the VB and VBX models for predicting VOC emission from a liquid mixture.

In addition to the dry materials whose VOC emissions can be well described and predicted using the models already reviewed, a variety of wet materials, mostly coatings such as wood stains, varnishes and paints, are also frequently used indoors. As suggested in several chamber experiments, VOC emissions from wet coating materials tend to consist of two stages: the early

stage during which the material is still quite wet and characterized by high emission rates and fast decay; and a subsequent dry stage during which the VOC is released at a much slower rate (Guo, 2002a). The fast emissions are mainly due to evaporation at the material surface and internal diffusion is immaterial during this early stage, while in the subsequent dry stage, internal diffusion acts as the main controlling factor. A transition phase usually exists between the two stages (Yang et al., 2001c; Yang et al., 2001d), which makes the prediction of VOC emissions from wet materials more complicated.

Early mass-transfer models for wet materials considered emission a pure evaporative process. Examples include the Vapor pressure and Boundary layer (VB) model for total volatile organic compounds (TVOCs) (Tichenor et al., 1993) and the subsequent VBX model employing the same mass-transfer principles for individual VOCs (Guo et al., 1998). The VB and VBX models assume that the coating on the substrate is a uniform liquid mixture of VOCs (Figure 2.4), which evaporate into air and do not penetrate into the substrate. With reference to Figure 2.4, assuming the influent air concentration is zero, the mass balance equation on the VOC in the well-mixed chamber air is

$$\frac{dy(t)}{dt} \cdot V = A \cdot E(t) - Q \cdot y(t) \tag{2.24}$$

where y(t) is the bulk air concentration, V is the chamber volume, Q is the air flow rate through the chamber, A is the surface area of the source, E(t) is the emission rate of the specific VOC from the source, and t is time. The emission rate is controlled by mass transfer through the boundary layer, or

$$E(t) = h_m (y_0(t) - y(t)) \tag{2.25}$$

where $y_0(t)$ is the gas-phase concentration of the VOC in equilibrium with the wet source, and h_m is the convective mass-transfer coefficient. Equations (2.24) and (2.25) therefore use the same approach as (2.9) and (2.10) for external convective mass transfer and mass balance in the chamber air. In the case of the VBX model (Guo et al., 1998), y_0 is equal to P_i, the partial pressure of the VOC expressed in units of gas-phase concentration. It is obtained from Raoult's Law, or

$$P_i = x_i P_i^{sat} \tag{2.26}$$

where for the i-th component of VOC in the mixture, P_i is the partial pressure, x_i is the mole fraction in the mixture, and P_i^{sat} is the vapor pressure of the pure liquid component. Because the various components may be present in the liquid mixture at different concentrations (or mole fractions) and have different liquid vapor pressures, y_0 varies from component to component. This means that the emission rate for individual components can also vary widely, causing the composition of the liquid mixture to change over time. To keep track of this change, an additional mass-balance equation for each component in the liquid mixture is required, or

$$\frac{dM_i}{dt} = -E_i \tag{2.27}$$

where M_i is the mass of the i-th component in the liquid mixture and E_i is its emission rate. Therefore, Equations (2.24), (2.25) and (2.27) for each individual VOC in the liquid mixture should be combined altogether to solve the model. A detailed application of the VB and VBX models can be found in the literature (Guo et al., 1999). The VB and VBX models ignored the mass transfer between the coating film and the substrate and the diffusion within the film itself, both of which may be negligible at the wet stage when evaporation and external convective mass transfer dominate, but become important when the film is dry. Therefore, although they predict the short-term emissions with reasonable accuracy, they are not applicable to the dry stage.

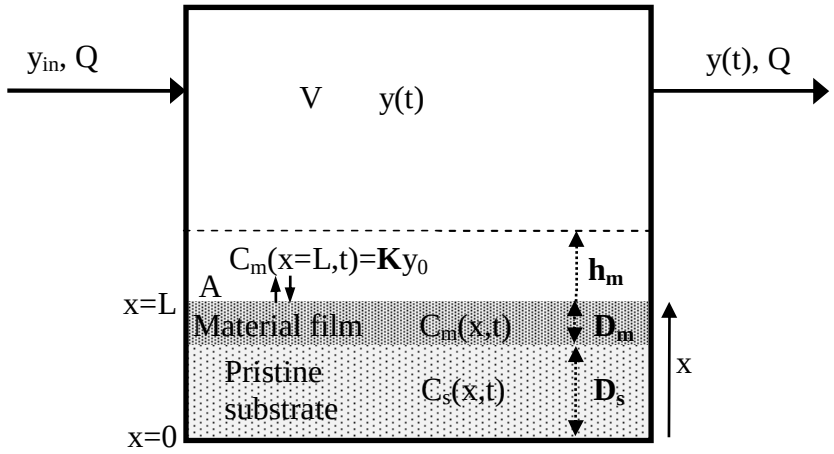

Figure 2.5 Schematic representation of VOC emission from a wet coating.

To examine the entire emission process, a semi-analytical model was developed considering diffusion within the coating (Sparks et al., 1999), although this does not have a sound mass-

transfer basis. A comprehensive mass-transfer model was proposed by Yang et al. (2001c), which was adopted and modified later in other studies (Haghighat and Huang, 2003; Zhang and Niu, 2003). According to the mass-transfer analysis, the wet material can be divided into two separate layers (Yang et al., 2001c). The upper layer (material film) is the substrate intruded with liquids while the lower layer is the pristine substrate (Figure 2.5) and each of the two layers can be treated as a continuum. Therefore, the mass-transfer mechanisms include evaporation and convective mass transfer at the material film surface, diffusion within the material film, mass transfer at the interface of the material film and the pristine substrate, and diffusion within the pristine substrate. Fick's law can be used to describe transient diffusion within the material film and the pristine substrate, as

$$\frac{\partial C_m}{\partial t} = \frac{\partial}{\partial x}\left(D_m \frac{\partial C_m}{\partial x} \right) \tag{2.28}$$

$$\frac{\partial C_s}{\partial t} = \frac{\partial}{\partial x}\left(D_s \frac{\partial C_s}{\partial x} \right) = D_s \frac{\partial^2 C_s}{\partial x^2} \tag{2.29}$$

where C_m and C_s are the VOC concentrations in the material film (upper layer) and in the pristine substrate (lower layer) and D_m and D_s are effective diffusion coefficient in the material film and in the pristine substrate. Since C_m is generally quite high initially and then decreases substantially, D_m may change with decreasing C_m. Therefore a third-power empirical equation (Yang et al., 2001c; Zhang and Niu, 2003) or a second-order empirical equation (Haghighat and Huang, 2003) has been proposed to describe the dependence of D_m on C_m. In contrast, C_s is generally low so that D_s can be assumed constant. At the material film/pristine substrate interface, the mass flux and the concentration should be continuous, with

$$-D_m \frac{\partial C_m}{\partial x} = -D_s \frac{\partial C_s}{\partial x} \tag{2.30}$$

$$C_m = C_s \tag{2.31}$$

At the bottom of the substrate, zero-flux, as for Equation (2.2), or zero-concentration, $C_s=0$, can be taken as the boundary condition. At the material film/air interface, an instantaneous reversible partition equilibrium is assumed as

$$C_m\big|_{x=L} = K y_0 \tag{2.32}$$

which is the same as Equation (2.4) or (2.11). Combined with CFD analysis of mass transfer in the chamber air (Yang et al., 2001c; Zhang and Niu, 2003) or a simple emission rate expressed

by Equation (2.9) and a mass balance equation for the chamber air as in Equation (2.10) (Haghighat and Huang, 2003), this equation set can be solved numerically. This idealized model for wet materials is similar to the two-layer dry model in principle and the same governing equations and boundary conditions are involved, except that the dependence of D_m on C_m needs considered. To eliminate the complexity due to the concentration dependence of D_m, Li et al. (2006) proposed a simplification for the previous model by assuming that the VOC concentration in the material film is always uniform so that diffusion within the film can be ignored. Their simplified model should work well for cases with a thin material film, but caution may be needed during the late period of emission when the internal diffusion in the material film becomes important.

Recently, a more complicated numerical model was developed by Altinkaya (2009) to predict VOC emissions from wet coatings. By assuming an impermeable substrate, the model can be also represented by the one-layer configuration shown in Figure 2.4. More comprehensive than the VB and VBX models, this model took account of both internal and external mass transfer resistances along with a moving coating/air interface caused by the emission process. Furthermore, it considered a concentration-dependent diffusion coefficient and a nonlinear equilibrium relationship at the air/coating interface, described by Vrentas-Duda free volume theory (Vrentas and Duda, 1977a; Vrentas and Duda, 1977b) and Flory-Huggins theory (Flory, 1953), respectively. These advancements make this model more physically plausible compared to the previous models which use empirical expressions to describe the concentration-dependence of the diffusion coefficient and use Henry's Law to describe the equilibrium relationship at the coating/air interface. However, because most model parameters are not readily available and a moving boundary is considered in the numerical calculation, this model is inherently complicated to use.

2.3.3 Dry/SVOC models

While VOC emissions have been studied for two decades, the scientific understanding of SVOC emissions has only emerged recently (Bennett and Furtaw, 2004; Liu et al., 2011; Webster et al., 2009; Xu and Little, 2006; Zhang et al., 2009). The low gas-phase concentrations of SVOCs,

strong adsorption onto interior surfaces and ubiquitous laboratory contamination cause great challenges during SVOC emission studies.

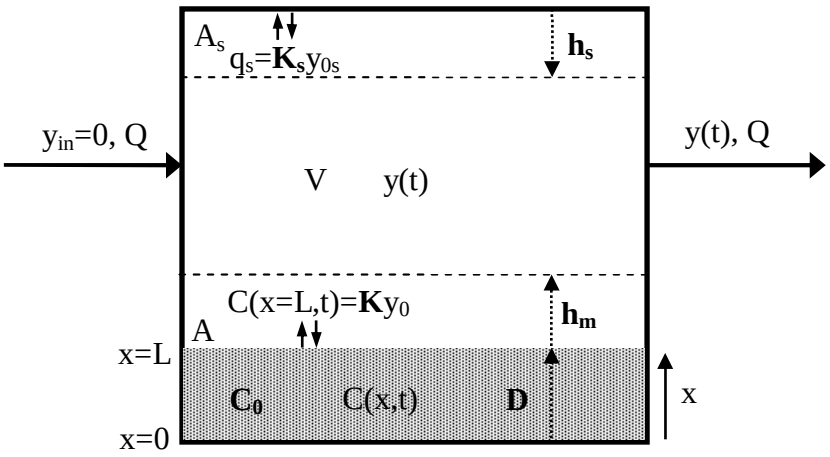

Figure 2.6 Schematic representation of SVOC emission from a homogeneous solid material.

SVOC emissions from dry materials can be modeled following essentially the same scheme as for VOCs, as shown in Figure 2.6 (Liu et al., 2011; Xu and Little, 2006). The governing equation describing transient diffusion within the material, boundary conditions at the lower and upper surfaces are also given by Equations (2.1), (2.2), (2.9) and (2.11). However, the mass balance equation for the SVOC in the bulk air should take the adsorption onto interior surfaces into account, and can be given by

$$\frac{dy(t)}{dt}\cdot V = h_m\left(y_0(t)-y(t)\right)\cdot A - Q\cdot y(t) - \frac{dq_s(t)}{dt}\cdot A_s \tag{2.33}$$

where A_s is the total area of the interior sorption surface and $q_s(t)$ is the corresponding surface concentration. The third term on the right-hand side is the SVOC accumulation rate on the surface, which is also the SVOC loss rate from the bulk air due to the adsorption onto the sorption surface. In addition, assuming a boundary layer at the sorption surface, which is analogous to that at the emission surface, the accumulation rate on the surface is equal to the convective mass-transfer rate through the boundary layer, or

$$\frac{dq_s(t)}{dt} = h_s\left(y(t)-y_{0s}(t)\right) \tag{2.34}$$

where h_s is the convective mass-transfer coefficient near the sorption surface, which is analogous to h_m, and $y_{0s}(t)$ is the SVOC concentration in the air adjacent to the sorption surface, which is

analogous to $y_0(t)$. A linear and instantaneously reversible equilibrium is also assumed between the surface and the air adjacent to the surface, or

$$q_s(t) = K_s y_{0s}(t) \tag{2.35}$$

where K_s is the partition coefficient between the surface and air for the SVOC. Assuming the initial material-phase concentration (C_0) is uniform and that the initial surface concentration and initial chamber concentration are zero, the set of equations is closed and can be solved numerically.

With respect to the emission process only, there are also two mass-transfer resistances for SVOCs, which are the same as for VOCs. However Bi_m/K values for typical SVOCs emitted from solid sources are much smaller than those for VOCs because K of SVOCs are generally several orders of magnitude larger than those of VOCs due to very low volatility, while the difference in D or h_m for VOCs and SVOCs is relatively small compared to that for K. For example, D, h_m and K for di-2-ethylhexyl phthalate (DEHP) in vinyl flooring are estimated to be 10^{-13} m^2/s, 10^{-4} m/s and 10^{11} (Xu and Little, 2006) so that Bi_m/K is much smaller than 1. Therefore, external convective mass transfer controls the emissions of SVOCs and the internal diffusion is negligible. From another perspective, K is so large that the emitted mass is tiny compared to the total amount of the SVOC in the source and therefore, the internal mass transfer is not important and the material-phase concentration is virtually constant. For example, only 0.002% of the total DEHP mass is released from the vinyl flooring after 800 days (Xu and Little, 2006). Therefore, the model can be simplified by assuming a constant and uniform material-phase concentration C_0 and a constant y_0. Equation (2.33) can then be simplified to

$$\frac{dy(t)}{dt} \cdot V = h_m (y_0 - y(t)) \cdot A - Q \cdot y(t) - \frac{dq_s(t)}{dt} \cdot A_s \tag{2.36}$$

where the first term on the right-hand side is the emission rate. Equations (2.34)-(2.36) together provide the simplified SVOC emission model, which can be calculated rather easily.

2.4 Estimation of key model parameters

2.4.1 Model parameters in the dry/VOC models

In addition to those readily measurable parameters such as V, Q, A, and L, the key parameters in the dry/VOC models primarily include material-phase diffusion coefficient D (or effective

diffusion coefficient for porous materials), material/air partition coefficient K, initial material-phase concentration C_0, and convective mass-transfer coefficient h_m. Besides the inherent errors stemming from the simplifications and assumptions of the models, the accuracy of predictions is largely dependent on reliable model parameters (Huang and Haghighat, 2003). Therefore, estimation of model parameters is a prerequisite to apply the models and has received plenty of attention. Haghighat et al. (2002) reviewed the experimental techniques to measure the diffusion coefficient of VOCs in building materials. In contrast, the comprehensive review by Guo (2002b) focused on correlations established between model parameters and physical and chemical properties of VOCs such as vapor pressure, molecular weight and mean molecular diameter. Because accurate measurements of these parameters for specific VOCs and materials are the basis of establishing correlations, and a universal correlation applicable to myriad VOCs and materials appears difficult to achieve, the following sections focus on techniques for estimating model parameters instead of those for developing correlations.

Before feasible experiment approaches were available, least square regression was often employed to estimate model parameters by fitting the emission models to emission chamber test data to obtain the "best-fitting" model parameters. This quick and easy approach is quite common during the initial stage of model development (Little et al., 1994; Yang et al., 2001(a)). He and Yang (2005) studied in detail the dependence of regression results on emission data and concluded that both the measurement errors and data abundance affect the regression results substantially. It was shown that the regression approach risks the problem of multi-solution if more than one unknown parameter needs to be determined and when the degree of freedom increases, the uncertainties of regression are larger. Furthermore, they concluded that an accurate D is more likely to be obtained from the regression, rather than K, which tends to be less sensitive. Also, taking C_0 into the regression as the third degree of freedom may deteriorate the regression results so that it needs to be determined independently (He and Yang, 2005). Meanwhile, an inverse analysis based on the Levenberg-Marquardt iterative algorithm (Marquardt, 1963) was proposed to simultaneously determine VOC diffusion and partition coefficients in building materials (Li and Niu, 2005a; Li and Niu, 2005b; Luo and Niu, 2006), which is a more robust extension of the conventional least square regression technique. In addition, regression methods based on emission chamber data can be combined with other

techniques for estimating model parameters to reduce the degree of freedom so that the accuracy of regression results can be improved. For example, Zhang et al. (2007) measured C_0 of several materials using an extraction method, calculated K from C_0 and the gas-phase concentration in equilibrium with the materials, and then obtained D by regression based on their emission chamber test results. Wang and Zhang (2009) measured C_0 and K simultaneously by a newly developed multi-injection method and then obtained D by regression based on emission chamber test results.

Considering the dependence of the above-mentioned approaches on emission chamber test data and the likely errors from multivariate regressions, it is more rigorous to obtain the model parameters from independent approaches, which can then be used for model validation and emission prediction. The inconvenience associated with the long test period required by emission chamber measurements also highlights the need for rapid estimation methods for model parameters.

2.4.1.1 Diffusion coefficient (D)

Existing techniques for determining D other than regression based on emission chamber test data generally follow two approaches. The first one is conducting a simple and well-controlled diffusion experiment where quite often, D and K can be simultaneously obtained by analyzing the experimental data. In some cases, such as the cup method (Hansson and Stymne, 2000; Kirchner et al., 1999) and the CLIMPAQ method (Meininghaus et al., 2000), a simple explicit theoretical relation between the model parameters and observed experimental data exists, which can be used to calculate the model parameters directly. In other cases, such as the two chamber method (Bodalal et al., 2000) and the microbalance method (Cox et al., 2001a), a simple diffusion model can be developed to describe the mass-transfer phenomena in the experiment so that the model parameters can be obtained by fitting the model to the experiment data. Essentially this is the same idea as the regression methods based on emission chamber test data while designing such diffusion experiments aims to eliminate the impact of other environmental conditions and model parameters, such as C_0, reducing the degree of freedom and regression uncertainties. Also, much less time is needed to carry out these simpler experiments. The second approach is the porosity test method (Blondeau et al., 2003; Xiong et al., 2008), which assumes

that diffusion within the porous material occurs in the pores by means of molecular diffusion and Knudsen diffusion. It measures the porosity and tortuosity of the test material and calculates the overall effective diffusion coefficient based on the microstructure of the material. Therefore, it is applicable for porous materials only.

Cup method

The cup method is one of the simplest techniques to measure D (Hansson and Stymne, 2000; Kirchner et al., 1999). The test material with a thickness of L and a single-sided surface area of A is tightly fastened to the open end of a cup containing a liquid VOC. As the VOC diffuses from the saturated cup air through the material, the weight decrease of the cup is recorded over time. The steady-state mass flux of the VOC through the material, $\dot{m}$, which is the slope of the weight loss curve, is dependent on D and K, or

$$\dot{m} = A \cdot D \frac{y_{sat} \cdot K - y_{amb} \cdot K}{L} \tag{2.37}$$

where y_{sat} and y_{amb} are the VOC concentrations in the saturated cup air and in the ambient air. $y_{sat} \cdot K$ and $y_{amb} \cdot K$ are therefore the material-phase concentrations at the material surface facing the cup and that exposed to the ambient air, respectively. When y_{amb} is 0, Equation (2.37) simplifies to

$$D \cdot K = \frac{\dot{m} \cdot L}{y_{sat} \cdot A} \tag{2.38}$$

Therefore, if either K or D is known, the other can be determined from Equation (2.38). However, D has been shown to be concentration dependent at high concentration levels and $y_{sat} \cdot K$ is much higher than the usual material-phase concentrations in real indoor environments. Therefore, D obtained using this method may be not applicable to realistic conditions. To eliminate the saturated concentration in the cup air, Haghighat et al. (2002) proposed a dry cup method. VOC absorbent is placed in the dry cup and a constant gas-phase VOC concentration is introduced on the other side so that the VOC diffuses into the dry cup through the material. Employing a similar idea to Equation (2.38), $D \cdot K$ can be obtained from the steady-state mass flux of the VOC through the material, which is simply the slope of the weight increase curve of the dry cup. Although very simple in both experiment and calculation, this technique alone cannot provide the values of D and K and remains inconvenient.

CLIMPAQ method

Only one VOC can be tested at a time by the cup method. Employing a similar idea, the CLIMPAQ method (Meininghaus et al., 2000) is more complicated but can test several VOCs simultaneously. The test material is placed between two CLIMPAQs (Gunnarsen et al., 1994), referred to as the primary chamber and the secondary chamber. Air with a desirable concentration of VOCs is led into the primary chamber while the secondary chamber is ventilated with clean air. Taking advantage of the special design of the CLIMPAQ, the air can be recirculated at a very large rate inside the chambers so that the steady-state concentration within each chamber can be assumed uniform. VOC concentrations in the supply and the exhaust air of each chamber are measured. The steady-state mass flux of each VOC from the primary chamber through the material to the secondary chamber, $\dot{m}$, can be calculated either from the mass-transfer aspect or from the mass-balance perspective,

$$\dot{m} = A \cdot D \frac{y_{primary} \cdot K - y_{secondary} \cdot K}{L} = Q_{secondary} \cdot y_{secondary} \tag{2.39}$$

where $Q_{secondary}$ is the clean air flow rate in the secondary chamber, $y_{primary}$ and $y_{secondary}$ are the steady-state concentrations in the primary and the secondary chamber and $y_{primary} \cdot K$ and $y_{secondary} \cdot K$ are therefore the material-phase concentrations at the material surfaces. Equation (2.39) can be rearranged into

$$D \cdot K = \frac{L \cdot Q_{secondary}}{A} \frac{y_{secondary}}{y_{primary} - y_{secondary}} \tag{2.40}$$

In addition, considering the mass balance from the beginning of the experiment until steady state, the absorbed mass of a VOC into the material when steady state is reached, m_{ab}, can be calculated by a numerical integration based on discrete measurements of exhaust concentrations, or

$$m_{ab} = \sum_{i=1}^{n} \left[Q_{primary} y_{supply} - \left(Q_{primary} y_{primary\_i} + Q_{secondary} y_{secondary\_i} \right) \right] \cdot \Delta t_i \tag{2.41}$$

where $Q_{primary}$ is the supply air flow rate in the primary chamber, y_{supply} is the supply air concentration in the primary chamber, $y_{primary\_i}$ and $y_{secondary\_i}$ are the i^{th} measurement of the exhaust concentration of the primary and the secondary chamber, and Δt_i is the time interval

between single measurements. Assuming the test material is clean at the beginning and the concentration gradient in the material is linear at steady state, K can be calculated as

$$K = \frac{m_{ab}/(A \cdot L)}{\left(\frac{y_{primary} + y_{secondary}}{2}\right)} \tag{2.42}$$

which can therefore be combined with Equations (2.40) and (2.41) to determine D and K. Using two identical regular chambers instead of CLIMPAQs, the same methodology was used to measure D and K of formaldehyde and toluene in calcium silicate (Xu et al., 2009) and D·K of several VOCs in ceiling tiles (Farajollahi et al., 2009). Also employing the same methodology, two FLECs (Wolkoff et al., 1991) were used to measure D·K of several chlorinated compounds in gypsum board (Meininghaus and Uhde, 2002). The CLIMPAQ method is therefore a particular representative of the steady-state twin chamber method, which can be also achieved using other types of chambers as long as the assumptions are satisfied. The main drawback of this method comes from neglecting external convective mass-transfer resistance at the material surfaces when applying Equation (2.39), which may result in an underestimation of D (Haghighat et al., 2002).

Two chamber method

Employing a two-airtight-chamber test, Bodalal et al. (2000) proposed a method to determine D and K simultaneously. The test material free of VOCs separates two identical 50-L chambers. Initially, one chamber has a gas-phase VOC concentration of $y_{initial}$ and is called the high-concentration chamber. The other one is clean, and is called the low-concentration chamber. During the experiment, the VOC diffuses from the high-concentration chamber through the test material into the low-concentration chamber. Assuming both chambers are well-mixed, the concentrations in the high-concentration chamber (y_1) and the low-concentration chamber (y_2) can be calculated by

$$y_1 = y_{initial} - (DA/V)\int_0^t \left(\frac{\partial C}{\partial x}\right)_{x=0} dt \tag{2.43}$$

$$y_2 = (DA/V)\int_0^t \left(\frac{\partial C}{\partial x}\right)_{x=L} dt \tag{2.44}$$

where D is diffusion coefficient, A is the area of the material, V is the volume of the two chambers, L is the thickness of the material, C is the material-phase concentration, t is time, x denotes the coordinate along the diffusion direction, or the direction normal to the material surface and x=0 is the surface facing the high-concentration chamber while x=L is the surface facing the low-concentration chamber. Transient diffusion within the material is given by

$$\frac{\partial C}{\partial t} = D\frac{\partial^2 C}{\partial x^2} \tag{2.45}$$

An instantaneous partition equilibrium is assumed between each material surface and the chamber air in contact, or

$$C\big|_{x=0} = K \cdot y_1 \tag{2.46}$$

$$C\big|_{x=d} = K \cdot y_2 \tag{2.47}$$

With the initial concentrations in the two chambers ($y_{initial}$ and zero) and in the test material (zero), the solution to Equations (2.43) - (2.47) is (Bodalal et al., 2000):

$$\ln\left(\frac{y_1 - y_2}{y_{initial}}\right) = \ln\left[\frac{4K \cdot A \cdot d/V}{q_1^2 + (K \cdot A \cdot d/V)(2 + K \cdot A \cdot d/V)}\right] - \frac{q_1^2 D}{d^2}t \tag{2.48}$$

where q_1 is the first positive root of the characteristic equation

$$\tan(q) = \frac{2(K \cdot A \cdot d/V)q}{q^2 - (K \cdot A \cdot d/V)^2} \tag{2.49}$$

Equation (2.48) gives a linear relation between the left-side term and t, with the slope and intercept dependent on D and K, respectively. Therefore, D and K can be easily obtained by linear regression of the experimental data. The problems associated with this air-tight test include air leakage in the chambers and the pressure difference caused by careless selection of sampling volume (Bodalal et al., 2000). This method also neglects the impact of external convective mass-transfer resistance and may have the same problem as the CLIMPAQ method.

Microbalance method

A method which could measure D and K separately was developed by Cox et al (2001a) for vinyl flooring and later successfully applied to polyurethane foam (Zhao et al., 2004), polystyrene foam, and oriented strand board (Yuan et al., 2007b). A thin slab sample is cut from the test material and put into a small glass chamber attached to a high-resolution dynamic

microbalance, which records the mass of the slab sample. Before testing, the sample is conditioned by ventilating clean carrier gas into the glass chamber until the mass of the slab sample becomes stable, indicating there is no VOC remaining in the sample. When the experiment begins, carrier gas with a constant VOC concentration is introduced into the glass chamber for a sorption test until partition equilibrium is reached between the sample and the carrier gas. During this period, the mass gain of the sample due to VOC sorption is recorded, generating a sorption curve. Then clean carrier gas is ventilated into the glass chamber for a desorption test until the sample is clean and the mass decrease of the sample due to VOC desorption is recorded, generating a desorption curve. Figure 2.7 shows the transient mass gain/loss of a polymeric sample during a sorption/desorption test. Based on the microbalance data, K can be determined directly as

$$K = C_{equ} / y_{sorption} \tag{2.50}$$

where $y_{sorption}$ is the VOC concentration in the incoming carrier gas for the sorption test, and C_{equ} is the material-phase concentration in equilibrium with $y_{sorption}$, which can be calculated by dividing the total mass gain at the end of the sorption test by the sample volume. D is determined by fitting a Fickian diffusion model for a thin slab to the sorption and desorption curve, which is given by (Crank, 1975):

$$\frac{M_t}{M_\infty} = 1 - \sum_{n=0}^{\infty} \frac{8}{(2n+1)^2 \pi^2} \cdot \exp\left[\frac{-D(2n+1)^2 \pi^2 t}{L^2}\right] \tag{2.51}$$

where M_t is the total mass of the VOC that has entered or left the sample in time t, M_∞ is the total mass gain when equilibrium is reached, and L is the thickness of the sample. The samples used for the microbalance method are normally quite small and thin so that it is only applicable for uniform materials. Ignoring external convective mass-transfer resistance in Equation (2.51) may also lead to the same problem as the CLIMPAQ method.

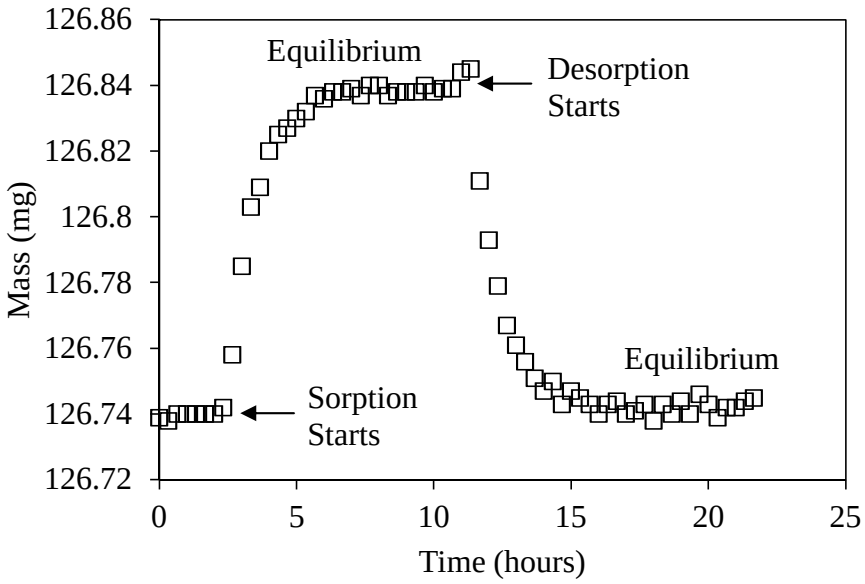

Figure 2.7 Transient mass gain/loss of a polymeric material sample during sorption/desorption cycles of toluene.

Porosity test method

In contrast to the methods discussed above, the porosity test method determines the diffusion coefficient based on the microstructure of the porous material. The methodology of the porosity test method to determine diffusion coefficient of gaseous species in porous materials was developed by Carniglia (1986) for catalysts and oxidants, and subsequently applied to building materials (Blondeau et al., 2003). It first requires carrying out a mercury intrusion porosimetry (MIP) test, intruding mercury into the porous material under stringently controlled pressures, to characterize the pore size distribution. MIP considers that the porosity of the porous material can be described as the sum of pore groups of progressively increasing radius with the i^{th} group characterized by radius r_i having a void volume of ΔV_i of all pores in the group. ΔV_i is also the volume of mercury penetrating the pores of radius r_i when an increasing pressure p_i is applied. The MIP test results can be interpreted by

$$r_i = \frac{2\gamma \cos\theta}{p_i} \tag{2.52}$$

where γ is the mercury surface tension, 4.58×10^{-5} $N\cdot m^{-1}$, and θ is the contact angle of the meniscus of mercury in a pore, 130º-140º. Therefore, the porosity of the material, ε, is given by

$$\varepsilon = \rho \sum_{i=1}^{m} \Delta V_i \tag{2.53}$$

where i=1 and i=m refer to the minimum and maximum size groups which contributes a detectibly nonzero ΔV_i respectively and ρ is the bulk density of the material. Meanwhile, the tortuosity factor of the material, τ, can be obtained by Carniglia's (1986) model. Then the overall effective diffusion coefficient D can be related to ε and τ by

$$D = D^0 \frac{\varepsilon}{\tau} \tag{2.54}$$

where D^0 is the mean (reference) diffusion coefficient in the pores of the material, which accounts for both molecular diffusion and Knudsen diffusion. The next step of the porosity test method is to determine D^0. Blondeau et al. (2003) employed a simple equation without differentiating molecular diffusion or Knudsen diffusion for different pore sizes,

$$D^0 = \frac{\sum_{i=1}^{m} D_p(r_i)\Delta V_i}{\sum_{i=1}^{m} \Delta V_i} \tag{2.55}$$

where $D_p(r)$ describes the way the diffusion coefficient varies as a function of the pore radius r, which can be defined as

$$D_p(r) = \frac{D_{air}}{1 + (\lambda / 2r)} \tag{2.56}$$

where D_{air} is the molecular diffusion coefficient in the air, and λ is the mean free path of molecules, given by

$$\lambda = \frac{3.2\mu}{p}\left(\frac{RT}{2\pi \cdot MW_{air}}\right) \tag{2.57}$$

where p is the pressure, T is the temperature, R is the universal gas constant, μ is the dynamic viscosity of air at given pressure and temperature, and MW_{air} is the molecular weight of air. Based on the pore size distribution obtained by the MIP test, D^0 can be determined by Equations (2.55)-(2.57) and then Equation (2.54) can be used to calculate D. However, the determination of D^0 by Blondeau et al. (2003) is a relatively rough estimation with large uncertainties. Given the critical impact of D^0 in the porosity test method, Xiong et al. (2008) developed a new method to determine D^0. According to the pore diameter, all the pores are divided into macro pores, whose diameters are larger than 10λ so that the diffusion is molecular diffusion, and meso pores, whose

diameters are less than 10λ in which Knudsen diffusion applies. The porosity ε_1 and average diameter d_1 of the macro pore as well as those of the meso pore, ε_2 and d_2, can be determined from the pore size distribution. Assuming macro and meso pores are connected physically in series and that they have the same tortuosity factor τ, D^0 can be determined using Fick's law,

$$\frac{1}{\varepsilon D^0} = \frac{\left[\varepsilon_1 d_2^2 / \left(\varepsilon_1 d_2^2 + \varepsilon_2 d_1^2\right)\right]^2}{\varepsilon_1 D_1} + \frac{\left[1 - \varepsilon_1 d_2^2 / \left(\varepsilon_1 d_2^2 + \varepsilon_2 d_1^2\right)\right]^2}{\varepsilon_2 D_2} \tag{2.58}$$

where D_1 is the diffusion coefficient within the macro pore, which is equal to D_{air}, the molecular diffusion coefficient in the air; and D_2 is the diffusion coefficient within the meso pore, given by

$$\frac{1}{D_2} = \frac{1}{D_{air}} + \frac{1}{D_K} \tag{2.59}$$

where D_K is the Knudsen diffusion coefficient and is calculated by

$$D_K = \frac{97 d_2}{2} \sqrt{T / MW_{VOC}} \tag{2.60}$$

where T is the temperature and MW_{VOC} is the molecular weight of the VOC. Knowing D^0, Equation (2.55) can be used to calculate D.

C-history method

An innovative method which can determine D, K and C_0 simultaneously was recently developed by Xiong et al. (2011a). The test material with a uniform initial VOC concentration is tested in an air-tight chamber and the chamber concentration development is measured. The chamber concentration y(t) and the equilibrium chamber concentration y_{equ} can be described by an emission model as shown by Figure 2.2, with the chamber flow rate set to zero. Based on the model, the logarithm of the dimensionless excess concentration, which is defined as $(y_{equ}-y)/y_{equ}$, is linearly dependent on time, or

$$\ln\left(\frac{y_{equ} - y(t)}{y_{equ}}\right) = SL \cdot t + INT \tag{2.61}$$

where SL and INT are the slope and intercept of the linear relationship, respectively. Furthermore, SL and INT are functions of both D and K as well as the geometry of the test material and the air-tight chamber while y_{equ} is dependent on C_0 and K. Therefore, the measured chamber concentration over time has the form of the logarithm of the dimensionless excess concentration as in Equation (2.61) allowing the determination of SL and INT by a linear

regression over time. Then D and K can be calculated from SL and INT and C_0 can be further determined from y_{equ} and the known value of K. This so-called C-history method has been well employed to determine the D, K and C_0 values of formaldehyde in several building materials and the determined parameters were validated using independent chamber test data (Xiong et al., 2011a). This promising method can determine three parameters simultaneously under realistic environmental conditions and is quite convenient and time-efficient to employ (Xiong et al., 2011a; Yao et al., 2011).

2.4.1.2 Partition coefficient (K)

Being the ratio of the material-phase concentration and the gas-phase concentration in equilibrium, as shown in Equation (2.4), K describes the thermodynamic status of partition equilibrium and is in principle easier to measure than D. As shown in previous section, several methods can determine both D and K simultaneously, including the CLIMPAQ method, the two chamber method, the microbalance method, and the C-history method, and therefore are not reiterated here. The headspace method is a simple and straightforward way to determine K by measuring both the material-phase concentration and the gas-phase concentration at equilibrium (Zhang et al., 2007). Analytical procedures for measuring the gas-phase VOC concentration have been well-developed while techniques for measuring the material-phase concentration will be discussed in the following section. Furthermore, several sensitive methods, which employ the basic idea of the headspace method and measure K and C_0 simultaneously, have been developed recently (Wang et al., 2008; Wang and Zhang, 2009; Xiong et al., 2009; Xiong et al., 2011b).

Multi-injection regression method

In the multi-injection regression method (Wang et al., 2008; Wang and Zhang, 2009), the test material with a uniform initial material-phase concentration (C_0, denoted by $C_{m,0}$ in this method) is placed in a well-mixed airtight chamber with a initial chamber concentration $C_{a,0}$. Partition equilibrium between the material and the chamber air is reached after some time with the material-phase and gas-phase concentrations changing to $C_{m,1}$ and $C_{a,1}$. When the chamber volume V is much larger than the volume of the material V_m, the mass conservation of the VOC gives rise to

$$C_{m,0}V_m + C_{a,0}V = C_{m,1}V_m + C_{a,1}V \quad (2.62)$$

At equilibrium, $C_{m,1}$ is equal to $K \cdot C_{a,1}$ so that Equation (2.62) can be rearranged to

$$\frac{V}{V_m}\left(C_{a,0} - C_{a,1}\right) = KC_{a,1} - C_{m,0} \tag{2.63}$$

Then a suitable mass of the VOC, q_1, is injected into the chamber air and $C_{a,1}$ increases to $C_{h,1}$ instantly while the material-phase concentration does not change within a very short period of time. Therefore, q_1 can be expressed by

$$q_1 = V(C_{h,1} - C_{a,1}) \tag{2.64}$$

After some time, partition equilibrium is established again, and the material-phase and gas-phase concentrations change to $C_{m,2}$ and $C_{a,2}$. The mass balance from the initial state to the new equilibrium after the injection of q_1 is given as

$$C_{m,0}V_m + C_{a,0}V + q_1 = C_{m,2}V_m + C_{a,2}V \tag{2.65}$$

Substituting Equation (2.64) and the equilibrium relation between $C_{m,2}$ and $C_{a,2}$ into Equation (2.65), it can be rearranged to

$$\frac{V}{V_m}\left[(C_{a,0} + C_{h,1} - C_{a,1}) - C_{a,2}\right] = KC_{a,2} - C_{m,0} \tag{2.66}$$

Similarly, the mass balance from the initial state to the equilibrium established after the i^{th} injection q_i leads to

$$\frac{V}{V_m}\left\{\left[C_{a,0} + \sum_{j=1}^{i}\left(C_{h,j} - C_{a,j}\right)\right] - C_{a,i+1}\right\} = KC_{a,i+1} - C_{m,0} \tag{2.67}$$

Equations (2.63), (2.66) and (2.67) practically define a linear relationship between the term on the left-hand side, which can be calculated from the measured gas-phase concentrations, and the equilibrium gas-phase concentration, $C_{a,i}$. Therefore, after several discrete injections, a linear regression can be carried out to determine K and $C_{m,0}$ from the slope and the intercept. Measuring gas-phase concentrations accurately is critical to obtain reliable K and C_0. However, the mass transfer between the chamber air and the material brings large uncertainties to the determination of $C_{h,i}$ and therefore may reduce the reliability of the method.

Multi-emission/flush regression method

To overcome the drawbacks of the multi-injection method, an improved method was developed (Xiong et al., 2009; Xiong and Zhang, 2010). The test material is placed in an initially clean

airtight chamber. After some time when equilibrium is reached between the material and the chamber air, the mass balance of the VOC is given by

$$C_{m,0}V_m = KC_{a,1}V_m + C_{a,1}V \tag{2.68}$$

or

$$C_{a,1} = \frac{C_{m,0}}{K + V/V_m} \tag{2.69}$$

where the notation is the same as in the multi-injection regression method. Clean air is supplied to flush the chamber rapidly and, assuming that no VOC is lost from the material during the flushing, the mass balance when the new equilibrium is established is given as

$$KC_{a,1}V_m = KC_{a,2}V_m + C_{a,2}V \tag{2.70}$$

Combing Equations (2.69) and (2.70) leads to

$$C_{a,2} = \frac{K}{K + V/V_m}C_{a,1} = \frac{K}{(K + V/V_m)^2}C_{m,0} \tag{2.71}$$

Similarly, after the $(i-1)^{th}$ flushing, the equilibrium gas-phase concentration is

$$C_{a,i} = \frac{K^{i-1}}{(K + V/V_m)^i}C_{m,0} \tag{2.72}$$

which can be rearrange into a linear form, or

$$\ln C_{a,i} = \ln\frac{K}{K + V/V_m}\cdot i + \ln\frac{C_{m,0}}{K} \tag{2.73}$$

Therefore, after several emission/flushing cycles, K and $C_{m,0}$ can be determined from the linear regression of $\ln C_{a,i}$ and i, according to Equation (2.73).

Variable volume loading method

The variable volume loading method (Xiong et al., 2011b) is another method using the similar principles and experiment apparatus as the multi-injection regression method and the multi-emission/flush regression method. Equation (2.69) can be rearranged to (ignoring the subscript of the equilibrium gas-phase concentration)

$$\frac{1}{C_a} = \frac{1}{C_{m,0}}(V/V_m) + \frac{K}{C_{m,0}} \tag{2.74}$$

As shown in Equation (2.74), reciprocal of the equilibrium gas-phase concentration ($1/C_a$) is linearly related to V/V_m for a specific material. Therefore, by carrying out airtight chamber tests using various specimen volumes V_m and measuring the corresponding equilibrium gas-phase concentration C_a, a data set of the two linearly related terms ($1/C_a$ and V/V_m) can be obtained. Employing linear regression according to Equation (2.74), $C_{m,0}$ and K can be determined from the slope and the intercept.

2.4.1.3 Initial material-phase concentration (C_0)

Traditional methods for measuring VOC concentrations in solid materials have used solvents or heat to extract target compounds. However, as discussed by Cox et al. (2001b) using the free volume theory and the dual-mobility model, the total VOC concentration can be apportioned to mobile and partially immobilized fractions. C_0 in the emission models should be the concentration of the readily emittable compound or the mobile fraction, which however cannot be distinguished by solvent or heat extraction methods. They also found that the emittable concentration of several VOCs in vinyl flooring measured by a new CM-FBD method is 30%-70% lower than the concentration measured by a direct thermal desorption method. The emittable formaldehyde concentration in building materials measured by the multi-injection regression method is also much lower than the total concentration measured by a thermal extraction method (Wang and Zhang, 2009). Recently, it is reported that the emittable concentration of formaldehyde in building materials increases significantly at elevated temperatures (Xiong and Zhang, 2010). Therefore, it is necessary to measure C_0 under environmental conditions resembling those of real indoor environments. In addition to the multi-purpose methods discussed above, two methods measuring C_0 exclusively are discussed here, both of which actually aim to extract all the emittable VOCs from the test materials at moderate environmental conditions and measure the total recovered mass.

CM-FBD method

As discussed in the first part of this review, internal diffusion often controls the emission rate so that complete depletion of VOCs from building materials may require a long time. Cox et al. (2001b) therefore pulverized vinyl flooring samples into powder using a ball mill in a liquid nitrogen bath at -140 °C. This cryogenic milling (CM) technique reduces the diffusion path

length and increases the emission surface area. This reduces VOC extraction time while the low temperature significantly reduces VOC vapor pressure and minimizes VOC loss during the grinding process. The extraction of VOCs from the powder was accomplished at room temperature using a fluidized-bed desorption (FBD) method. The powder was placed in a fluidized-bed vessel ventilated continuously with clean air, which extracted VOCs from the powder. The effluent concentration was measured at suitable time intervals until all the VOCs were extracted and the total amount of emitted VOCs was determined based on the air flow rate. The combination of the CM and the FBD accelerates the extraction greatly under room temperature. However, the experimental system is complicated and there is concern that the property of the test material may change after being ground into powder.

Multi-flushing extraction method

Placing the ground test material in an airtight chamber, the multi-flushing extraction method involves multiple equilibrium cycles and entails flushing the chamber air at each equilibrium state (Smith et al., 2008). The test continues until the equilibrium chamber air concentration of the last cycle is less than 10% of the first cycle so that most of the VOCs are extracted from the materials. Therefore, a series of equilibrium chamber air concentrations can be obtained during the entire process and the initial emittable mass, M_0, can be calculated as

$$M_0 = \sum_{i=1}^{n} VC_i + \frac{VC_n}{C_{n-1}/C_n - 1} \tag{2.75}$$

The first term on the right-hand side is the amount of the VOC emitted during the entire experiment period and the second term estimates the mass remaining in the material after the experiment, where V is the volume of the chamber, C_i is the equilibrium chamber air concentration for cycle i and n is the last cycle of the experiment. Since this method may require many cycles for the equilibrium concentration of the last cycle to reach the required condition, a very long experimental period may be needed.

2.4.1.4 Convective mass-transfer coefficient (h_m)

The effect of external convective mass transfer on the emission process has been discussed above. When the external convective mass-transfer resistance is large compared with that due to internal diffusion, h_m can be incorporated into the emission models to account for the external

convective mass transfer. However, it has been shown that h_m only affects the initial emission period and that emission is not very sensitive to h_m even during the initial period (Cox et al., 2010; Deng and Kim, 2004; Li and Niu, 2005a; Xu and Zhang, 2003). h_m is dependent on the air flow condition near the emission surface and generally inconvenient to measure experimentally. Therefore, estimating h_m based upon heat and mass transfer analogy empirical relations is generally adopted.

The empirical relations are generally established by several dimensionless numbers, including Sherwood number (Sh), Reynolds number (Re) and Schmidt number (Sc). The empirical correlation most commonly employed for VOC emissions modeling is (Kays and Crawford, 1980; White, 1988):

For laminar flow ($Re<5\times10^5$)

$$Sh = 0.664 \cdot Sc^{1/3} \cdot Re^{1/2} \quad (2.76)$$

For turbulent flow ($Re>5\times10^5$)

$$Sh = 0.037 \cdot Sc^{1/3} \cdot Re^{4/5} \quad (2.77)$$

Combined laminar/turbulent flow ($5\times10^4 \leq Re \leq 10^7$)

$$Sh = \left(0.037 \cdot Re^{4/5} - 8700\right) \cdot Sc^{1/3} \quad (2.78)$$

where $Sh= h_m \cdot l/D_{air}$, $Sc=\nu/D_{air}$, and $Re=u \cdot l/\nu$, ν is the kinematic viscosity of the air, u is the mean air velocity over the emission surface, l is the characteristic length of the material, and D_{air} is the VOC diffusion coefficient in the air. D_{air} can be obtained directly from the literature (Rafson, 1998) or estimated simply based on empirical correlations, such as the commonly used Fuller-Schettler-Giddings method and Wilke-Lee method (Guo, 2002b). If the mean air velocity over the emission surface u is measured during the emission chamber test, the correlation can be used to estimate h_m.

Haghighat and Zhang (1999) developed another method to determine h_m, incorporating wall shear stress. Other correlations which can be used to estimate h_m have been extensively reviewed by Guo (2002b).

2.4.2 Model parameters in the wet/VOC models

Although the VB and VBX models require several parameters, most of them are readily measurable, including V, A, and Q. h_m can be obtained using the method introduced above for the dry/VOC models. When the composition of VOCs in the solvent (initial M_i) is known, Equations (2.24), (2.25) and (2.27) for each VOC component can be combined to solve the chamber concentration of each VOC, with the partial pressure of each VOC at any time calculated using Raoult's Law.

The wet models based on Figure 2.5 are analogous to the double-layer dry model in principle but the model parameters are more difficult to determine. Some of them, such as D_s, K and h_m can be determined using the same methods as for the dry/VOC models and the initial material-phase concentration in the substrate layer ($C_{0,s}$) can be simply assumed to be zero. The dependence of D_m on the concentration is however still unclear and can be only estimated using some empirical equations (Haghighat and Huang, 2003; Yang et al., 2001c; Zhang and Niu, 2003). The initial material-phase concentration in the material film ($C_{0,m}$) can be estimated from the initial concentration in the applied liquid solvent and the liquid expansion factor, which means that once a liquid solvent is applied to a substrate, the volume of the liquid film absorbed by the substrate will expand by a given factor, and the initial VOC concentration in the film will decrease by the same factor. The thickness of the material film and the substrate layer can be also determined from the liquid expansion factor and the initial volume of the applied liquid solvent (Yang et al., 2001c). However, the value of the liquid expansion factor depends on the liquid solvent and the substrate and is difficult to obtain.

2.4.3 Model parameters in the dry/SVOC models

Some of the model parameters (V, Q, A, L, and A_s) in Figure 2.6 are readily measurable, and h_m and h_s can be estimated using the correlation given by Equations (2.76)-(2.78). A new method for measuring K_s has been developed recently, which exposes the sorption surface to air with a constant SVOC concentration until the sorption equilibrium is reached. Then K_s can be determined from the gas-phase and surface concentrations in equilibrium (Liu et al., 2011). Very little work has been done in determining C_0, D, and K experimentally for SVOCs. However, as discussed above, C_0 is usually effectively constant and the source can be simply represented by a constant y_0 value, bypassing C_0, D, and K. In some cases, y_0 can be approximated by the vapor

pressure of the SVOC. For example, it has been demonstrated that the DEHP plasticizer present in vinyl flooring at a concentration of 15% by mass behaves as a thermodynamically separate liquid phase and its y_0 is equal to the vapor pressure of pure liquid DEHP (Clausen et al., 2010; Clausen et al., 2012; Ekelund et al., 2010). Unfortunately, y_0 is not well approximated by vapor pressure in all cases. For example, another phthalate plasticizer, di-n-butyl phthalate (DnBP) is generally used in polymer products at much lower concentrations so that it behaves very differently from its pure liquid form. Another example, 2,2',4,4'-tetrabromodiphenyl ether (BDE-47) is a common brominated flame retardants and is sometimes present at high concentrations in polyurethane foam products. However, it is a solid at room temperature. y_0 for DnBP and BDE-47 may therefore be much lower than their vapor pressures. The material-phase concentration (C_0) of SVOC additives such as DnBP and BDE-47 in different products can vary substantially, and the dependence of y_0 on C_0 is presently unknown. The simple linear partition relationship is generally only applicable at concentrations below 1% by mass and therefore, K in the SVOC models cannot be simply taken as a constant partition coefficient as done for the VOC models although they share the same form in Equation (2.11). Raoult's Law does not apply to polymer solutions either owing to the extremely large polymer molecules compared to the size of the added SVOC molecules (Hawkes, 1995; Nicholson, 2006). Therefore, y_0 is not directly available for many SVOCs and the development of methods to measure or estimate y_0 for SVOCs is an area that requires further research.

2.5 Conclusions

In the context of the renewed drive for "air-tight" energy-efficient buildings, source control is a more straightforward and probably better approach to reduce indoor VOC and SVOC concentrations: preventing the problem rather than curing it (Bluyssen, 2009). The understanding of emission mechanisms and the ability to predict emissions from various indoor sources is prerequisite for characterizing the source-to-effect continuum and for developing environmentally benign products. The present paper reviews the major mechanistic models for predicting VOC and SVOC emissions from building materials and consumer products and also elaborates the current state of knowledge about the mass-transfer mechanisms controlling emissions. The validation and application of these models require reliable determination of

model parameters and therefore, major techniques for determining the key model parameters are also reviewed.

In general, the mass-transfer mechanisms of VOC emissions from dry and wet materials are reasonably well understood and a variety of validated mass-transfer models have been developed, with the capability to predict chamber test results as well as more realistic and complicated indoor emission scenarios. However, there are still knowledge gaps in the understanding of VOC emissions. For example, the emission characteristics of sources are much more complicated in the real indoor environment with several sources and sinks present at the same time; indoor and surface chemistry could generate secondary sources; and the impact of various environmental factors on emissions are not fully understood. Furthermore, the lack of simple and effective estimation methods for model parameters hinders the application of some models, especially for the wet/VOC models. Although considerable progress has been achieved and several techniques have been developed, most of them are still quite complicated and time-consuming. Great concern about the reliability of these techniques also exists. For example, diffusion coefficients measured by different methods may have deviations of up to 700% (Haghighat et al., 2002). Therefore, further development of simple and reliable methods for estimating model parameters is needed and inter-method comparisons for same materials and VOCs are required to verify the reliability of the methods.

On the other hand, the understanding of the mass-transfer mechanisms controlling SVOC emissions is just emerging. Although SVOC emissions from dry materials may be modeled following a similar scheme to VOCs, SVOC emissions are inherently more complicated than VOCs and sorption onto interior surfaces affects emissions substantially. Therefore, more chamber studies are needed to characterize both the emission and sorption behavior of SVOCs and to determine the required model parameters.

2.6 Acknowledgements

Financial support from the National Science Foundation (Grant Numbers: BES 9624488; CMS 0122165; BES 0504167; CMS 0600090) is acknowledged.

2.7 References

Altinkaya, S.A. (2009) Predicting emission characteristic of volatile organic compounds from wet surface coatings, *Chemical Engineering Journal*, **155**, 586-593.

Bako-Biro, Z., Wargocki, P., Weschler, C.K. and Fanger, P.O. (2004) Effects of pollution from personal computers on perceived air quality, SBS symptoms and productivity in offices, *Indoor Air*, **14**, 178-187.

Bennett, D.H. and Furtaw, E.J. (2004) Fugacity-based indoor residential pesticide fate model, *Environmental Science and Technology*, **38**, 2142-2152.

Billionnet, C., Gay, E., Kirchner, S., Leynaert, B. and Annesi-Maesano, I. (2011) Quantitative assessments of indoor air pollution and respiratory health in a population-based sample of French dwellings, *Environmental Research*, **111**, 425-434.

Blondeau, P., Tiffonnet, A.L., Allard, F. and Haghghat, F. (2008) Physically based modeling of the material and gaseous contaminant interactions in buildings: Models, experimental data and future developments, *Advances in Building Energy Research*, **2**, 57-93.

Blondeau, P., Tiffonnet, A.L., Damian, A., Amiri, O. and Molina, J.L. (2003) Assessment of contaminant diffusivities in building materials from porosimetry tests, *Indoor Air*, **13**, 302-310.

Bluyssen, P.M. (2009) Towards an integrative approach of improving indoor air quality, *Building and Environment*, **44**, 1980-1989.

Bluyssen, P.M., Fernandes, E.D.O., Groes, L., Clausen, G., Fanger, P.O., Valbjørn, O., Bernhard, C.A. and Roulet, C.A. (1996) European indoor air quality audit project in 56 office buildings, *Indoor Air*, **6**, 221-238.

Bodalal, A., Zhang, J.S. and Plett, E.G. (2000) A method for measuring internal diffusion and equilibrium partition coefficients of volatile organic compounds for building materials, *Building and Environment*, **35**, 101-110.

Boeglin, M.L., Wessels, D. and Henshel, D. (2006) An investigation of the relationship between air emissions of volatile organic compounds and the incidence of cancer in Indiana counties, *Environmental Research*, **100**, 242-254.

Carniglia, S.C. (1986) Construction of the tortuosity factor from porosimetry, *Journal of Catalysis*, **102**, 401-418.

Chang, J.C. and Guo, Z. (1992) Modeling of the fast organic emissions from a wood-finishing product - floor wax, *Atmospheric Environment*, **26A**, 2365-2370.

Clausen, P.A., Liu, Z., Kofoed-Sørensen, V., Little, J.C. and Wolkoff, P. (2012) Influence of temperature on the emission of di-(2-ethylhexyl)phthalate (DEHP) from PVC flooring in the emission cell FLEC, *Environmental Science and Technology*, **46**, 909-915.

Clausen, P.A., Liu, Z., Xu, Y., Kofoed-Sørensen, V. and Little, J.C. (2010) Influence of air flow rate on emission of DEHP from vinyl flooring in the emission cell FLEC: measurements and CFD simulation, *Atmospheric Environment*, **44**, 2760-2766.

Clausen, P.A., Wolkoff, P., Holst, E. and Nielsen, P.A. (1991) Long-term emission of volatile organic compounds from waterborne paints-methods of comparison, *Indoor Air*, **4**, 562-576.

Clausen, P.A., Xu, Y., Kofoed-Sørensen, V., Little, J.C. and Wolkoff, P. (2007) The influence of humidity on the emission of di-(2-ethylhexyl) phthalate (DEHP) from vinyl flooring in the emission cell "FLEC", *Atmospheric Environment*, **41**, 3217-3224.

Cox, S.S., Little, J.C. and Hodgson, A.T. (2002) Predicting the emission rate of volatile organic compounds from vinyl flooring, *Environmental Science and Technology*, **36**, 709-714.

Cox, S.S., Little, J.C. and Hodgson, A.T. (2001b) Measuring concentrations of volatile organic compounds in vinyl flooring, *Journal of Air and Waste Management Association*, **51**, 1195-1201.

Cox, S.S., Liu, Z., Little, J.C., Howard-Reed, C., Nabinger, S.J. and Persily, A. (2010) Diffusion-controlled reference material for VOC emissions testing: proof of concept, *Indoor Air*, **20**, 424-433.

Cox, S.S., Zhao, D. and Little, J.C. (2001a) Measuring partition and diffusion coefficients for volatile organic compounds in vinyl flooring, *Atmospheric Environment*, **35**, 3823-3830.

Crank, J. (1975) *The Mathematics of Diffusion, Second Edition*, Clarendon Press, Oxford, England.

Deng, B. and Kim, C.N. (2004) An analytical model for VOCs emission from dry building materials, *Atmospheric Environment*, **38**, 1173-1180.

Deng, B., Tang, S., Kim, J.T. and Kim, C.N. (2010) Numerical modeling of volatile organic compound emissions from multi-layer dry building materials, *Korean Journal of Chemical Engineering*, **27**, 1049-1055.

Dunn, J.E. and Tichenor, B.A. (1988) Compensating for sink effects in emissions test chambers by mathematical modeling, *Atmospheric Environment*, **22**, 885-894.

Ekelund, M., Azhdar, B. and Gedde, U.W. (2010) Evaporative loss kinetics of di(2-ethylhexyl)phthalate (DEHP) from pristine DEHP and plasticized PVC, *Polymer Degradation and Stability*, **95**, 1789-1793.

Fanger, P.O. (2006) What is IAQ? *Indoor Air*, **16**, 328-334.

Farajollahi, Y., Chen, Z. and Haghighat, F. (2009) An experimental study for examining the effects of environmental conditions on diffusion coefficient of VOCs in building materials, *Clean*, **37**, 436-443.

Flory, P.J. (1953) *Principles of Polymer Chemistry*, Cornell University Press, Ithaca, NY.

Gunnarsen, L., Nielsen, P.A. and Wolkoff, P. (1994) Design and characterization of the CLIMPAQ, chamber for laboratory investigations of materials, pollution and air quality, *Indoor Air*, **4**, 56-62.

Guo, Z. (2002a) Review of indoor emission source models. Part 1. Overview, *Environmental Pollution*, **120**, 533-549.

Guo, Z. (2002b) Review of indoor emission source models. Part 2. Parameter estimation, *Environmental Pollution*, **120**, 551-564.

Guo, Z., Chang, J.C.S., Sparks, L.E. and Fortmann, R.C (1999) Estimation of the rate of VOC emissions from solvent-based indoor coating materials based on product formulation, *Atmospheric Environment*, **33**, 1205-1215.

Guo, Z., Sparks, L.E., Tichenor, B.A. and Chang, J.C.S. (1998) Predicting the emissions of individual VOCs from petroleum-based indoor coatings, *Atmospheric Environment*, **32**, 231-237.

Haghighat, F. and Huang, H. (2003) Integrated IAQ model for prediction of VOC emissions from building material, *Building and Environment*, **38**, 1007-1017.

Haghighat, F., Huang, H. and Lee, C.-S. (2005) Modeling approaches for indoor air VOC emissions from dry building materials-A review, *ASHRAE Transactions*, **111**, 635-645.

Haghighat, F., Lee, C.-S. and Ghaly, W.S. (2002) Measurement of diffusion coefficients of VOCs for building materials: review and development of a calculation procedure, *Indoor Air*, **12**, 81-91.

Haghighat, F. and Zhang, Y. (1999) Modelling of emission of volatile organic compounds from building materials-estimation of gas-phase mass transfer coefficient, *Building and Environment*, **34**, 377-389.

Hansson, P. and Stymne, H. (2000) 'VOC diffusion and absorption properties of indoor materials-consequences for indoor air quality' In: *Proceedings of Healthy Buildings 2000*, Espoo, Finland, Healthy Buildings 2000.

Hawkes, S. J. (1995) Raoult's law is a deception, *Journal of Chemical Education*, **72**, 204-205.

He, G. and Yang, X. (2005) On regression method to obtain emission parameters of building materials, *Building and Environment*, **40**, 1282-1287.

Heudorf, U., Mersch-Sundermann, V. and Angerer, J. (2007) Phthalates: toxicology and exposure, *International Journal of Hygiene and Environmental Health*, **210**, 623-634.

Hu, H., Zhang, Y., Wang, X. and Little, J.C. (2007) An analytical mass transfer model for predicting VOC emissions from multi-layered building materials with convective surfaces on both sides, *International Journal of Heat and Mass Transfer*, **50**, 2069-2077.

Huang, H. and Haghighat, F. (2002) Modeling of volatile organic compounds emission from dry building materials, *Building and Environment*, **37**, 1127-1138.

Huang, H. and Haghighat, F. (2003) Building materials VOC emissions - a systematic parametric study, *Building and Environment*, **38**, 995-1005.

Jaakkola, J.J.K. and Knight, T.L. (2008) The role of exposure to phthalates from polyvinyl chloride products in the development of asthma and allergies: a systematic review and meta-analysis, *Environmental Health Perspectives*, **116**, 845-853.

Jie, Y., Ismail, N.H., Jie, X. and Isa, Z.M. (2011) Do indoor environments influence asthma and asthma-related symptoms among adults in homes? A review of the literature, *Journal of the Formosan Medical Association*, **110**, 555-563.

Kays, W.M. and Crawford, M.E. (1980) *Convective Heat and Mass Transfer, Second Edition*, McGraw-Hill, New York.

Kirchner, S., Badey, J.R., Knudsen, H.N., Meininghaus, R., Quenard, D., Sallee, H. and Sarrinen, A. (1999) 'Sorption capacities and diffusion coefficients of indoor surface materials exposed to VOCs: proposal of new test procedures' In: *Proceedings of the 8th International Conference on Indoor Air Quality and Climate*, Edinburg, Scotland, Indoor Air 1999.

Kumar, D. and Little, J.C. (2003a) Single-layer model to predict the source/sink behavior of diffusion-controlled building materials, *Environmental Science and Technology*, **37**, 3821-3827.

Kumar, D. and Little, J.C. (2003b) Characterizing the source/sink behavior of double-layer building materials, *Atmospheric Environment*, **37**, 5529-5537.

Latini, G., De Felice, C. and Verrotti, A. (2004) Plasticizers, infant nutrition and reproductive health, *Reproductive Toxicology*, **19**, 27-33.

Lee, C.-S., Haghighat, F. and Ghaly, W.S. (2005) A study on VOC source and sink behavior in porous building materials - analytical model development and assessment, *Indoor Air*, **15**, 183-196.

Lee, C.-S., Haghighat, F. and Ghaly, W.S. (2006) Conjugate mass transfer modeling for VOC source and sink behavior of porous building materials: When to apply it? *Journal of Building Physics*, **30**, 91-111.

Li, F. and Niu, J. (2007) Control of volatile organic compounds indoors – Development of an integrated mass-transfer-based model and its application, *Atmospheric Environment*, **41**, 2344-235.

Li, F. and Niu, J. (2005a) An inverse technique to determine volatile organic compounds diffusion and partition coefficients in dry building materials, *Heat and Mass Transfer*, **41**, 834-842.

Li, F. and Niu, J. (2005b) Simultaneous estimation of VOCs diffusion and partition coefficients in building materials via inverse analysis, *Building and Environment*, **40**, 1366-1374.

Li, F., Niu, J. and Zhang, L. (2006) A physically-based model for prediction of VOCs emissions from paint applied to an absorptive substrate, *Building and Environment*, **41**, 1317-1325.

Little, J.C. and Hodgson, A.T. (1996) 'A strategy for characterizing homogeneous, diffusion-controlled, indoor sources and sinks' In: *ASTM Standard Technical Publication 1287*, American Society for Testing and Materials, Philadelphia, PA.

Little, J.C., Hodgson, A.T. and Gadgil, A.J. (1994) Modeling emissions of volatile organic compounds from new carpets, *Atmospheric Environment*, **28**, 227-234.

Liu, Z., Xu, Y. and Little, J.C. (2011) 'Characterizing emissions of di-2-ethylhexyl phthalate from vinyl flooring in a specially-designed chamber' In: *Proceedings of the 12th*

International Conference on Indoor Air Quality and Climate, Austin, Texas, Indoor Air 2011.

Luo, R. and Niu, J. (2006) Determining diffusion and partition coefficients of VOCs in cement using one FLEC, *Building and Environment*, **41**, 1148-1160.

Marion, M., Tiffonnet, A.L., Santa-Cruz, A. and Makhloufi, R. (2011) Study of the resistances to transfer of gaseous pollutant between material and indoor air, *Building and Environment*, **46**, 356-362.

Marquardt, D.W. (1963) An algorithm for least-squares estimation of nonlinear inequalities, *Journal of the Society for Industrial and Applied Mathematics*, **11**, 431-441.

Matsumoto, M., Hirata-Koizumi, M. and Ema, M. (2008) Potential adverse effects of phthalic acid esters on human health: a review of recent studies on reproduction, *Regulatory Toxicology and Pharmacology*, **50**, 37-49.

McKee, R.H., Butala, J.H., David, R.M. and Gans, G. (2004) NTP center for the evaluation of risks to human reproduction reports on phthalates: addressing the data gaps, *Reproductive Toxicology*, **19**, 1-22.

Meininghaus, R., Gunnarsen, L. and Knudsen, H.N. (2000) Diffusion and sorption of volatile organic compounds in building materials – Impact on indoor air quality, *Environmental Science and Technology*, **34**, 3101-3108.

Meininghaus, R. and Uhde, E. (2002) Diffusion studies of VOC mixtures in a building material, *Indoor Air*, **12**, 215-222.

Missia, D.A., Demetriou, E., Michael, N., Tolis, E.I. and Bartzis, J.G. (2010) Indoor exposure from building materials: A field study, *Atmospheric Environment*, **44**, 4388-4395.

Mølhave, L. (1989) The sick buildings and other buildings with indoor climate problems, *Environment International*, **15**, 65-74.

Nicholson, J. W. (2006) *The Chemistry of Polymers*, Royal Society of Chemistry, Cambridge, UK.

NTP (2011) *Report on Carcinogens, Twelfth Edition*, U.S. Department of Health and Human Services, National Toxicology Program.

Rafson, H.J. (1998) *Odor and VOC control handbook*, McGraw-Hill, New York.

Rennix, C.P., Quinn, M.M., Amoroso, P.J., Eisen, E.A. and Wegman, D.H. (2005) Rish of breast cancer among enlisted army women occupationally exposed to volatile organic compounds, *American Journal of Industrial Medicine*, **48**, 157-167.

Ritter, L. and Arbuckle, T.E. (2007) Can exposure characterization explain concurrence of discordance between toxicology and epidemiology? *Toxicological Sciences*, **97**, 241-252.

Rudel, R.A. and Perovich, L.J. (2009) Endocrine disrupting chemicals in indoor and outdoor air, *Atmospheric Environment*, **43**, 170-181.

Sax, S.N., Bennett, D.H., Chillrud, S.N., Ross, J., Kinney, P.L. and Spengler, J.D. (2006) A cancer risk assessment of inner-city teenagers living in New York City and Los Angeles, *Environmental Health Perspectives*, **114**, 1558-1566.

Silberstein, S., Grot, R.A., Kunimichi, I. and Mulligan, J.L. (1988) Validation of models for predicting formaldehyde concentrations in residences due to pressed-wood products, *Journal of Air Pollution Control Association*, **38**, 1403-1411.

Sparks, L.E., Guo, Z., Chang, J.C. and Tichenor, B.A. (1999) Volatile organic compound emissions from Latex paint – Part 1. Chamber experiments and source model development, *Indoor Air*, **9**, 10-17.

Smith, J.F., Zhang, J.S., Guo, B. and Xu, J. (2008) 'Determination of emittable initial VOC concentrations in building materials and sorption isotherm for VOCs' In: *Proceedings of the 11th International Conference on Indoor Air Quality and Climate*, Copenhagen, Denmark, Indoor Air 2008.

Tichenor, B.A., Guo, Z., Dunn, J.E., Sparks, L.E. and Mason, M.A. (1991) The interaction of vapor phase organic compounds with indoor sinks, *Indoor Air*, **1**, 23-35.

Tichenor, B.A., Guo, Z. and Sparks, L.E. (1993) Fundamental mass transfer model for indoor air emissions from surface coatings, *Indoor Air*, **3**, 263-268.

Tiffonnet, A.L., Blondeau, P., Allard, F. and Haghighat, F. (2002) Sorption isotherms of acetone on various building materials, *Indoor and Built Environment*, **11**, 95-104.

Vrentas, J.S. and Duda, J.L. (1977a) Diffusion in polymer-solvent systems: I. Re-examination of the free volume theory, *Journal of Polymer Science: Polymer Physics Edition*, **15**, 403-416.

Vrentas, J.S. and Duda, J.L. (1977b) Diffusion in polymer-solvent systems: II. A predictive theory for the dependence of diffusion coefficients on temperature concentration and molecular weight, *Journal of Polymer Science: Polymer Physics Edition*, **15**, 417-439.

Wang, X. and Zhang, Y. (2009) A new method for determining the initial mobile formaldehyde concentrations, partition coefficients and diffusion coefficients of dry building materials, *Journal of Air and Waste Management Association*, **59**, 819-825.

Wang, X., Zhang, Y. and Xiong, J. (2008) Correlation between the solid/air partition coefficient and liquid molar volume for VOCs in building materials, *Atmospheric Environment*, **42**, 7768-7774.

Webster, T.F., Harrad, S., Millette, J. R., Holbrook, R.D., Davis, J.M., Stapleton, H.M., Allen, J.G., McClean, M.D., Ibarra, C., Abdallah, M.A.. and Covaci, A. (2009) Identifying transfer mechanisms and sources of decabromodiphenyl ether (BDE 209) in indoor environments using environmental forensic microscopy, *Environmental Science and Technology*, **43**, 3067-3072.

Weschler, C.J. (2009) Changes in indoor pollutants since the 1950s, *Atmospheric Environment*, **43**, 153-169.

Weschler, C.J. and Nazaroff, W.W. (2008) Semivolatile organic compounds in indoor environments, *Atmospheric Environment*, 42, 9018-9040.

White, F.M. (1988) *Heat and Mass Transfer*, Addison-Wesley, Reading, MA.

Wolkoff, P., Clausen, P.A., Nielsen, P.A., Gustaffson, H., Jonsson, B. and Rasmussen, E. (1991) 'Field and laboratory emission cell: FLEC' In: *Proceedings of Healthy Building 1991*, Washington, D.C.

Wolkoff, P. and Nielsen, G.D. (2001) Organic compounds in indoor air-their relevance for perceived indoor air quality? *Atmospheric Environment*, **35**, 4407-4417.

Xiong, J., Chen, W., Smith, J.F., Zhang, Y. and Zhang, J.S. (2009) An improved extraction method to determine the initial emittable concentration and the partition coefficient of VOCs in dry building materials, *Atmospheric Environment*, **43**, 4102-4107.

Xiong, J., Yan, W. and Zhang Y. (2011b) Variable volume loading method: A convenient and rapid method for measuring the initial emittable concentration and partition coefficient of formaldehyde and other aldehydes in building materials, *Environmental Science and Technology*, **45**, 10111-10116.

Xiong, J., Yao, Y. and Zhang, Y. (2011a) C-history method: rapid measurement of the initial emittable concentration, diffusion and partition coefficients for formaldehyde and VOCs in building materials, *Environmental Science and Technology*, **45**, 3584-3590.

Xiong, J. and Zhang, Y. (2010) Impact of temperature on the initial emittable concentration of formaldehyde in building materials: experimental observation, *Indoor Air*, **20**, 523-529.

Xiong, J., Zhang, Y., Wang, X. and Chang, D. (2008) Macro-meso two-scale model for predicting the VOC diffusion coefficients and emission characteristics of porous building materials, *Atmospheric Environment*, **42**, 5278-5290.

Xu, J., Zhang, J.S., Grunewald, J., Zhao, J., Plagge, R., Ouali, A. and Allard, F. (2009) A study on the similarities between water vapor and VOC diffusion in porous media by a dual chamber method, *Clean*, **37**, 444-453.

Xu, Y. and Little, J.C. (2006) Predicting emissions of SVOCs from polymeric materials and their interaction with airborne particles, *Environmental Science and Technology*, **40**, 456-461.

Xu, Y. and Zhang, Y. (2003) An improved mass transfer based model for analyzing VOC emissions from building materials, *Atmospheric Environment*, **37**, 2497-2505.

Xu, Y. and Zhang, Y. (2004) A general model for analyzing single surface VOC emission characteristics from building materials and its application, *Atmospheric Environment*, **38**, 113-119.

Yan, W., Zhang, Y. and Wang, X. (2009) Simulation of VOC emissions from building materials by using the state-space method, *Building and Environment*, **44**, 471-478.

Yang, X., Chen, Q., Zeng, J., Zhang, J.S. and Shaw, C.Y. (2001c) A mass transfer model for simulating volatile organic compound emissions from "wet" coating materials applied to absorptive substrates, *International Journal of Heat and Mass Transfer*, **44**, 1803-1815.

Yang, X., Chen, Q., Zeng, J., Zhang, J.S. and Shaw, C.Y. (2001d) Effects of environmental and test conditions on VOC emissions from "wet" coating materials, *Indoor Air*, **11**, 270-278.

Yang, X., Chen, Q., Zhang, J.S., An, Y., Zeng, J. and Shaw, C.Y. (2001b) A mass transfer model for simulating VOC sorption on building materials, *Atmospheric Environment*, **35**, 1291-1299.

Yang, X., Chen, Q., Zhang, J.S., Magee, R., Zeng, J. and Shaw, C.Y. (2001a) Numerical simulation of VOC emissions from dry materials, *Building and Environment*, **36**, 1099-1107.

Yao, Y., Xiong, J., Liu, W., Mo, J. and Zhang, Y. (2011) Determination of the equivalent emission parameters of wood-based furniture by applying C-history method, *Atmospheric Environment*, **45**, 5602-5611.

Yuan, H., Little, J.C. and Hodgson, A.T. (2007b) Transport of polar and non-polar volatile compounds in polystyrene foam and oriented strand board, *Atmospheric Environment*, **41**, 3241-3250.

Yuan, H., Little, J.C., Marand, E. and Liu, Z. (2007a) Using fugacity to predict volatile emissions from layered materials with a clay/polymer diffusion barrier, *Atmospheric Environment*, **41**, 9300-9308.

Zhang, L. and Niu, J. (2003) Mass transfer of volatile organic compounds from painting material in a standard field and laboratory emission cell, *International Journal of Heat and Mass Transfer*, **46**, 2415-2423.

Zhang, L. and Niu, J. (2004) Modeling VOCs emissions in a room with a single-zone multi-component multi-layer technique, *Building and Environment*, **39**, 523-531.

Zhang, X., Diamond, M.L., Ibarra, C. and Harrad, S. (2009) Multimedia modeling of polybrominated diphenyl ether emissions and fate indoors, *Environmental Science and Technology*, **43**, 2845-2850.

Zhang Y., Luo, X., Wang, X., Qian, K. and Zhao, R. (2007) Influence of temperature on formaldehyde emission parameters of dry building materials, *Atmospheric Environment*, **41**, 3203-3216.

Zhang, Y. and Xu, Y. (2003) Characteristics and correlations of VOC emissions from building materials, *International Journal of Heat and Mass Transfer*, **46**, 4877-4883.

Zhao, D., Little, J.C. and Cox, S.S. (2004) Characterizing polyurethane foam as a sink for or source of volatile organic compounds in indoor air, *Journal of Environmental Engineering*, **130**, 983-989.

Zhao, D., Little, J.C. and Hodgson, A.T. (2002) Modeling the reversible, diffusive sink effect in response to transient contaminant sources, *Indoor Air*, **12**, 184-190.

Chapter 3 – Diffusion-controlled Reference Material for VOC Emissions Testing

Zhe Liu[1], Cynthia Howard-Reed[2], Steven S. Cox[1] and John C. Little[1]

[1]Department of Civil and Environmental Engineering, Virginia Tech, Blacksburg, VA 24061
[2]National Institute of Standards and Technology, Gaithersburg, MD 20899

3.1 Abstract

There is growing awareness of the need to reduce emissions of volatile organic compounds (VOCs) from building materials and interior products. To comply with regulatory requirements and to meet consumer demand for low VOC-emitting materials and furnishings, manufacturers usually submit their products to independent laboratories for emissions testing. However the same product tested by different laboratories often results in very different emissions profiles due to unidentified errors and uncertainties within testing procedures. There is thus a need for a standard reference VOC source that will have known VOC emission profiles when tested by different laboratories. Virginia Tech (VT) and the National Institute of Standards and Technology (NIST) have created a program to develop reference materials for VOC emissions testing. The prototype reference material consists of a thin polymethylpentene (PMP) film that has been loaded to equilibrium with a representative VOC. Its emissions under various chamber testing configurations can be accurately predicted by a mechanistic model. The model predicted emission profiles can therefore be used as reference values to validate individual laboratories' testing results and calibrate testing procedures. The feasibility of the reference material has been extensively evaluated and its capability in assessing emissions testing performance has been demonstrated in a series of inter-laboratory studies. Such reference materials have the potential to build consensus and confidence in emissions testing as well as to "level the playing field" for VOC emissions testing laboratories and product manufacturers.

3.2 Introduction

Indoor air pollution has been recognized as one of the primary environmental health risks in the world, considering people typically spend over 80% of their time indoors (Adgate et al., 2004; Klepeis et al., 2001; Leech et al., 2002). Volatile organic compounds (VOCs) constitute an

important class of indoor air pollutants (Weschler et al., 2009) and indoor VOC concentrations generally far exceed outdoor levels due to the presence of strong indoor sources (Jia et al., 2008; Missia et al., 2010; Ohura et al., 2006). Exposure to VOCs can cause acute health effects such as eye and respiratory irritations, headaches, fatigue and asthmatic symptoms (Mølhave, 1989; Wolkoff, 2001) to chronic illnesses such as cancers (Boeglin et al., 2006; Rennix et al., 2005; Sax et al., 2006). Indoor sources of VOCs include a vast array of building materials and furnishings, such as wood products, sealants, carpets, adhesive, styrene-butadiene rubber and vinyl flooring (Bluyssen et al., 1996; Missia et al., 2010).

To reduce indoor exposure to toxic VOCs, low emitting products are increasingly in demand. These products are usually tested in emission chambers by independent laboratories. However, very different emission profiles are often obtained for the same product tested in different laboratories, with coefficients of variation between measured emission rates on the order of 50% and as large as 300% (De Bortoli et al., 1999; Howard-Reed and Nabinger, 2006; Wilke et al., 2009). The large uncertainties in emissions testing results are due to errors and variations in every aspect of the entire testing procedure, including specimen preparation, chamber operation, sampling strategy, and analytical technique. For example, the World Calibration Centre for Volatile Organic Compounds (WCC-VOC) coordinated a comprehensive inter-comparison exercise involving nine laboratories to examine their analytical procedures (Rappenglück et al., 2006). A synthetic standard mixture of 73 VOCs in nitrogen gas was provided to each participant, but only 18 VOCs were accurately determined by at least 50% of all the laboratories. Although inter-laboratory emission studies using the same materials as the emission source could help strengthen reliability and establish equivalence among emissions testing laboratories, they are very costly and may lead to inconclusive results because they cannot identify the true emission value for comparison. Therefore, several approaches have been proposed to provide standard sources for individual laboratories to evaluate and calibrate the chamber systems. Both gas mixtures injected from cylinders and permeation tubes releasing VOCs at constant rates can serve as standard sources in chambers. However, the chamber concentration measurements are not affected by all chamber parameters such as temperature, humidity and air velocity, or by the procedures associated with preparing and loading specimens into the chamber. A convenient approach has been specified in ASTM Standard D6670-01 (ASTM, 2001), which uses a Petri

dish containing a pure liquid VOC as a standard source with the emission rate determined by weighing the change in mass. However, emissions from pure VOC liquids and those from solid materials are governed by distinct mass-transfer mechanisms and follow very different patterns. Recently, a new standard source call LIFE (liquid-inner tube diffusion-film emission) was developed (Wei et al., 2012). It is comprised of a small Teflon cylinder containing a pure liquid VOC and a permeable membrane covering the opening of the cylinder, through which the VOC diffuses into the chamber at a constant rate. Although its emission rate is dependent on chamber temperature and humidity, the LIFE works more like an improved permeation tube and is still different in nature to real building materials and furnishings.

Concerning the urgent demand for a standard source and the limitations of available approaches, Virginia Tech (VT) and the National Institute of Standards and Technology (NIST) have initiated a multi-phase project to develop a reference material for VOC emissions testing which can mimic real building materials and has a known emission rate. Briefly, a polymer film was selected as the substrate that can be loaded with a representative VOC through a diffusion process. The loaded film has an emission profile similar to a typical "dry" material (e.g., flooring or wood panels) that can be measured in small emissions testing chambers. A unique advantage of this emission source is that its emission profiles can be predicted accurately by a fundamental mass transfer model. The predicted emission profile therefore serves as a reference value for validating the measured results of different laboratories, evaluating the test performance, and helping to identify the root causes of variability.

This paper presents a comprehensive review of the approaches and results in the three phases of the project. In Phase I, a prototype reference material was created by infusing toluene into a thin polymeric film and proof-of-concept emission tests using the toluene reference material were performed to validate the ability of a mechanistic model in predicting its true emissions (Cox et al., 2010; Liu et al., 2011). The shelf-life property of the toluene reference material was also investigated (Howard-Reed et al., 2011a). In Phase II, three inter-laboratory studies (ILSs) were conducted using the toluene reference material to assess its performance in practical applications. The first inter-laboratory study (ILS 1) was a pilot study involving four laboratories in North America (Howard-Reed et al., 2011b). The second one (ILS 2) involved two laboratories in the

US and Germany and was a pilot international inter-laboratory study (Howard-Reed et al., 2011c). Finally, a full international inter-laboratory study (ILS 3) was carried out among fourteen laboratories from seven countries. In Phase III, the method for creating the toluene reference material was expanded to other VOCs, such as n-butanol. Via extensive emission chamber tests and inter-laboratory studies, the feasibility and capability of using the reference material to assess emissions testing performance has been well demonstrated. Such reference materials have the potential to build consensus and confidence in emissions testing as well as to "level the playing field" for VOC emissions testing laboratories and product manufacturers.

3.3 Research methods

3.3.1 Creating reference materials

An ideal reference material should emit VOCs at a predictable rate and in quantities comparable to those generated by typical building materials. Critical material properties include purity, stability, and mass-transfer properties such as diffusion coefficient and partition coefficient. Considering all these factors, a commercially available pure polymer, polymethylpentene (PMP), was selected as the substrate. According to a microbalance test measuring the mass change of a PMP film in the presence of dry clean air, its mass stabilized after a few hours, suggesting that the material does not contain significant amount of volatile additives or contaminants (Cox et al., 2010).

Toluene was chosen as the first representative VOC for the reference material. To load the PMP films with a specific amount of toluene, a gas calibrator (Dynacalibrator 190, VICI Metronics Inc., Santa Clara, CA) with a mass flow controller (FC-280S, Tylan General, Carson, CA) was used to generate a continuous dry air stream with a constant toluene concentration. As shown in Figure 3.1(a), the toluene-laden dry air was passed through one or several stainless steel vessels connected in series, each containing several PMP films (6 cm×6 cm×0.0254 cm) on aluminum screen fixtures. The outlet air stream from the last vessel was further passed across an extra film, whose mass was monitored by a high-resolution (0.1 μg) dynamic microbalance (Thermo Cahn D-200, Thermo Fisher Scientific, Waltham, MA) throughout the loading process. During the loading process (about 10 days), airborne toluene diffused into the films until sorption equilibrium was reached between the material-phase and gas-phase. Because the film on the

microbalance was undergoing the same mass transfer process as the others in the loading vessels, its mass change data recorded by the microbalance, as shown in Figure 3.1(b), could be used to monitor the loading process and to determine when sorption equilibrium was reached. The material-phase concentration of toluene in the loaded films (C_0) can be also derived from the microbalance data by dividing the total mass gain of the microbalance-monitored film by its volume.

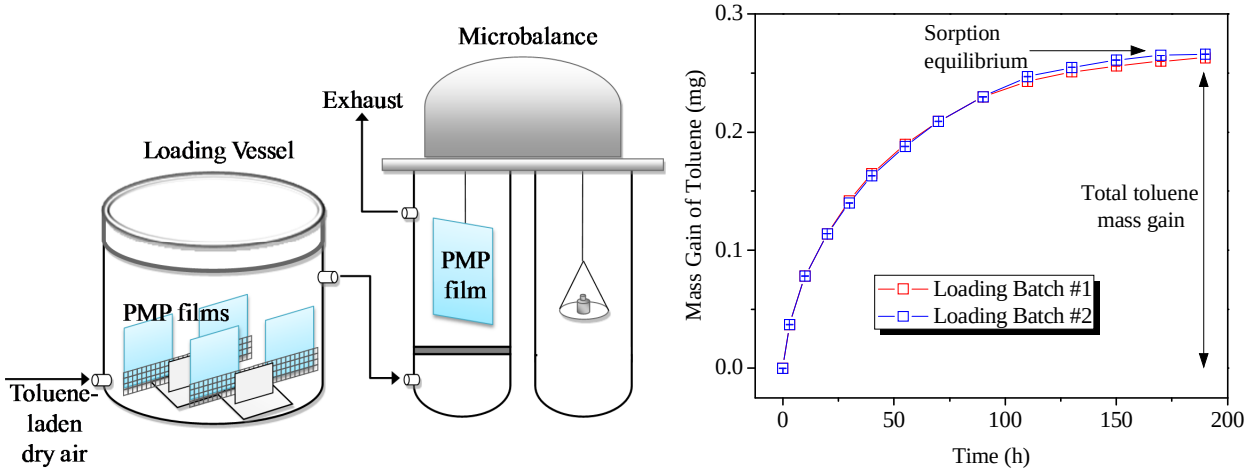

(a) (b)

Figure 3.1 Loading process to produce reference materials: (a) schematic diagram of the loading system; (b) toluene mass gain recorded by the microbalance during two loadings.

3.3.2 Distributing reference materials for emissions testing

When the microbalance data indicated that sorption equilibrium had been reached, the loading process was considered complete. The films were removed from the loading vessels one at a time for packaging to minimize exposure to ambient air. The packaging procedure included wrapping each film in heavy-duty aluminum foil, placing it in a small sealable plastic bag, and carefully evacuating air at each step. The bags were then coded, placed in coolers containing dry ice, and sent by express delivery to emissions testing laboratories. After arriving at the laboratories, the reference materials were retained in the original packages and stored in freezers at -20 ^{o}C until being tested in chambers.

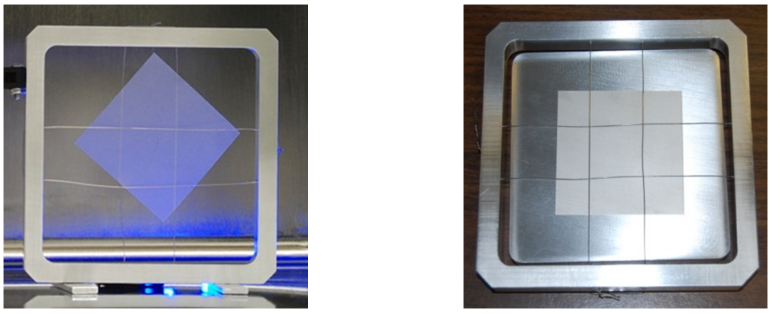

(a) (b)

Figure 3.2 Film holders for securing films in chambers: (a) a vertical film holder that exposes both sides of the film to chamber air; (b) a horizontal film holder that allows only one side of the film to be exposed to chamber air.

The emissions testing laboratories, including NIST and others that participated in the three ILSs, generally measured the emission profile of each film in small chambers following ASTM Standard D5116-2010 (ASTM, 2010). Testing protocols have been discussed in detail elsewhere (Cox et al., 2010; Howard-Reed et al., 2011b) and are recapitulated here. Before being tested, each film was removed from the freezer and maintained in the package at room temperature for 5 minutes, restoring it to ambient temperature. Then it was taken out of the package and placed in the emissions testing chamber using a specified film holder. In this project, two specially-designed holders were employed. Figure 3.2(a) shows the vertical film holder which can expose both sides of the film to chamber air. The horizontal one in Figure 3.2(b) aimed to press the film flat against the bottom platform so that expose only the upper surface to chamber air. During the emission tests, the chamber volume and air flow rate may vary among different laboratories but the testing temperature was fixed at 23 ºC. Chamber air samples were collected on sorbent tubes at time intervals practicable for individual laboratories and were quantified by the thermal desorption and gas chromatography/mass spectrometry (TD-GC/MS) method.

3.3.3 Predicting emission profiles using a mechanistic model

The emissions of toluene from the reference material under various chamber configurations can be predicted using a mechanistic mass-transfer model (Cox et al., 2010; Liu et al., 2011). The principles of the model and the method used to obtain the model parameters are briefly summarized here. The emission of a VOC from a homogeneous dry material to a well-mixed

chamber occurs through three steps: internal diffusion within the material which is characterized by diffusion coefficient (D), partition between the material and the air at their interface which is characterized by partition coefficient (K), and external convective mass transfer near the material surface, which can be neglected for our diffusion-controlled reference materials (Cox et al., 2010). When surface area (A), thickness of the material (L), chamber volume (V) and chamber air flow rate (Q) are known, assuming a uniform initial VOC concentration in the material (C_0), the chamber air concentration (y) can be predicted as a function of time.

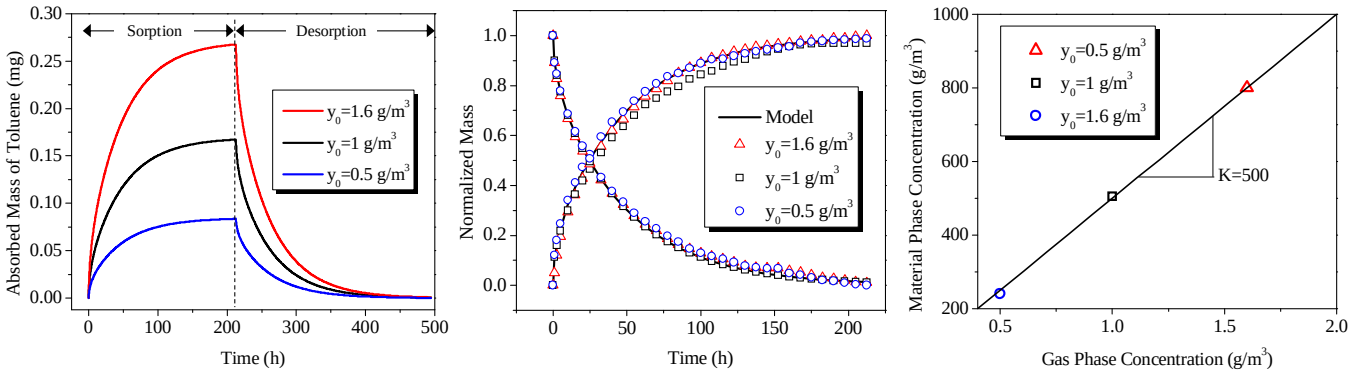

(a) (b) (c)

Figure 3.3 (a) Microbalance sorption/desorption test results under three gas-phase concentrations (y_0); (b) fitting a Fickian diffusion model to the sorption and desorption data to get D; (c) determining K by linear regression.

The model parameters include D, K, C_0 and other directly measurable parameters (A, L, V, and Q). C_0 depends on the loading and should be determined from the total mass gain of the film monitored by the microbalance during the corresponding loading process. D and K were determined by independent microbalance sorption/desorption tests at 23 ºC. During the sorption test, dry air with a constant toluene concentration (y_0) was passed across a clean PMP sample on the microbalance until partition equilibrium was reached and the transient mass gain of the sample was recorded, generating a sorption curve. After partition equilibrium was reached, clean air was then passed across the film for the desorption test, with a desorption curve generated from the mass loss data (Cox et al., 2001a; Cox et al., 2010). The microbalance sorption/desorption tests were performed under three different gas concentrations and the resulting sorption and desorption curves are displayed in Figure 3.3(a). As shown in Figure

3.3(b), D can be determined by fitting a Fickian diffusion model to the normalized sorption and desorption data (Cox et al., 2001a). D of toluene in PMP was found to be $(3.6\pm0.7)\times10^{-14}$ m^2/s at 23 ^oC and was independent of concentration. Also from the sorption curve, the material-phase concentration in equilibrium with the corresponding gas-phase concentration can be obtained with K found to be 500±30 from the linear correlation between the material-phase and gas-phase concentrations in equilibrium, as shown in Figure 3.3(c) (Cox et al., 2001a).

3.3.4 Measuring toluene concentration in the reference materials

While C_0 can be determined from the microbalance data during each loading process, independent measurement of the toluene concentration in the loaded films using a direct thermal desorption method (Cox et al., 2001b) was also performed to assess the toluene loss during the storage period, which would reduce the shelf-life of the reference material. To measure the material-phase toluene concentration in a loaded film, 3-mm diameter disks were obtained from the film using a rubber stopper hole punch as soon as it was removed from the freezer and each disk was immediately transferred to a small borosilicate glass tube. Then the glass tube was placed in a sleeve heater, heated to 150 ºC for 20 min and then cooled to 50 ºC. Meanwhile, a helium gas flow of 50 mL/min was passed through the glass tube and the outlet stream was pumped through a sorbent tube to collect toluene desorbed from the disk. To ensure toluene in the disk was completely desorbed during this process, it was repeated with another sorbent tube. Finally, sorbent tubes were analyzed by TD-GC/MS with the material-phase concentration calculated by dividing the total recovered toluene mass by the volume of the disk.

3.4 Results

3.4.1 Phase I – Developing the prototype toluene reference material

Proof of concept tests

Figure 3.4 shows the concentration development profiles of two identical tests conducted by NIST in a 0.051 m^3 chamber with a flow rate of 0.065 m^3/h, except that one was performed with the chamber fan off and the other with the fan on (Howard-Reed et al., 2011b). Both sides of the reference material were exposed to the chamber air by using the vertical film holder as shown in Figure 3.2(a). The black line is the model prediction using mean values of D, K and C_0. The shaded band indicates uncertainties of the model predicted concentrations associated with

uncertainties of D, K and C_0, which were estimated by a Monte Carlo analysis (Cox et al., 2010). As shown in the figure, the two tests generated very similar emission profiles, implying that the chamber air was well mixed in both cases. The model prediction with independently measured parameters matches the chamber test results very well, validating the model for predicting the true emission profiles and providing proof-of-concept for the reference material.

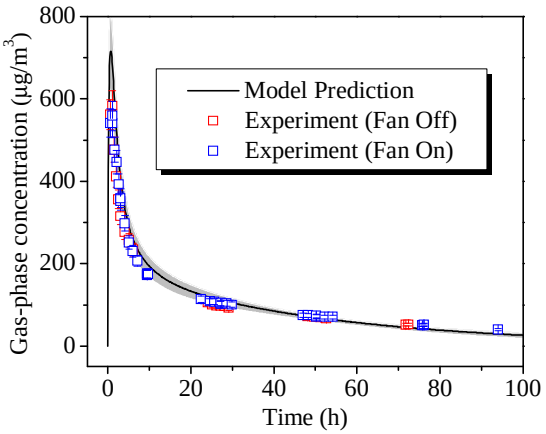

Figure 3.4 Comparisons between model predicted and measured emission profiles for NIST's chamber tests.

Shelf-life tests

As discussed previously, the reference materials were wrapped in aluminum foil and then sent to different laboratories with dry ice. Using dry ice in shipment and storing films at sub-zero temperatures aims to reduce or even eliminate volatile loss of toluene from the films by minimizing the volatility of toluene, or more specifically, diminishing D while increasing K. To explore the effectiveness of these practices, several films produced in a single batch were divided into two groups: films in one group were sent to an analytical laboratory and stored at -20 ºC following the regular procedure elaborated above; while the films in the other group were also wrapped in aluminum foil but sent and stored at ambient temperature. Then the material-phase concentration of toluene in the films in each group was measured using direct thermal desorption over a period of time, with results plotted in Figure 3.5(a). It is shown that shipping and storing at ambient temperature lead to substantial loss of toluene while shipping with dry ice and storing at sub-zero temperatures effectively reduced volatile loss during shipping and storage period although in the long run, some toluene still escaped from the films.

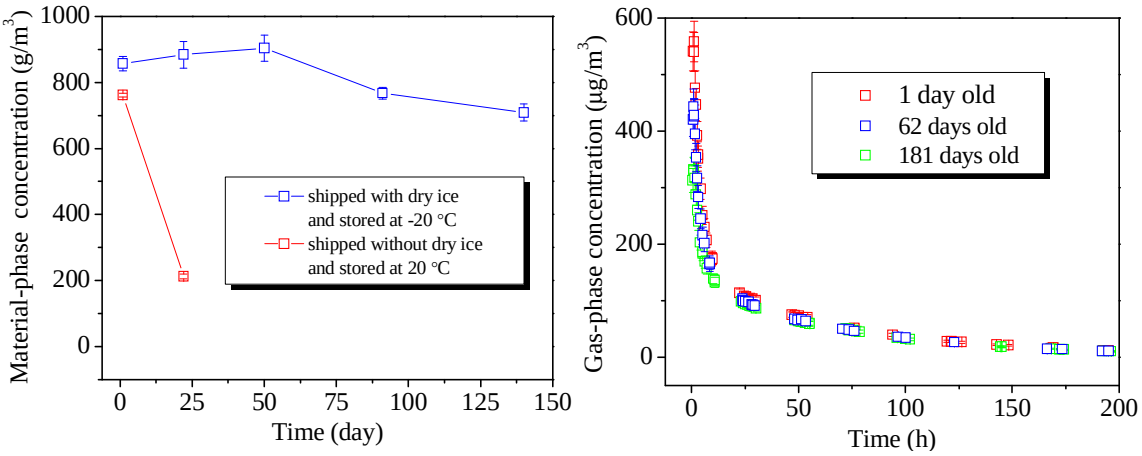

(a) (b)

Figure 3.5 Shelf-life effect of the toluene reference material: (a) change of material-phase toluene concentration in films; (b) emission profiles of reference materials with different shelf-life.

To further examine the shelf-life effect on emissions testing results, eight films (6 cm×6 cm×0.0254 cm) were produced in a single batch and sent to NIST in the regular way. These films were stored at -20 ºC for different time spans and then tested in emission chambers at 23 ºC, with both sides exposed and chamber fan on. Figure 3.5(b) shows the measured emission profiles of the 1-day-old (the freshest one), 62-day-old and 181-day-old (the oldest one) reference materials as examples. Either from these three films' results alone or from all the eight films' data (Howard-Reed et al., 2011a), it can be found that the toluene concentration in the first 24 h of the chamber test decreased with sample age but this effect diminished as testing time increased. The reason is that some toluene at/near the film surface would escape during the storage period, which however only affects the early-period emission instead of the long-term emission. Furthermore, total toluene mass in the eight films can be estimated from the chamber concentration and the chamber flow rate, assuming material-phase toluene was completely depleted at the end of the emission tests. For example, the total mass in the 1-day-old, 62-day-old and 181-day-old films were calculated to be about 790, 720 and 640 µg, respectively. The implied mass loss is very consistent with the data shown in Figure 3.5(a) even though they were in fact studying films from two completely separate batches: Figure 3.5(a) indicates the toluene mass in a 6 cm×6 cm×0.0254 cm film dropped from 780 µg on the 1st day to 700 µg on the 90th

day and to 650 µg on the 140th day. Overall, these shelf-life tests demonstrate that shipping and storing the toluene reference materials at sub-zero temperatures effectively reduces volatile loss to an acceptable level but a small amount of toluene loss still occurs during a long-term storage period. Therefore, it is critical to minimize the storage time to examine emissions during the early stage while the shelf-life effect is low if long-term emissions (>24 h) are of primary concern.

3.4.2 Phase II – Inter-laboratory studies

ILS 1

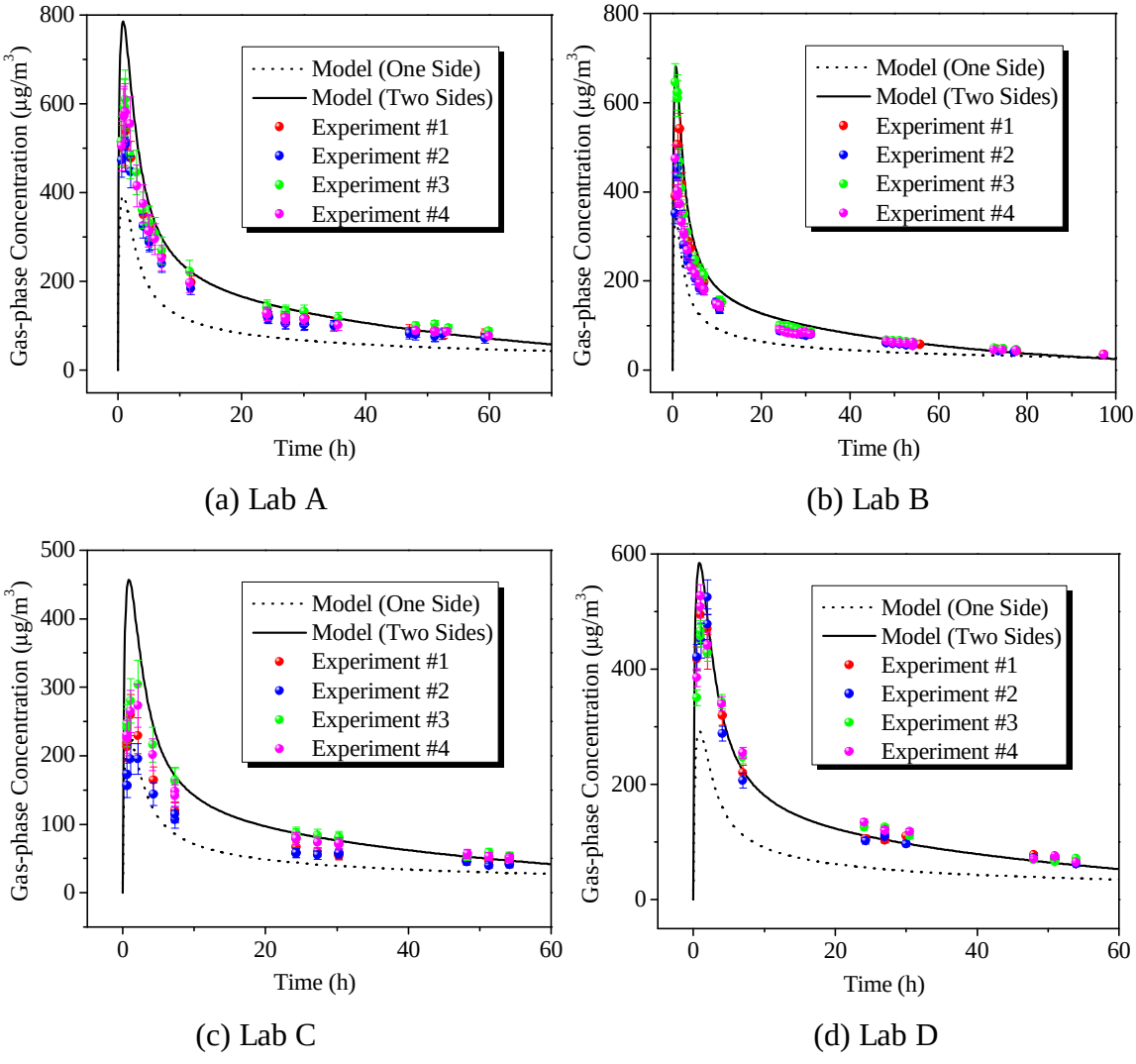

Figure 3.6 Comparison of model predicted and measured emission profiles in ILS 1.

Four laboratories in North America participated in the pilot ILS (ILS 1) and each of them received four identical reference material samples (6 cm×6 cm×0.0254 cm). In ILS 1, the horizontal film holder shown in Figure 3.2(b) was used to secure reference material films in the emission chambers, with toluene expected to emit from the upper side of the material only (Howard-Reed et al., 2011b).

Figure 3.6 shows the measured emission profiles of four replicates tested by each laboratory. As shown in the figure, the emission model assuming that one side of the material was exposed substantially underestimates the measured results for all the laboratories, while the model considering both sides as emission surfaces overestimates the results for lab A, B, and C but predicts the observed emission profiles in lab D quite well. It was thus hypothesized that toluene escaped from the bottom surface of the film in contact with the platform so that the real emission profiles fell between the ideal one-sided and two-sided cases. It was later confirmed by the laboratories that the samples were not held perfectly flat on the platform and that some air gaps existed beneath the samples, thus highlighting the value of the predictive model. The fact that the source was standardized and well-characterized by the mechanistic model greatly facilitated the identification and resolution of the problem.

ILS 2

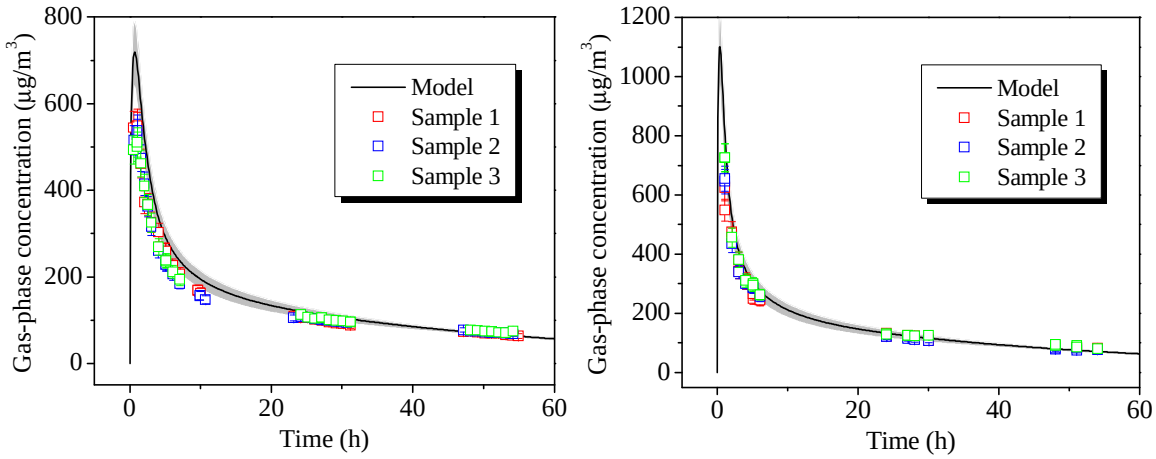

Figure 3.7 Comparison of model predicted and measured emission profiles in ILS 2.

Due to the horizontal film holder's problem revealed in ILS 1, the vertical type in Figure 3.2(a) was employed in all the later chamber studies. To further validate the reference material using the vertical film holder and explore several practical issues associated with coordination and logistics, a pilot international ILS (ILS 2) was performed prior to the full international ILS (ILS 3). In ILS 2, six identical reference material samples (6 cm×6 cm×0.0254 cm) were produced in a single batch and NIST and BAM (BAM Federal Institute for Materials Research and Testing, Germany) each received three, with emissions testing results presented in Figure 3.7 (Howard-Reed et al., 2011c). In general, there was very good agreement between the emission profiles measured in triplicate in both laboratories, and the measured emission profiles agree well with model predictions, with deviations of less than 10%. It should be noted that the two laboratories employed very different chamber configurations (V and Q) in their tests, resulting in different chamber concentrations. Although it is hard to directly compare their chamber concentration measurements when very different chamber configurations were used, the model predictions can still be used as reference values to validate individual laboratories' data and as two of the top emissions testing laboratories in the world, both NIST and BAM demonstrated satisfactory performance in this ILS.

ILS 3

Based on the knowledge from ILS 1 and ILS 2, the full international ILS (ILS 3) was designated to expand the number of participants to 14 laboratories from 7 countries: Canada, China, Demark, Finland, France, Germany, and the United States. The objectives of ILS 3 were to: (1) diversify and increase the number of participants to provide greater scrutiny of the emissions testing procedure and ensure its clarity and correctness; (2) evaluate the performance of the reference material and the model to predict the emission profiles in a wider range of test facilities and environments; and (3) work toward establishing global harmonization of emissions testing validation methods.

Because the chamber size varied substantially among the 14 laboratories, from 0.024 m^3 to 1 m^3, they were categorized into two groups: the small chamber group consisting of 10 laboratories (Lab A to J) with the chamber size ranging from 0.024 m^3 to 0.12 m^3, and the large chamber group consisting of 4 laboratories (Lab K to N) with the chamber size ranging from 0.225 m^3 to

1 m^3. Each laboratory was asked to run two tests using the same chamber. One film was supplied for each test carried out by laboratories in the small chamber group while two films were supplied for each test by laboratories in the large chamber group to increase chamber concentrations. All the reference material samples (6 cm×6 cm×0.0254 cm) were produced simultaneously in a 36 L loading vessel and C_0 was determined to be 820±20 g/m^3. The films were sent to the laboratories in the regular way together with vertical film holders. The testing protocols were the same as in previous studies. All the tests were required to be performed at 23 ºC and the chamber flow rate was specified as 0.055 m^3/h for the small chamber group and 0.3 m^3/h for the large chamber group, although there were small deviations in temperature and flow rate during the actual tests. Use of a mixing fan during the test was not specified and participants simply followed their routine procedure. All the laboratories were asked to collect duplicate chamber air samples at 24 h, 48 h, and 72 h in each test but a few of them collected air samples at additional time points. Finally, all the tests were run within 45 days of the reference material manufacture with most laboratories running both tests within 14 days of manufacture. Therefore, the shelf-life effect was negligible.

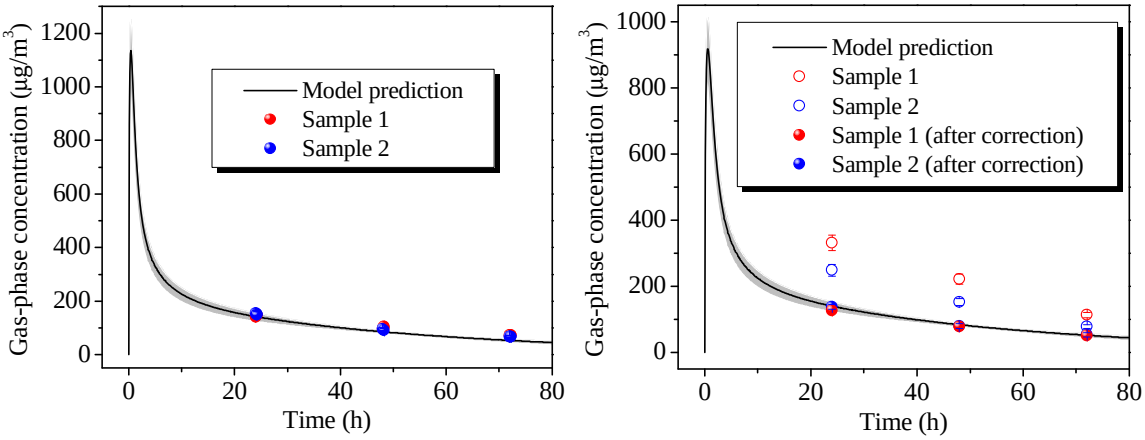

(a) Lab A (b) Lab C

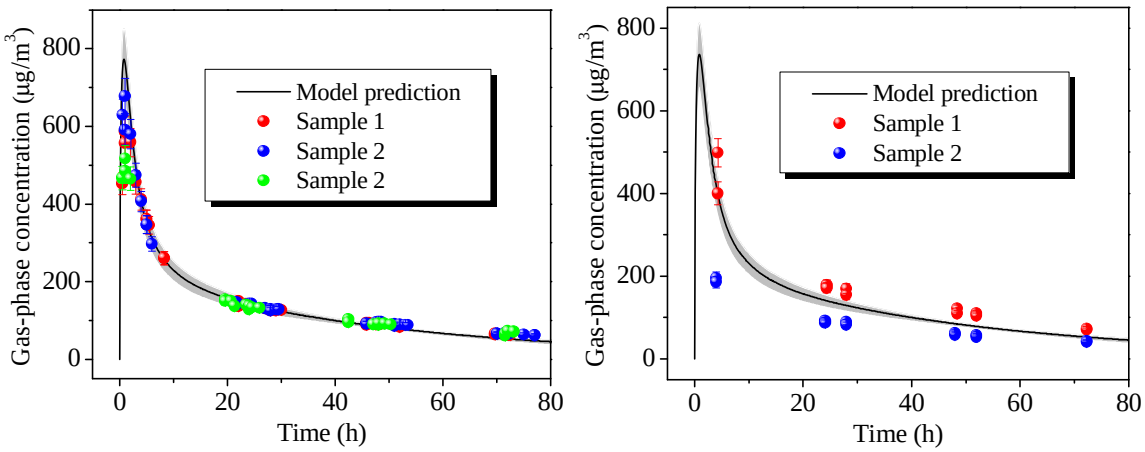

(c) Lab F (d) Lab J

Figure 3.8 Comparison of model predicted and measured emission profiles in ILS 3 (the small chamber group).

The ten laboratories in the small chamber group were successful at running two chamber tests. Figure 3.8 shows the testing results of four laboratories and their comparisons with model predictions as examples. Lab F was NIST, which tested three films for confirmation purposes. Lab A and F obtained very close concentration measurements for the films they tested. In fact, considering concentration measurements at 24 h, 48 h, and 72 h, most laboratories in the small chamber group had variations between the two runs of less than 10%. Lab A and F met all the ILS specifications and their measured chamber concentrations match the model predicted reference values reasonably well. In Figure 3.8(b), empty circles indicate original data reported for the two runs of Lab C. Although Lab C followed the ILS instruction well in sample preparation and chamber operation, a large discrepancy was found between the two runs and the measured concentrations were much higher than the model predictions. An analytical problem was discovered after the completion of the ILS that affected the results. Figure 3.8(b) also shows the chamber concentrations with an analytical correction (filled circles), which are very consistent with the model predictions. The data of Lab J shown in Figure 3.8(d) also illustrate a large discrepancy in the results for the two successive runs. In fact, Lab J mistakenly stored the reference material samples in a laboratory refrigerator rather than a freezer and therefore encountered much greater loss of toluene in the second sample, which resulted in the substantial decrease of the chamber concentrations in the second run. This emphasizes the necessity to ship and store the reference materials at sub-zero temperatures.

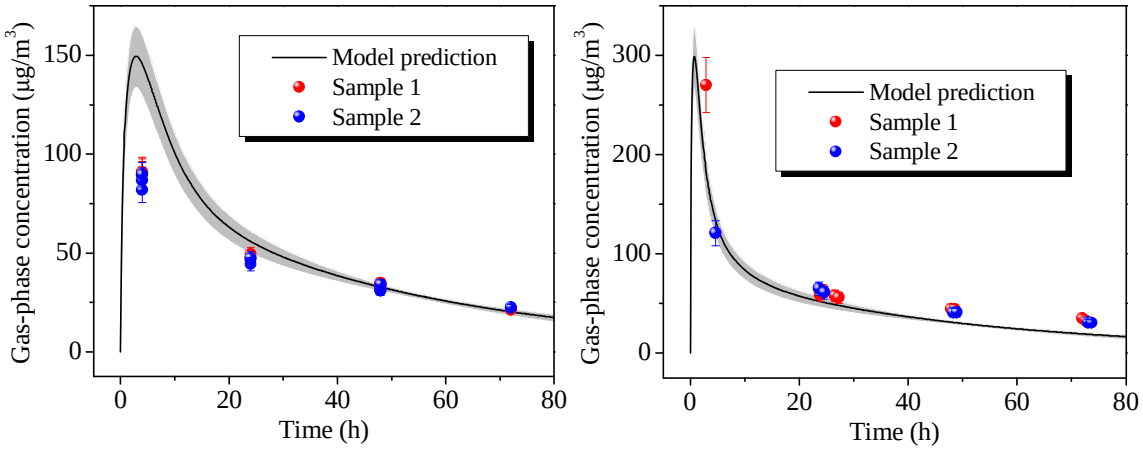

(a) Lab K (b) Lab L

Figure 3.9 Comparison of model predicted and measured emission profiles in ILS 3 (the large chamber group).

All laboratories in the large chamber group were able to successfully run both tests and two reference material samples were used in each test. Figure 3.9 shows the measured and model predicted emission profiles of two laboratories in the large chamber group. Both Lab K and L had very similar results between the two tests, with a variation of less than 10%. Due to a several-day delay in Customs transit, dry ice in the package was depleted when received by Lab K, which may explain the discrepancy between the observed chamber concentrations and the model predictions. The measured emission profiles for Lab L agree with the model prediction reasonably well, demonstrating that the reference material should work not only with small chambers, but also with large chambers.

3.4.3 Phase III – Extending reference material concept to n-butanol in PMP

In Phase III, the reference material approach was extended to n-butanol, a polar and somewhat more difficult VOC to handle experimentally than toluene. Figure 3.10(a) shows sorption and subsequent desorption profiles for n-butanol in PMP at three different gas-phase concentrations. The same as toluene in PMP, the profiles were highly symmetrical and completely reversible. Figure 3.10(b) shows that the diffusion coefficient values obtained from the six normalized data sets for n-butanol in PMP (three sorption and three desorption cycles) were all essentially the same, proving again that D is independent of concentration, as required by the model. Figure

3.10(c) shows the equilibrium concentration of n-butanol in PMP as a function of the imposed gas-phase concentration and again confirms a linear relationship. Although the validity of the approach remains to be proven by comparing model predictions to measured emissions of n-butanol in emissions testing chambers, the initial results suggest that it is feasible to create reference materials for other VOCs, such as n-butanol.

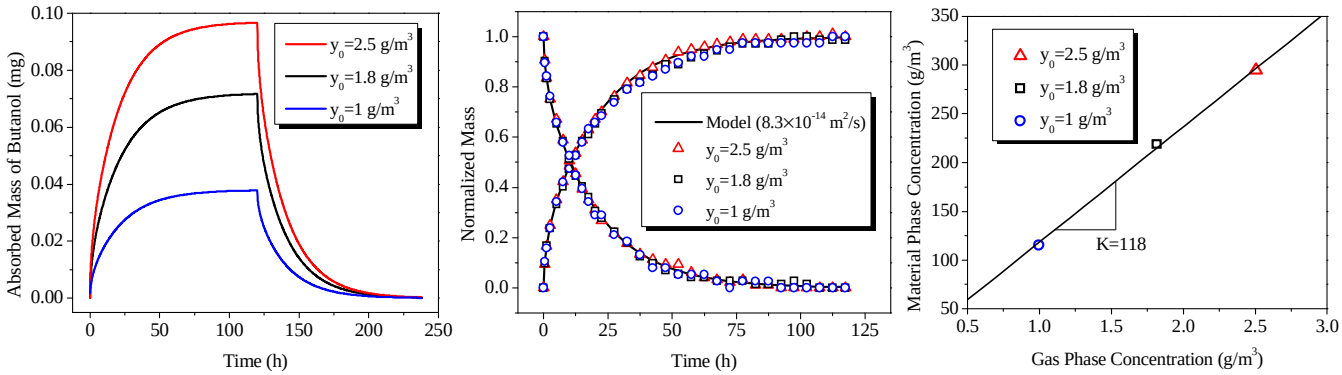

(a) (b) (c)

Figure 3.10 (a) Microbalance results showing transient mass gain/loss during sorption/desorption cycles of butanol in PMP; (b) fitting a Fickian diffusion model to the sorption and desorption data to get D; (c) determining K by linear regression.

3.5 Discussion and conclusions

The proof-of-concept tests and inter-laboratory studies have demonstrated that the toluene reference material mimics a real building material and can be used as a reference emission source to evaluate emissions testing performance in different laboratories. Because the production of the reference material is very well controlled and its emission profiles under various chamber settings can be predicted accurately using a mass-transfer model, the reference material not only provides a standard emission source for inter-laboratory studies, but also allows individual laboratories to independently check their emission chamber measurements and diagnose problems in testing procedures without the need for an organized inter-laboratory study. Furthermore, as validated by the proof-of-concept tests, reliable values of D, K and C_0 can also be obtained for the reference material. Therefore, in addition to validating VOC emissions testing, the reference material can also be used to validate techniques for measuring the mass-

transfer parameters themselves (such as D, K and C_0), which are general requirements in emissions modeling and also substantial challenges in material emission research.

However, it has also been learned that further investigation and refinement of the prototype toluene reference material is needed. For example, all the emission tests prior to ILS 3 were in small-scale chambers with the chamber volume less than 0.086 m^3 and only four laboratories with fairly large chambers (0.225 m^3 to 1 m^3) participated in ILS 3. Therefore, the performance of the reference material in large chambers is still unclear. In fact, large or full-scale chambers with volume larger than 1 m^3 are often used by emissions testing laboratories, especially for determining emissions from wood products (ASTM, 2001; BSI, 2004; ISO, 2007). The impact of temperature and humidity on the performance of the reference material is also not yet well understood. The dependence of D and K on temperature and humidity will be studied and the emission model will be validated at different temperature and humidity levels by further proof-of-concept emission tests in our future research. This will allow the application of the reference material under different environmental conditions and provide a theoretical basis for assessing uncertainties of emissions testing results stemming from variations in temperature and humidity. Moreover, the current approach using dry ice for shipping requires considerable effort, slows processing of the shipment, and makes the films brittle and vulnerable. It is also of concern that very low temperature during shipment and storage may cause permanent changes to the polymer's property, leading to additional variability. Therefore, an improved shipping and storage approach may be needed to facilitate the distribution and preservation of the reference material in large quantities.

Finally, as shown by the preliminary data for n-butanol, the reference material concept should be applicable to other VOCs. The key criteria for developing reference materials for other VOCs include: (1) the compound should have sufficient solubility in the substrate (K) so that enough mass can be loaded into the film; (2) mass transfer of the compound in the substrate should be dominated by Fickian diffusion so that the emission model is applicable in predicting its emissions; and (3) values of D and K should be in appropriate ranges and L and A should be optimized so that the VOC emissions of reference materials in chambers can meet the requirements in source strength and duration. Therefore, for different VOCs, different polymer

substrates and different L and/or A may be needed to meet specific emission requirements. Fortunately, the emission model can be of great help in this process by providing emission predictions in response to different model parameters and estimating parameters needed for achieving specific target emission profiles.

3.6 Acknowledgements

Financial support for the contributions of the authors from Virginia Tech was provided by the National Institute of Standards and Testing (NIST) (Award Number: 60NANB6D6156 and 60NANB9D9154). We thank Al Hodgson at Berkeley Analytical Associates for kind help in measuring toluene concentrations in the reference materials. We also thank other colleagues at Air Quality Sciences (US), BAM Federal Institute for Materials Research and Testing (Germany), Bayer Material Science (US), Berkeley Analytical Associates (US), California Department of Public Health (US), Centre Scientifique et Technique du Bâtiment (CSTB) (France), Danish Technological Institute (Denmark), Eurofins (Denmark), National Research Council (Canada), Tsinghua University (China), US Environmental Protection Agency (US), VTT Technical Research Centre of Finland (Finland), and Fraunhofer Wilhelm-Klauditz-Institut (WKI) (Germany) for participating in the inter-laboratory studies and providing valuable feedbacks on the prototype reference material.

3.7 References

Adgate, J.L., Church, T.R., Ryan, A.D., Ramachandran, G., Fredrickson, A.L., Stock, T.H., Morandi, M.T. and Sexton, K. (2004) Outdoor, indoor, and personal exposure to VOCs in children, *Environmental Health Perspectives*, **112**, 1386-1392.

ASTM (2001) *ASTM D6670-01, Standard Practice for Full-scale Chamber Determination of Volatile Organic Emissions from Indoor Materials/Products*, ASTM International, West Conshohocken, PA.

ASTM (2010) *ASTM D5116-10, Standard Guide for Small-scale Environmental Chamber Determinations of Organic Emissions from Indoor Materials/Products*, ASTM International, West Conshohocken, PA.

Bluyssen, P.M., Fernandes, E.D.O., Groes, L., Clausen, G., Fanger, P.O., Valbjørn, O., Bernhard, C.A. and Roulet, C.A. (1996). European indoor air quality audit project in 56 office buildings, *Indoor Air*, **6**, 221-238.

Boeglin, M.L., Wessels, D. and Henshel, D. (2006) An investigation of the relationship between air emissions of volatile organic compounds and the incidence of cancer in Indiana counties, *Environmental Research*, **100**, 242-254.

BSI (2004) *BS EN 717-1, Wood-based Panels - Determination of Formaldehyde Release- Part 1: Formaldehyde Emission by the Chamber Method*, British Standards Institution, London, United Kingdom.

Cox, S.S., Little, J.C. and Hodgson, A.T. (2001b) Measuring concentrations of volatile organic compounds in vinyl flooring, *Journal of Air and Waste Manage Association*, **51**, 1195-1201.

Cox, S.S., Liu, Z., Little, J.C., Howard-Reed, C., Nabinger, S.J. and Persily, A. (2010) Diffusion controlled reference material for VOC emissions testing: proof of concept, *Indoor Air*, **20**, 424-433.

Cox, S.S., Zhao, D. and Little, J.C. (2001a) Measuring partition and diffusion coefficients for volatile organic compounds in vinyl flooring, *Atmospheric Environment*, **35**, 3823-3830.

De Bortoli, M., Kephalopoulos, S., Kirchner, S., Schauenburg, H. and Vissers, H. (1999) State-of-the-art in the measurement of volatile organic compounds emitted from building products: results of European interlaboratory comparison, *Indoor Air*, **9**, 103-116.

Howard-Reed, C., Liu, Z., Benning, J., Cox, S.S., Samarov, D., Leber, D., Hodgson, A.T., Mason, S., Won, D. and Little, J.C. (2011b) Diffusion-controlled reference material for volatile organic compound emissions testing: pilot inter-laboratory study, *Building and Environment*, **46**, 1504-1511.

Howard-Reed, C., Liu, Z., Cox, S.S., Little, J.C., Horn, W., Wilke, O., Wiegner, K. and Persily, A. (2011c) 'Inter-laboratory study approach to validate the performance of a prototype reference material for product emissions tests' In: *Proceedings of the 12th International Conference on Indoor Air Quality and Climate – Indoor Air 2011*, Austin, Texas, Indoor Air 2011.

Howard-Reed, C., Liu, Z., Samarov, S., Leber, D. and Little, J.C. (2011a) 'Assessing the shelf-life of a prototype reference material for product emissions testing' In: *Proceedings of the*

12th International Conference on Indoor Air Quality and Climate – Indoor Air 2011, Austin, Texas, Indoor Air 2011.

Howard-Reed, C. and Nabinger, S.J. (2006) 'Developing a standard reference material for VOC emissions testing' In: *Proceedings of the Indoor Environmental Quality: Problems, Research and Solutions Conference*, Research Triangle Park, NC, EPA/AWMA conference.

ISO (2007) *ISO 12460-1, Wood-based Panels – Determination of Formaldehyde Release – Part 1: Formaldehyde Emission by the 1-cubic-metre Chamber Method*, International Organization for Standardization, Geneva, Switzerland.

Jia, C., Batterman, S. and Godwin, C. (2008) VOCs in industrial, urban and suburban neighborhoods, Part 1: Indoor and outdoor concentrations, variation, and risk drivers, *Atmospheric Environment*, **42**, 2083-2100.

Klepeis, N.E., Nelson, W.C., Ott, W.R., Robinson, J.P., Tsang, A.M., Switzer, P., Behar, J.V., Hern, S.C. and Englemann, W.H. (2001) The national human activity pattern survey (NHAPS): a resource for assessing exposure to environmental pollutants, *Journal of Exposure Analysis and Environmental Epidemiology*, **11**, 231-252.

Leech, J.A., Nelson, W.C., Burnett, R.T., Aaron, S. and Raizenne, M.E. (2002) It's about time: a comparison of Canadian and American time-activity patterns, *Journal of Exposure Analysis and Environmental Epidemiology*, **12**, 427-432.

Liu, Z., Howard-Reed, C., Cox S.S. and Little J.C. (2011) 'Diffusion-controlled reference material for VOC emissions testing: validation and application of a mass transfer model' In: *Proceedings of the 12th International Conference on Indoor Air Quality and Climate – Indoor Air 2011*, Austin, Texas, Indoor Air 2011.

Missia, D.A., Demetriou, E., Michael, N., Tolis, E.I. and Bartzis, J.G. (2010) Indoor exposure from building materials: A field study, *Atmospheric Environment*, **44**, 4388-4395.

Mølhave, L. (1989) The sick buildings and other buildings with indoor climate problems, *Environmental International*, **15**, 65-74.

Ohura, T., Amagai, T., Senga, Y. and Fusaya, M. (2006) Organic air pollutants inside and outside residences in Shimizu, Japan: levels, sources and risks, *Science of the Total Environment*, **366**, 485-499.

Rappenglück, B., Apel, E., Bauerfeind, M., Bottenheim, J., Brickell, P., Čavolka, P., Cech, J., Gatti, L., Hakola, H., Honzak, J., Junek, R., Martin, D., Noone, C., Plass-Dülmer, Ch.,

Travers, D. and Wang D. (2006) The first VOC intercomparison exercise within the Global Atmosphere Watch (GAW), *Atmospheric Environment*, **40**, 7508-7527.

Rennix, C.P., Quinn, M.M., Amoroso, P.J., Eisen, E.A. and Wegman, D.H. (2005) Risk of breast cancer among enlisted army women occupationally exposed to volatile organic compounds, *American Journal of Industrial Medicine*, **48**, 157-167.

Sax, S.N., Bennett, D.H., Chillrud, S.N., Ross, J., Kinney, P.L. and Spengler, J.D. (2006) A cancer risk assessment of inner-city teenagers living in New York City and Los Angeles, *Environmental Health Perspectives*, **114**, 1558-1566.

Wei, W., Zhang, Y., Xiong, J. and Li, M. (2012) A standard reference for chamber testing of material VOC emissions: design principle and performance, *Atmospheric Environment*, **47**, 381-388.

Weschler, C.J. (2009) Changes in indoor pollutants since the 1950s, *Atmospheric Environment*, **43**, 153-159.

Wilke, O., Horn, W., Wiegner, K., Jann, O., Bremser, W., Brodner, D., Kalus, S., Juritsch, R. and Till, C. (2009) *Investigations for the improvement of the measurement of volatile organic compounds from flooring coverings within the health-related evaluation of construction products, BAM Final Report (ZP 52-5-20.49.1-1251/07)*, BAM Federal Institute for Materials Research and Testing, Berlin, Germany.

Wolkoff, P. and Nielsen, G.D. (2001) Organic compounds in indoor air-their relevance for perceived indoor air quality? *Atmospheric Environment*, **35**, 4407-4417.

Chapter 4 – Diffusion-controlled Reference Material for VOC Emissions Testing: Impact of Temperature and Humidity

Zhe Liu[1], Cynthia Howard-Reed[2], Steven S. Cox[1] and John C. Little[1]

[1]Department of Civil and Environmental Engineering, Virginia Tech, Blacksburg, VA 24061
[2]National Institute of Standards and Technology, Gaithersburg, MD 20899

4.1 Abstract

To improve the reliability and accuracy of chamber tests for measuring emissions of volatile organic compounds (VOCs) from interior materials, Virginia Tech (VT) and the National Institute of Standards and Technology (NIST) have created a program to develop reference materials for VOC emissions testing. A prototype reference material has been developed by loading toluene into a polymethylpentene (PMP) film. Its emission characteristic parameters, including material-phase diffusion coefficient (D) and material/air partition coefficient (K), have been measured at 23 ºC. A fundamental mass-transfer model can then be used to predict the true toluene emission rate from the reference material at 23 ºC, which serves as the reference value for validating the results measured by different laboratories. In this paper, the impact of temperature and humidity on the performance of the reference material was investigated. Emissions from the reference material were measured in chambers at 10, 23 and 30 ºC and at different relative humidity (RH) levels. D and K values at different temperature and RH levels were also determined using a completely independent microbalance method. It was found that RH level does not significantly affect D and K and has no impact on emission chamber test results. However, D and K depend strongly on temperature and emissions are enhanced substantially at elevated temperatures. At all the test temperatures, the model predictions match the chamber test results very well, suggesting that it can indeed predict the true emission rates at different temperatures. The reference material can therefore be applied to a wider range of emission chamber testing conditions.

4.2 Introduction

It has been well recognized that a variety of building materials and consumer products such as carpets, flooring, composite wood and paints are the main sources of volatile organic compounds (VOCs) in indoor air (Weschler, 2009). Due to their large surface area and permanent presence in the indoor environment, indoor VOC concentrations typically exceed outdoor levels substantially. Meanwhile, people spend over 80% of their time indoors (Adgate et al., 2004). Therefore, indoor VOC exposure has significant impacts on occupants' comfort, health and productivity, by causing Sick Building Syndromes (SBS), Building Related Illness (BRI), and Multiple Chemical Sensitivity (MCS) (Dorgan et al., 1998; EPA, 1991; WHO, 1983).

Variations of indoor temperature and humidity have been extensively documented. For example, Raja et al. (2001) measured a mean temperature of 24 ºC and a maximum of 33 ºC in 15 naturally ventilated buildings in UK in 1996-1997; Zhang and Yoshino (2010) measured relative humidity (RH) levels in residential houses across nine cities of China and observed very large variations among cities, from below 20% to above 80%; Dili et al. (2010) measured 100 households in India and reported a temperature range of 28 to 32 ºC and a RH range of 28 to 100%; Kim et al. (2011) measured over 1000 air-conditioned buildings in Korea, Japan and the US and reported a temperature range of 20.1 to 26 ºC and a RH range of 20.4 to 54.6%. These temperature and humidity variations are important because they may affect VOC emission rates from interior materials and thus indoor VOC concentrations. For example, formaldehyde emission rate from chipboard was found to double for every 7 ºC rise in temperature within the range of 14-31 ºC (Andersen et al., 1975). Similarly, Myers (1985) reported that formaldehyde emission rate from particleboard increased by a factor of 5.2 when temperature increased from 23 to 40 ºC. Positive correlations between emission rates and temperature were also obtained for other VOCs from some building materials (Crawford and Lungu, 2011; Lin et al., 2009). But little or negligible impact of temperature on VOC emissions from some materials were also observed (Sollinger et al., 1994; Wiglusz et al., 2002; Wolkoff, 1998) as well as an opposite trend (Haghighat and Bellis, 1998). The impact of RH on VOC emissions is also not clear. Andersen et al. (1975) reported a doubling in formaldehyde emission rate from chipboard when RH increased from 30% to 70%. Lin et al. (2009) reported emissions of several VOCs from wood flooring were enhanced at higher RH levels. However, the impact of humidity was negligible in some other cases and a decreasing trend was also observed (Wolkoff, 1998). The complicated impact of

temperature and humidity on VOC emissions may be explained by different interaction patterns between different types of materials and VOCs (Wolkoff, 1998) and further experimental and theoretical research is required.

Currently, the primary method to characterize VOC emissions from various materials and to develop low-emitting products is to perform emission chamber tests, measuring VOC emissions from test materials in chambers at specified temperature and humidity levels. To improve the reliability and accuracy of emission chamber tests, Virginia Tech (VT) and the National Institute of Standards and Technology (NIST) have developed a prototype reference material that mimics a real building material and has a known emission rate (Cox et al., 2010). A polymethylpentene (PMP) film was selected as the substrate that can be loaded with toluene through a diffusion process. The loaded film has an emission profile similar to a typical "dry" material (e.g., flooring) that can be measured in small emissions testing chambers. A unique advantage of this reference material is that its emission profile can be predicted accurately by a fundamental mass-transfer model with independently measured emission characteristic parameters (diffusion coefficient D, partition coefficient K, and initial material-phase concentration C_0). The predicted emission profile therefore serves as a reference value and can be compared to measured results by individual laboratories. The feasibility and capability of the reference material in validating emissions testing results and calibrating testing procedures have been demonstrated in a series of inter-laboratory studies (Howard-Reed et al., 2011a; Howard-Reed et al., 2011b). However, the prototype reference material was only validated at 23 ºC and employed in inter-laboratory studies at this temperature. Furthermore, the impact of humidity on its emissions was ignored.

In the present work, the impact of temperature and humidity on the reference material's emissions was investigated. Emission chamber tests were performed at 10, 23 and 30 ºC and at different RH levels. The characteristic parameters (D and K) of the reference material were also determined at various temperature and humidity levels. We found that RH level does not affect D and K and has no significant impact on the emission chamber test results. However, D and K are dependent on temperature and emissions are enhanced significantly at elevated temperatures. When the appropriate parameters are used, the model predictions match the chamber test results very well, suggesting that it can indeed predict the true emission profiles at different

temperatures. This work enables the reference material to be applied over a wider range of environmental conditions and provides a theoretical basis for assessing uncertainties of emissions testing results stemming from variations of temperature and humidity during the test period.

4.3 Methods

4.3.1 Producing reference materials for emissions testing

The reference materials were created by loading toluene vapor into clean PMP films through a diffusion process (Cox et al., 2010; Howard-Reed et al., 2011a). A diffusion vial containing pure liquid toluene was placed in a gas calibrator (Dynacalibrator 190, VICI Metronics Inc., Santa Clara, CA) with clean and dry cylinder air passing through to generate a continuous dry air stream with a constant toluene concentration. The gas-phase toluene concentration in the air stream was determined by weighing the diffusion vial regularly to obtain the toluene release rate. As shown in Figure 4.1(a), the toluene-laden dry air was passed through a stainless steel vessel containing several PMP films (6 cm×6 cm×0.0254 cm) on aluminum screen fixtures. The outlet air stream from the vessel was further passed across an extra film (3.6 cm×3.6 cm×0.0254 cm), whose mass was monitored by a high-resolution (0.1 μg) dynamic microbalance (Thermo Cahn D-200, Thermo Fisher Scientific, Waltham, MA) throughout the loading process. During the loading process (about 10 days), gas-phase toluene diffused into the films until sorption equilibrium was reached between the material-phase and gas-phase. Because the film on the microbalance was undergoing the same mass transfer process as all others in the loading vessel, its transient mass gain recorded by the microbalance, as shown in Figure 4.1(b), could be used to monitor the loading process and to determine when sorption equilibrium was reached. The material-phase concentration of toluene in the loaded films (C_0) can be also derived from the microbalance data by dividing the total toluene mass gain of the microbalance-monitored film by its volume. All the reference material samples tested in this study were produced in a single loading batch and C_0 was determined to be 780±30 g/m^3.

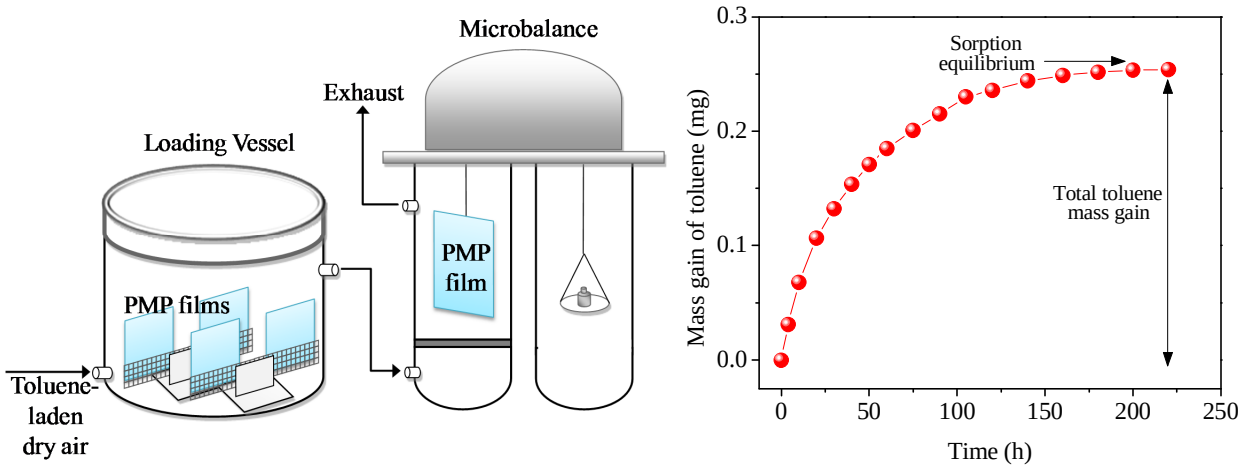

(a) (b)

Figure 4.1 Loading process to produce reference materials: (a) schematic diagram of the loading system; (b) transient toluene mass gain recorded by the microbalance during the loading process.

4.3.2 Measuring emissions at different temperature/RH levels

When the microbalance data indicated that sorption equilibrium had been reached, the loading process was considered complete. The films were removed from the loading vessel one at a time for packaging to minimize exposure to ambient air. The packaging procedure included wrapping each film in heavy-duty aluminum foil, placing it in a small sealable plastic bag, and carefully evacuating air at each step. The bags were then coded, placed in coolers containing dry ice, and sent by express delivery to NIST. After arriving at NIST, the reference materials were retained in the original packages and stored in a freezer at -20 ºC until being tested. The reference material samples were tested in a 51-L chamber with an air change rate of 1 h^{-1} following ASTM Standard D5116-2010 (ASTM, 2010). Testing protocols have been discussed in detail in the literature (Cox et al., 2010; Howard-Reed et al., 2011a) and are summarized here. Before being tested, each sample was removed from the freezer and maintained in the package at room temperature for 5 minutes, restoring it to ambient temperature. Then it was taken out of the package and placed in the emissions testing chamber with both sides fully exposed to the chamber air. Temperature and humidity set point values in each chamber test are summarized in Table 4.1. Temperature variations in all the tests were less than 0.2 ºC and RH variations were less 0.2%. During each chamber test period, chamber air samples were collected on sorbent

tubes at appropriate time intervals and toluene concentrations in the samples were quantified by thermal desorption and gas chromatography/mass spectrometry (TD-GC/MS) method.

Table 4.1 Emission chamber test conditions.

Test	1	2	3	4	5
Temperature (^{o}C)	23	23	23	10	30
Humidity (% RH)	15	70	50	50	47

4.3.3 Determining D and K at different temperature/RH levels

The key emission characteristic parameters include diffusion coefficient (D), partition coefficient (K) and initial material-phase concentration (C_0). C_0 should be determined from each loading process and is independent of temperature and RH because all the toluene in the reference material is emittable in chamber tests. However, D and K may change at different temperature and RH levels, as suggested for some VOC/material combinations (Deng et al., 2009; Xu and Zhang, 2011; Zhang et al., 2007), giving rise to different emission profiles in chamber tests. Therefore, the impact of temperature on D and K of the reference material was investigated by determining their values at 10, 23 and 30 ºC with the RH fixed at 0%. To evaluate the humidity impact on D and K, their values were also measured at 0% and 50% RH at 23 ºC.

The microbalance sorption/desorption method was employed to determine D and K of the reference material (Cox et al., 2010). Briefly, a clean PMP sample (3.6 cm×3.6 cm×0.0254 cm) was put into a small glass chamber and weighed continuously by the microbalance during the sorption/desorption cycles. During each sorption period, an air stream with a constant toluene concentration (y_∞) was swept across the sample until sorption equilibrium was reached between the gas-phase and material-phase and its transient mass gain due to sorption of toluene was recorded by the microbalance, generating a sorption curve. Then clean air was passed through the sample for the desorption test and the transient mass loss due to desorption was recorded, generating a desorption curve. The microbalance was placed in a temperature-controlled cabinet so that the temperature of each sorption/desorption cycle was accurately regulated. The temperature variations within all the sorption/desorption tests were less than 0.2 ºC. The RH at which each sorption/desorption test was conducted was adjusted by the RH of the air flow. To

acquire 50% RH, a dry air stream with toluene generated from the gas calibrator (or dry clean air for the desorption test) was mixed with a water-saturated clean air stream of the same flow rate. K can be determined from the sorption curve by

$$K = C_\infty / y_\infty \tag{4.1}$$

where C_∞ is the material-phase concentration in equilibrium with y_∞, which can be calculated by dividing the total mass gain when equilibrium is reached (M_∞) by the sample volume. D is determined by fitting a Fickian diffusion model for a thin slab to the sorption and desorption curve, which is given by (Crank, 1975):

$$\frac{M_t}{M_\infty} = 1 - \sum_{n=0}^{\infty} \frac{8}{(2n+1)^2 \pi^2} \cdot \exp\left[\frac{-D(2n+1)^2 \pi^2 t}{2H^2}\right] \tag{4.2}$$

where M_t is the total mass of the VOC that has entered or left the sample in time t, M_∞ is the total mass gain when equilibrium is reached, and 2H is the sample thickness.

4.3.4 Predicting emission profiles

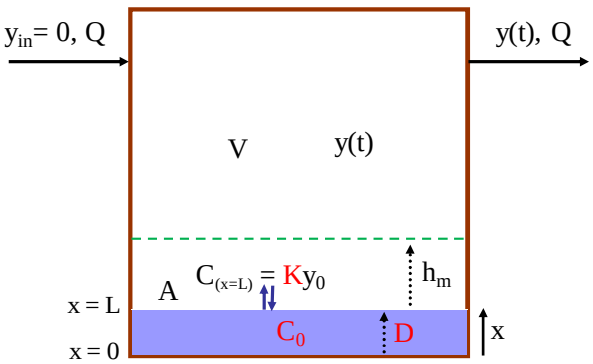

Figure 4.2 Schematic representation of the reference material in an emission chamber showing mechanisms governing VOC emission rate.

It has been proven that the emission profile of the reference material at 23 ºC can be accurately predicted by a fundamental mass-transfer model (Howard-Reed et al., 2011a; Liu et al., 2011). Figure 4.2 shows the mechanisms governing the VOC emission from the reference material in an emission chamber. These mechanisms include internal diffusion of the VOC within the material (characterized by the diffusion coefficient, D), partition between the material and air at the material/air interface (characterized by the partition coefficient between the material and air, K),

and external convective mass transfer near the emission surface (characterized by the convective mass-transfer coefficient, h_m). The external convective mass transfer is shown to be negligible compared to the internal diffusion for the reference material and the emission is diffusion controlled (Cox et al., 2010). Therefore, the boundary layer adjacent to the emission surface can be ignored and an instantaneous partition equilibrium can be assumed between the bulk chamber air and the material surface, or

$$K = \frac{C(x,t)\big|_{x=L}}{y(t)} \tag{4.3}$$

where C(x,t) is the material-phase concentration as a function of the distance from the bottom of the material x and time t, y(t) is the VOC concentration in the well-mixed chamber air as a function of time, and L is the material thickness. When a uniform initial VOC concentration in the material (C_0) is assumed, C(x,t) is given by (Little et al., 1994):

$$C(x,t) = 2C_0 \sum_{n=1}^{\infty} \left\{ \frac{\exp\left(-Dq_n^2 t\right)\left(h - kq_n^2\right)\cos\left(q_n x\right)}{\left[L\left(h - kq_n^2\right)^2 + q_n^2\left(L + k\right) + h\right]\cos\left(q_n L\right)} \right\} \tag{4.4}$$

where

$$h = \frac{Q/A}{D \cdot K} \tag{4.5}$$

$$k = \frac{V/A}{K} \tag{4.6}$$

and the q_ns are the positive roots of

$$q_n \tan\left(q_n L\right) = h - kq_n^2 \tag{4.7}$$

In Equation (4.4), A is the exposed surface area of the material, Q is the chamber flow rate, and V is the well-mixed chamber volume. When C is obtained by Equation (4.4), y can be derived from Equation (4.3). In the present work, C_0 was determined from the microbalance measured toluene mass gain in the loading process and is independent of temperature and RH. To predict emission profiles of the reference material at various temperature and RH conditions, D and K values at the corresponding conditions should be used while other parameters, including L, A, Q, and V, were obtained from the geometry of the reference material and the chamber configuration. Although the present model is constructed to predict emissions from a single-sided source, it is also applicable to emissions when both sides of the material are exposed to the

chamber air, with A indicating the total surface area of both sides and L indicating half of the material thickness.

4.4 Results and discussion

4.4.1 Emission chamber test results

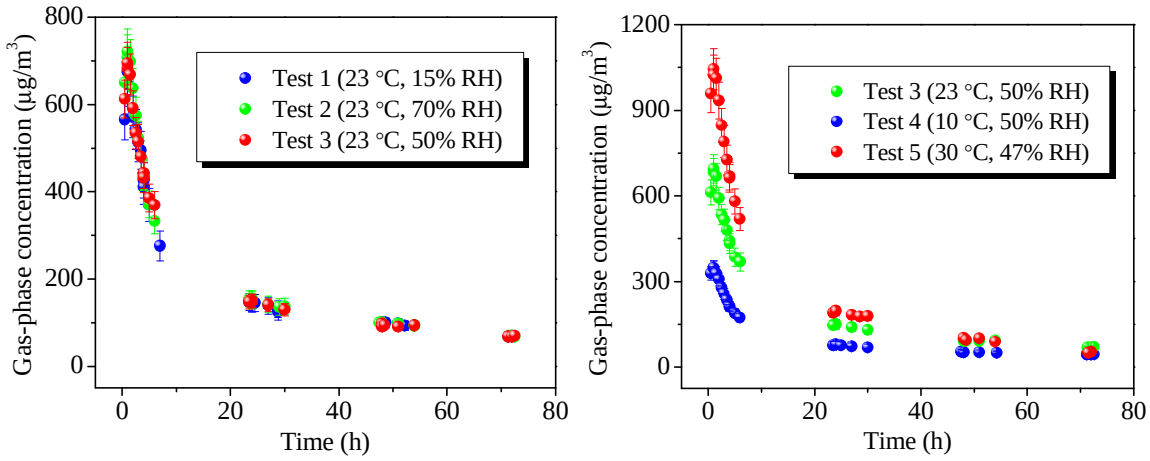

(a) (b)

Figure 4.3 Measured gas-phase toluene concentration profiles in emission chamber tests: (a) tests conducted at 23 ºC with different RH levels; (b) tests conducted at different temperatures and ~50% RH.

Figure 4.3 shows the measured chamber concentration profiles in all the five emission chamber tests, with Figure 4.3(a) comparing the results of the three tests (test 1, 2 and 3) carried out at the same temperature (23 ºC) and Figure 4.3(b) comparing the results of the three tests (test 3, 4, and 5) performed at roughly the same RH level (~50%). Figure 4.3(a) illustrates that test 1, 2 and 3 resulted in very close emission profiles, although their RH varied from 15% to 70%, demonstrating humidity does not affect the emission of the reference material significantly. Figure 4.3(b) shows, however, that the emission profiles measured at different temperatures were significantly different, with higher temperature accelerating emissions substantially. During the first 10 hours, chamber concentrations in test 5 (30 ºC) were ~1.5 times higher than concentrations in test 3 (23 ºC) and ~3 times higher than concentrations in test 4 (10 ºC). However, the differences became smaller as time went by because faster emissions at elevated temperatures also lead to faster depletion of the material-phase concentration and thus faster

decay of the chamber concentration. Therefore, when using the reference material in chamber studies, humidity is not important but temperature should be carefully controlled.

4.4.2 Diffusion and partition coefficients at different temperature/RH levels

To evaluate the temperature effect on D and K, microbalance sorption/desorption tests were carried out at 10, 23 and 30 ºC with a fixed 0% RH. Figures 4.4(a), 4.5(a) and 4.6(a) display the microbalance measured mass gain/loss data of the PMP film during the sorption/desorption cycles at the three temperatures, respectively. It is found that the sorption and desorption curves at the three temperatures were all symmetrical, implying that the sorption and desorption of toluene in the reference material is completely reversible. Furthermore, with the gas-phase concentrations (y_∞) roughly the same for the three sorption tests shown in the figures, more toluene mass was absorbed by the film at lower temperatures but it also took longer for the film and the gas to reach partition equilibrium. This is expected because at lower temperatures, the vapor pressure of toluene is reduced so that more molecules tend to be present in the material phase and the random motion of toluene molecules is less intense so that diffusion becomes slower. Figures 4.4(b), 4.5(b) and 4.6(b) show that D was obtained by fitting the Fickian diffusion model (Equation (4.2)) to the normalized sorption and desorption data for 10, 23 and 30 ºC, respectively. D was determined to be $(1.0\pm0.2)\times10^{-14}$, $(3.3\pm0.3)\times10^{-14}$ and $(6.4\pm0.3)\times10^{-14}$ m^2/s for 10, 23 and 30 ºC, respectively, increasing substantially with rising temperature. As shown by Equation (4.1), K can be calculated from the total toluene mass gain of the PMP film (M_∞) in each sorption test and the gas-phase concentration in equilibrium (y_∞). K was determined to be 1150±80, 500±30, and 369±20 for 10, 23 and 30 ºC, respectively, decreasing greatly with rising temperature. The dependence of D and K on temperature explains the difference among the measured emission profiles of the reference material at different temperatures (Figure 4.3(b)). At elevated temperatures, D increases and K decreases, thereby enhancing emissions and increasing the chamber concentration during the early period. However, because the toluene mass in the film is limited, the faster emission also leads to a faster decay of the chamber concentration during the later period.

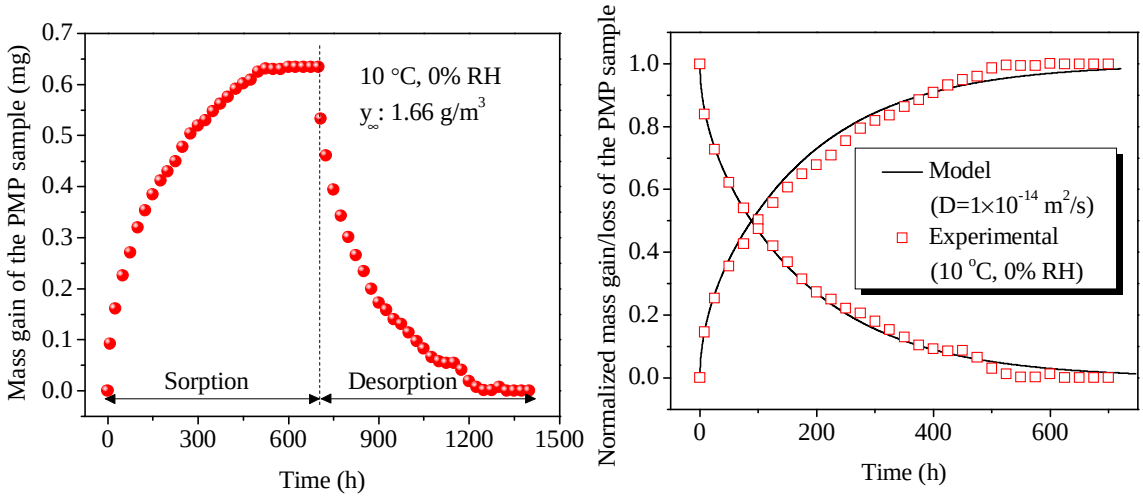

(a) (b)

Figure 4.4 (a) Transient mass gain/loss during the sorption/desorption test at 10 ºC and 0% RH; (b) fitting the Fickian diffusion model (Equation (4.2)) to the normalized sorption and desorption data to determine D at 10 ºC and 0% RH.

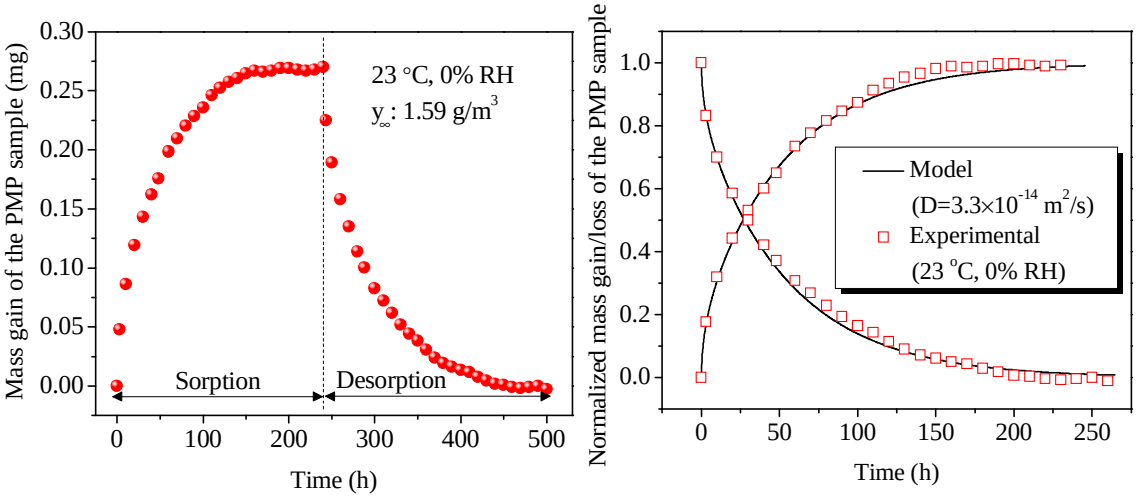

(a) (b)

Figure 4.5 (a) Transient mass gain/loss during the sorption/desorption test at 23 ºC and 0% RH; (b) fitting the Fickian diffusion model (Equation (4.2)) to the normalized sorption and desorption data to determine D at 23 ºC and 0% RH.

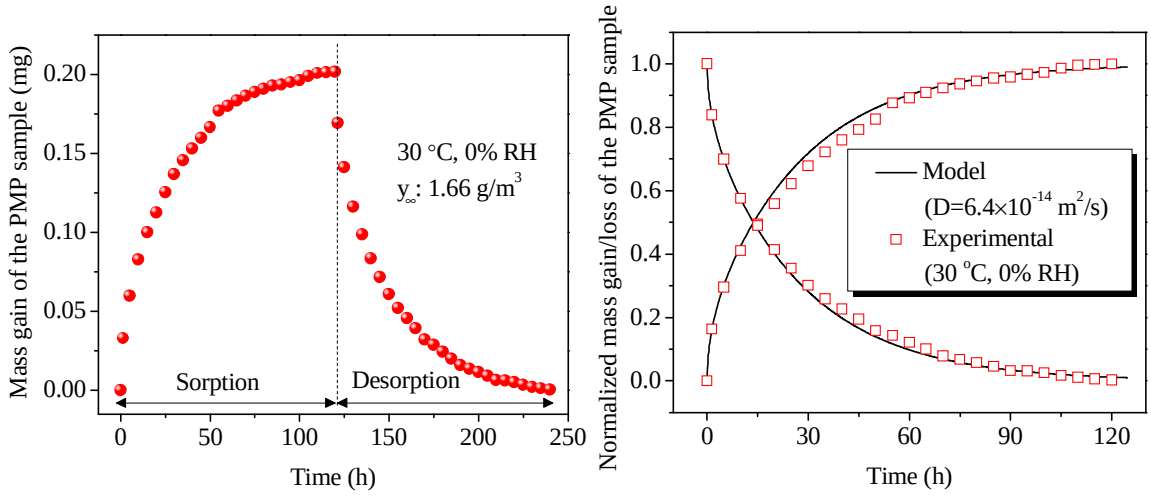

(a) (b)

Figure 4.6 (a) Transient mass gain/loss during the sorption/desorption test at 30 ºC and 0% RH; (b) fitting the Fickian diffusion model (Equation (4.2)) to the normalized sorption and desorption data to determine D at 30 ºC and 0% RH.

To evaluate the impact of humidity on D and K, an identical sorption/desorption test was performed at 50% RH and 23 ºC, with the transient mass gain/loss of the PMP sample shown in Figure 4.7 by red squares and lines. During the test, dry clean air was passed across the film and then switched to 50% RH clean air at about 70 h, with only a small amount of water rapidly absorbed by the PMP film. Maintaining 50% RH, the sorption/desorption test was carried out and when the desorption test was complete (~660 h), air flow was switched to dry air again to examine desorption of water vapor from the film. Comparing the 50% RH test results with the test carried out with dry air throughout (blue squares and lines in Figure 4.7), it appears the absorption of water vapor does not change the mass change profiles due to sorption and desorption of toluene (i.e. the sorption and desorption curves) and thereby does not change D and K. This further implies that D and K determined at 0% RH are also applicable to humid conditions and that humidity in chamber tests should have no significant impact on the emission from the reference material, which is consistent with our observations in the emission chamber tests at different RH levels (Figure 4.3(a)).

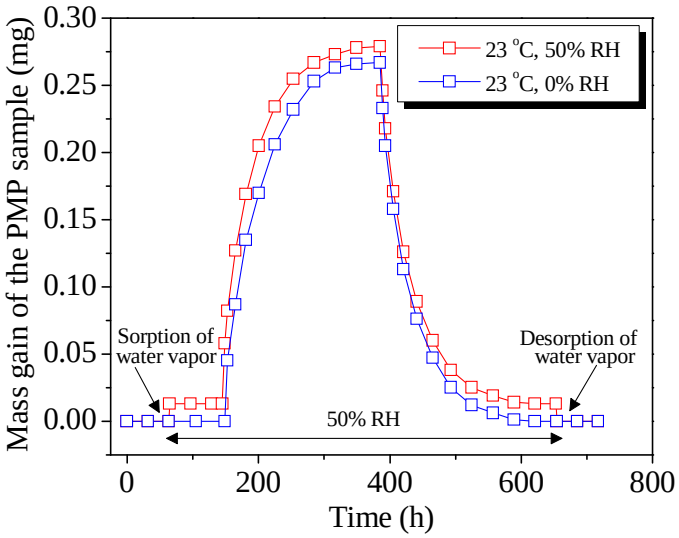

Figure 4.7 Microbalance measured mass gain/loss of the PMP sample during sorption/desorption tests at 0% and 50% RH levels, at 23 ºC.

Therefore, D and K of toluene in the reference material are exclusively dependent on temperature, for which we can thus develop simple correlations. The dependence of diffusion coefficient in polymers on temperature is frequently assumed to follow an Arrhenius-type equation (Chandak et al., 1997; Yang et al., 2001; Zhang and Niu, 2003; Zhao et al., 2006), or:

$$D = D_0 \exp\left(-E_d / RT\right) \tag{4.8}$$

where E_d is the activation energy for diffusion, R is the ideal gas constant, T is temperature and D_0 is a prefactor. Assuming E_d is constant, Equation (4.8) can be expressed as

$$D = B_1 \cdot \exp\left(-B_2 / T\right) \tag{4.9}$$

where B_1 and B_2 are both constant for a given VOC/material combination. Therefore, it can be fitted to the measured D to obtain B_1 and B_2 for toluene in the reference material. Figure 4.8(a) shows the experimental data obey the correlation very well and the obtained correlation can be used to estimate D values at different temperatures. Zhang et al. (2007) found that the relationship between K of dry building materials and temperature follows

$$K = P_1 \cdot T^{1/2} \exp\left(-P_2 / T\right) \tag{4.10}$$

where P_1 and P_2 are constant for a given VOC/material combination. Fitting the formula to the measured K, Figure 4.8(b) shows that K of the reference material follows this correlation well, which can be used to predict K values at different temperatures.

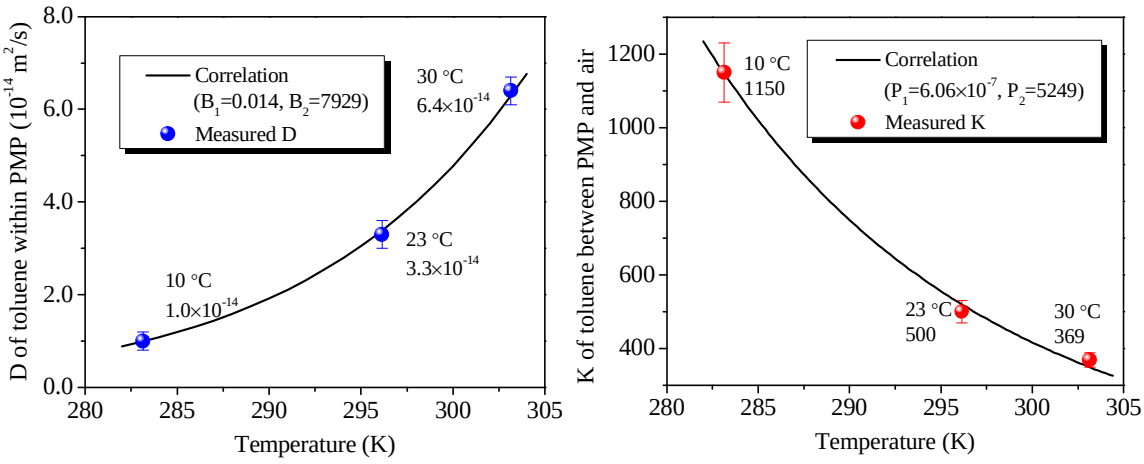

(a) (b)

Figure 4.8 Correlations for temperature dependence of (a) D (D=0.014·exp(-7929/T)) and (b) K ($K=6.06\times10^{-7}\cdot T^{1/2}\cdot\exp(5249/T)$).

4.4.3 Model predicted emission profiles

The model parameters required to predict the emission profiles of the reference material (Equations (4.3)-(4.7)) are D, K, C_0 and other directly measurable parameters, including L, A, Q, and V. The model parameter values for each chamber test are summarized in Table 4.2. The variability of V, Q, A, and L are ignored given they were very precisely controlled and had little variation. To estimate the uncertainties of model predicted chamber concentrations associated with the uncertainties of D, K and C_0, the Monte Carlo method (Cox et al., 2010) was employed. 10,000 repeated model simulations were carried out with D, K and C_0 randomly sampled from their distributions and the other parameters (L, A, Q, and V) fixed for each individual run. The results of the 10,000 model predictions were then pooled to assess the expected average value and variation of y as a function of time. Figure 4.9 shows the model predictions at the three temperatures, with the black solid line indicating the mean of the transient gas-phase toluene concentration in the chamber air and the shaded area indicting the range of mean ± standard deviation of the transient gas-phase concentration. For each temperature, the model predicted emission profile is very consistent with the experimental measurements, validating its predictive power under different environmental conditions. It has been proven that at 23 ºC, the toluene emission from the reference material is controlled by internal diffusion and that the external convective mass transfer can be ignored (Cox et al., 2010). A measure of the relative significance

of internal mass-transfer resistance versus external convective mass-transfer resistance can be given by Bi_m/K, where Bi_m (Biot number) is equal to $h_m \times L/D$. When Bi_m/K is much larger than one, internal diffusion controls the emission rate and external convective mass-transfer is negligible. It should be noted that given h_m is roughly 3×10^{-3} m/s (Cox et al., 2010), Bi_m/K values at all the three temperatures are on the order of 10^4, much larger than one. Therefore, the diffusion-based emission model is indeed applicable for the reference material.

Table 4.2 Model parameters for predicting emissions.

Test	**V (m^3)**	**Q (m^3/h)**	**A[a] (m^2)**	**L[b] (m)**	**C_0 (g/m^3)**	**D (m^2/s)**	**K (-)**
1, 2, 3 (23 ºC)	0.051	0.051	0.0072	1.27×10^{-4}	780±30	$(3.3\pm0.3)\times10^{-14}$	500±30
4 (10 ºC)	0.051	0.051	0.0072	1.27×10^{-4}	780±30	$(1.0\pm0.2)\times10^{-14}$	1150±80
5 (30 ºC)	0.051	0.051	0.0072	1.27×10^{-4}	780±30	$(6.4\pm0.3)\times10^{-14}$	369±20

[a] A is the total surface area of both sides of the reference material (two-sided source)

[b] L is the half thickness of the reference material (two-sided source)

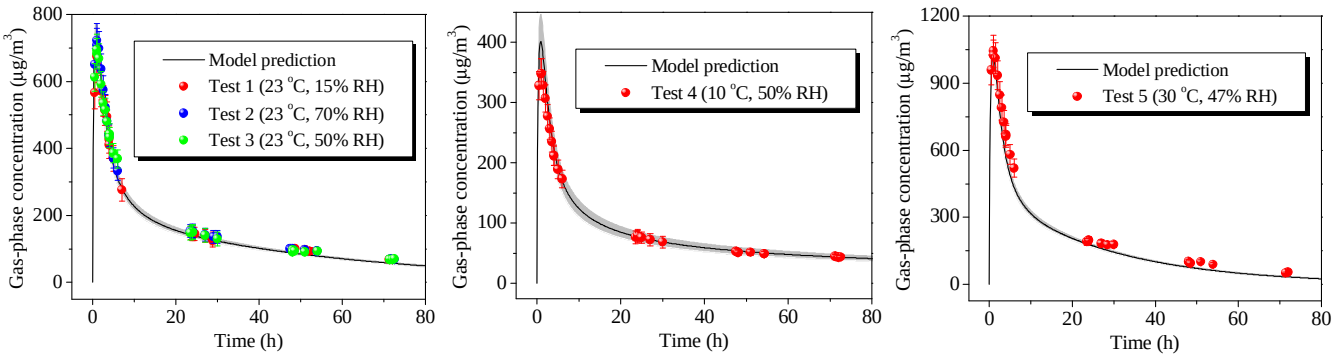

(a) (b) (c)

Figure 4.9 Comparison of measured and predicted emission profiles in emission chamber tests: (a) test 1, 2 and 3 (23 ºC); (b) test 4 (10 ºC); (c) test 5 (30 ºC).

4.5 Conclusions

In the present paper, toluene emissions from the reference material were measured in chamber tests at different temperature and RH levels and the emission characteristic parameters, diffusion coefficient and partition coefficient, were measured independently by the microbalance

sorption/desorption method. Both experiments show that humidity has no significant impact on diffusion and partition coefficients and thus does not affect the emission rate in chamber tests. However, elevated temperature significantly increases the diffusion coefficient and reduces the partition coefficient and thus enhances the emission rate substantially. Therefore, rigorous control of temperature in emission tests is necessary to ensure that measurements are comparable. On the other hand, the toluene emission from the reference material at different temperatures is controlled by internal diffusion and the diffusion-based emission model is able to predict its emission rate accurately when temperature-dependent diffusion and partition coefficients are known. Furthermore, the proposed correlations between D and K and temperature can be used to estimate D and K for various temperatures. Therefore, when the reference material is tested in chambers under different environmental conditions, the model can still supply reference values of the true emission rates for validating the experimental measurements, allowing the application of the reference material over a broader range of environmental conditions.

4.6 Acknowledgements

Financial support for the contributions of the authors from Virginia Tech was provided by the National Institute of Standards and Testing (NIST) (Award Number: 60NANB9D9154).

4.7 References

Adgate, J.L., Church, T.R., Ryan, A.D., Ramachandran, G., Fredrickson, A.L., Stock, T.H., Morandi, M.T. and Sexton, K. (2004) Outdoor, indoor, and personal exposure to VOCs in children, *Environmental Health Perspectives*, **112**, 1386-1392.

Andersen, I., Lundquist, R. and Mølhave, L. (1975) Indoor air pollution due to chipboard used as a construction material, *Atmospheric Environment*, **9**, 1121-1127.

ASTM (2010) *ASTM D5116-10, Standard Guide for Small-scale Environmental Chamber Determinations of Organic Emissions from Indoor Materials/Products*, ASTM International, West Conshohocken, PA.

Chandak, M.V., Lin, Y.S., Ji, W. and Higgins, R.J. (1997) Sorption and diffusion of VOCs in DAY zeolite and silicalite-filled PDMS membranes, *Journal of Membrane Science*, **133**, 231-243.

Cox, S.S., Liu, Z., Little, J.C., Howard-Reed, C., Nabinger, S.J. and Persily, A. (2010) Diffusion controlled reference material for VOC emissions testing: proof of concept, *Indoor Air*, **20**, 424-433.

Crank, J. (1975) *The Mathematics of Diffusion, Second Edition*, Clarendon Press, Oxford, England.

Crawford, S. and Lungu, C.T. (2011) Influence of temperature on styrene emission from a vinyl ester resin thermoset composite material, *Science of the Total Environment*, **409**, 3403-3408.

Deng, Q., Yang, X., Zhang, J.S. (2009) Study on a new correlation between diffusion coefficient and temperature in porous building materials, *Atmospheric Environment*, **43**, 2080-2083.

Dili, A.S., Naseer, M.A. and Zacharia Varghese, T. (2010) Thermal comfort study of Kerala traditional residential buildings based on questionnaire survey among occupants of traditional and modern buildings, *Energy and Buildings*, **42**, 2139-2150.

Dorgan, C.B., Dorgan, C.E., Kanarek, M.S. and Willman, A.J. (1998) Health and productivity benefits of improved indoor air quality, *ASHRAE Transactions*, **104**, 658-665.

EPA (1991) *Sick building syndrome (SBS), Indoor Air Facts No. 4 (revised)*, U.S. Environmental Protection Agency, Washington, D.C.

Haghighat, F. and Bellis, L.D. (1998) Material emission rates: literature review, and the impact of indoor air temperature and relative humidity, *Building and Environment*, **33**, 261-277.

Howard-Reed, C., Liu, Z., Benning, J., Cox, S.S., Samarov, D., Leber, D., Hodgson, A.T., Mason, S., Won, D. and Little, J.C. (2011a) Diffusion-controlled reference material for volatile organic compound emissions testing: pilot inter-laboratory study, *Building and Environment*, **46**, 1504-1511.

Howard-Reed, C., Liu, Z., Cox, S.S., Little, J.C., Horn, W., Wilke, O., Wiegner, K. and Persily, A. (2011b) 'Inter-laboratory study approach to validate the performance of a prototype reference material for product emissions tests' In: *Proceedings of the 12th International Conference on Indoor Air Quality and Climate – Indoor Air 2011*, Austin, Texas, Indoor Air 2011.

Kim, H., Chun, C., Kwok, A., Ota, A. and Tamura, A. (2011) Cross-city comparison of indoor air temperatures in air-conditioned spaces, *Indoor Air*, **21**, 311-318.

Lin, C.C., Yu, K.P., Zhao, P. and Lee, G.W.M. (2009) Evaluation of impact factors on VOC emissions and concentrations from wooden flooring based on chamber tests, *Building and Environment*, **44**, 525-533.

Little, J.C., Hodgson, A.T. and Gadgil, A.J. (1994) Modeling emissions of volatile organic compounds from new carpets, *Atmospheric Environment*, **28**, 227-234.

Liu, Z., Howard-Reed, C., Cox S.S. and Little J.C. (2011) 'Diffusion-controlled reference material for VOC emissions testing: validation and application of a mass transfer model' In: *Proceedings of the 12th International Conference on Indoor Air Quality and Climate – Indoor Air 2011*, Austin, Texas, Indoor Air 2011.

Myers, G.E. (1985) The effects of temperature and humidity on formaldehyde emission from UF-bonded boards: a literature critique, *Forest Products Journal*, **35**, 20-31.

Raja, I.A., Nicol, J.F., McCartney, K.J. and Humphreys, M.A. (2001) Thermal comfort: use of controls in naturally ventilated buildings, *Energy and Buildings*, **33**, 235-244.

Sollinger, S., Levsen, K. and Wunsch, G. (1994) Indoor pollution by organic emissions from textile floor coverings: climate test chamber studies under static conditions, *Atmospheric Environment*, **28**, 2369-2378.

Weschler, C.J. (2009) Changes in indoor pollutants since the 1950s, *Atmospheric Environment*, **43**, 153-169.

WHO (1983) *Indoor air pollutants: exposure and health effects*, *EURO Reports and Studies 78*, World Health Organization, Geneva, Switzerland.

Wiglusz, R., Sitko, E., Nikel, G., Jarnuszkiewicz, I. and Igielska, B. (2002) The effect of temperature on the emission of formaldehyde and volatile organic compounds (VOCs) from laminate flooring-case study, *Building and Environment*, **37**, 41-44.

Wolkoff, P. (1998) Impact of air velocity, temperature, humidity and air on long-term VOC emissions from building products, *Atmospheric Environment*, **32**, 2659-2668.

Xu, J. and Zhang, J.S. (2011) An experimental study of relative humidity effect on VOCs' effective diffusion coefficient and partition coefficient in a porous medium, *Building and Environment*, **46**, 1785-1796.

Yang, X., Chen, Q., Zhang, J.S., Magee, R., Zeng, J. and Shaw, C.Y. (2001) Numerical simulation of VOC emissions from dry materials, *Building and Environment*, **36**, 1099-1107.

Zhang, H. and Yoshino, H. (2010) Analysis of indoor humidity environment in Chinese residential buildings, *Building and Environment*, **45**, 2132-2140.

Zhang, L. and Niu, J. (2003) Effects of substrate parameters on the emissions of volatile organic compounds from wet coating materials, *Building and Environment*, **38**, 939-946.

Zhang, Y., Luo, X., Wang, X., Qian, K. and Zhao, R. (2007) Influence of temperature on formaldehyde emission parameters of dry building materials, *Atmospheric Environment*, **41**, 3203-3216.

Zhao, C., Li, J., Jiang, Z. and Chen, C. (2006) Measurement of the infinite dilution diffusion coefficients of small molecule solvents in silicone rubber by inverse gas chromatography, *European Polymer Journal*, **42**, 615-624.

Chapter 5 – Evaluation of Solid Phase Microextraction for Measuring Concentration of VOCs in Indoor Air

Zhe Liu and John C. Little

Department of Civil and Environmental Engineering, Virginia Tech, Blacksburg, VA 24061

5.1 Abstract

Measuring concentrations of volatile organic compounds (VOCs) in indoor air accurately is a necessary but challenging task to resolve problems associated with indoor VOCs. Cryogenic trapping and sorbent trapping are the primary air sampling techniques for measuring VOCs in indoor air. However, the apparatus and procedures are quite sophisticated and may lead to large uncertainties in the concentration measurement results. Recently, a new solid phase microextraction (SPME) technique has emerged as an increasingly popular alternative for air sampling. SPME integrates sampling, pre-concentration and sample introduction in a single step and eliminates the complicated cryogenic trapping and sorbent trapping procedures. In this paper, SPME fibers with polydimethylsiloxane (PDMS) coating were studied using experimental and modeling approaches to evaluate their capability for measuring VOC concentrations in indoor air. The sorption of benzene, toluene and p-xylene by test fibers was investigated at different temperatures using a gravimetric method, and partition and diffusion characteristic parameters were determined. Finally, standard gases with toluene were measured by the SPME technique to evaluate its practical application. Our results suggest that SPME is a simple, accurate, sensitive, and cost and time efficient technique for sampling VOCs in indoor air. While VOC reference materials can help to identify and resolve the errors and variability associated with chamber test procedures, SPME holds potential to eliminate the root causes of variability in the sampling and analytical procedures, given its simplicity and excellent repeatability.

5.2 Introduction

Since people typically spend over 80% of their time indoors (Klepeis et al., 2001), indoor air quality is of world-wide concern. Due to the toxicological properties, volatile organic compounds (VOCs) largely account for the degradation of indoor air quality (Weschler, 2009).

Exposure to VOCs may lead to acute health effects such as eye and respiratory irritation, headache, fatigue, and asthmatic symptoms (Mølhave, 1989; Wolkoff and Nielsen, 2001) and chronic illnesses such as cancers (Boeglin et al., 2006; Rennix et al., 2005; Sax et al., 2006). In addition, indoor VOC concentrations generally exceed outdoor levels (Jia et al., 2008; Ohura et al., 2006) due to the presence of many strong indoor sources, including building materials, consumer products and furniture.

Reliable concentration measurement is a prerequisite to address indoor VOC problems (Salthammer and Bahadir, 2009). Depending on specific circumstances and analytes, many sampling and analytical strategies have been developed to measure VOC concentrations in air. Common analytical methods consist of separation by capillary gas chromatography (GC), or high performance liquid chromatography (HPLC) for weakly volatile or thermally labile analytes, followed by detection and quantification techniques such as mass spectrometry (MS), flame ionization detection (FID) or electron capture detection (ECD) (Aragon et al., 2000; Wang and Austin, 2006). Direct detection and quantification of VOCs without separation in advance and online observation can also be achieved using some advanced detection techniques, such as proton transfer reaction mass spectrometry (PRT-MS) (Hewitt et al., 2003; Kuster et al., 2004; Weschler et al., 2007). However, due to the relatively small air sample volume and low VOC concentrations in the indoor air matrix (typically on the order of micrograms per cubic meter), sampling and sample preparation procedures involving a preconcentration scheme are generally needed for indoor VOCs and often require additional effort (Demeestere et al., 2007). Surveys reported that more than 80% of analysis time is spent on sampling and sample preparation (Vas and Vekey, 2004).

Sampling and sample preparation techniques for indoor VOCs primarily include cryogenic trapping and sorbent trapping. In a recent study assessing indoor VOC concentrations in nuclear power plants (Hsieh et al., 2006), cryogenic trapping was combined with whole air sampling and the air samples collected by canister samplers were introduced into a pre-concentration trap cooled at -170^{o}C. The enriched analytes in the cryogenic trap were then thermally desorbed into GC/MS. The same method has also been employed widely for monitoring VOC concentrations in the outdoor air (Chang et al., 2005; Colon et al., 2001; Warneke et al., 2003) due to its simple

principle and clean and complete thermal desorption. However, simultaneous condensation of water and other matrix compounds with target compounds may block the trap passage and later produce serious problems in the GC column, such as peak distortion, variability in the retention time and sensitivity suppression (Wang et al., 1999). A three-stage cryogenic preconcentration method followed by GC/MS analysis was consequently developed to overcome the matrix effects (Ochiai et al., 2003), which makes the cryogenic trapping system more cumbersome. In contrast, sorbent trapping by pumping air through tubes packed with organic or inorganic sorbents to collect and enrich VOCs at moderate temperature overcomes the drawbacks of cryogenic trapping. Single-sorbent tubes, mostly packed with Tenax TA (a porous polymer resin based on 2,6-diphenylene oxide), have been widely used in indoor VOC sampling (Claeson and Sunesson, 2005; Hippelein, 2004; Salthammer and Mentese, 2008). Although exhibiting low water vapor retention, low background contamination and low reactivity, Tenax TA does not favor some polar compounds and is not suitable for low molecular weight compounds in alkane, alkene and unsaturated alkyl halide categories as well as very volatile VOCs such as aldehydes, nitriles and amines due to poor adsorptive capacity and low breakthrough volume (Wang and Austin, 2006). Therefore, multi-sorbent tubes can be utilized to cover a wider spectrum of VOCs (Chien and Yin, 2009; Claeson et al., 2007; Zhu et al., 2005; Zuraimi et al., 2004). After sampling, analytes enriched in sorbent tubes are normally thermally desorbed into a GC for analysis. However, the higher thermal resistance and longer diffusion path compared with the cryogenic trap may result in slow desorption and incomplete recovery and therefore thermo-desorption apparatus refocusing the analytes is needed prior to GC in order to achieve high peak resolution (Demeestere et al., 2007). Although well established and extensively used for indoor VOCs, cryogenic trapping and sorbent trapping involve sophisticated apparatus and procedures and are subject to a large number of human and environmental factors. Uncertainty is augmented by variations and errors associated with the procedures and the integrity of each sample may be compromised (Huxham and Thomas, 2000). For example, the World Calibration Centre for Volatile Organic Compounds (WCC-VOC) coordinated a comprehensive intercomparison exercise among nine laboratories to examine the sampling and analytical procedures of either cryogenic trapping or sorbent trapping (Rappenglück et al., 2006). A synthetic standard mixture of 73 VOCs in nitrogen was provided to each participant but only 18 VOCs were accurately determined by at least 50% of all the laboratories.

Since invented (Berlardi and Pawliszyn, 1989), solid phase microextraction (SPME) has been successfully applied as a sampling technique in water and soil chemistry, food and beverage chemistry, biology, and biomedical analysis (Eisert and Levsen, 1996; Kataoka et al., 2000; Lord and Pawliszyn, 2000; Mills and Walker, 2002; Ulrich, 2000). Recently, SPME has emerged as an increasingly popular alternative to cryogenic trapping and sorbent trapping for air sampling (Hippelein, 2006; Huang et al., 2011; Huang et al., 2012; Nicolle et al., 2008; Nicolle et al., 2009; Pacenti et al., 2010; Pacolay et al., 2006; Ras et al., 2008; Tassi et al., 2012; Toscano et al., 2011; Tumbiolo et al., 2004; Wang et al., 2009). For commonly used equilibrium sampling, the SPME fiber, consisting of a thin fused-silica or metal core coated with a polymeric film, is exposed to the air sample until partition equilibrium is reached between the air sample and the SPME coating. The SPME fiber is then inserted into a GC injection port for analysis. The amount of the analyte extracted onto the fiber is linearly proportional to its equilibrium concentration in the air (Vas and Vekey, 2004), which is determined by the linear partition relationship between the air and the fiber coating. Various coating materials are available to accommodate different analytes with polydimethylsiloxane (PDMS) being the most common coating material for airborne VOCs (Vas and Vekey, 2004). SPME integrates sampling, preconcentration and sample introduction in a single step, eliminates the uncertainties caused by complicated cryogenic trapping and sorbent trapping procedures, and has been shown to offer significant superiority to conventional air sampling techniques (Koziel and Novak, 2002; Namiesnik et al. 2000).

Although quantification of VOC concentrations by SPME is mostly achieved by calibration methods (Ouyang and Pawliszyn, 2006) without the knowledge about the sorption behavior between the SPME fiber and the air sample, examining the mass transfer of VOCs between the air and the SPME fiber is valuable for evaluating the application of SPME in measuring indoor VOCs (Martos and Pawliszyn, 1997). In this paper, using a microbalance sorption test, the sorption behavior of benzene, toluene and p-xylene by PDMS coated SPME fibers were investigated at different temperatures. The partition and diffusion characteristic parameters were determined from the sorption data. In addition, standard gases with toluene were measured by SPME to evaluate its practical application. The results confirm the potential to apply SPME for indoor VOC sampling and provide useful guidance for equilibrium sampling strategies.

5.3 Materials and methods

5.3.1 Chemicals and SPME fibers

Benzene, toluene and p-xylene were selected as target VOCs. Toluene (99.9%) was purchased from Honeywell Burdick & Jackson (Muskegon, MI) and benzene (99.9%) and p-xylene (99.8%) were purchased from Thermo Fisher Scientific (Fair Lawn, NJ). All chemicals were used as purchased without purification. For the sorption test, pristine SPME fibers with three different configurations were obtained from Supelco (Bellefonte, PA). They had the same fused-silica core with a diameter of 0.11 mm but were coated with 95-μm-thick, 30-μm-thick and 7.5-μm-thick PDMS phase respectively and each fiber was 1 meter in length. These pristine SPME fiber samples were exactly the same as the nominal 100-μm, 30-μm and 7-μm SPME PDMS fibers commercially available from Supelco. To accommodate the fibers in the microbalance chamber, they were cut into lengths of 39.3 cm for the 7-μm fiber, 11.9 cm for the 30-μm fiber, and 11.6 cm for the 100-μm fiber. In addition, 1-cm × 100-μm PDMS fibers assembled with fiber holders for manual sampling were purchased from Supelco and used for measuring standard gases.

5.3.2 Gas generation

Gas samples were prepared with a gas dynacalibrator (Model 190, VICI Metronics Inc., Santa Clara, CA). The pure VOC liquid was placed in a glass diffusion vial (VICI Metronics Inc.), which was held at a constant temperature in the dynacalibrator. USP medical air (UN1002, Airgas Inc., Radnor, PA) regulated by a mass flow controller (Model FC-280S, Tylan General, Carson, CA) was passed through the dynacalibrator so that an air stream with a constant VOC concentration was generated. The gas-phase concentration (y_∞) was calculated by dividing the gravimetrically determined emission rate of the diffusion vial by the air flow rate. Maintaining a constant flow rate, the gas-phase concentration can be varied by adjusting the temperature of the dynacalibrator.

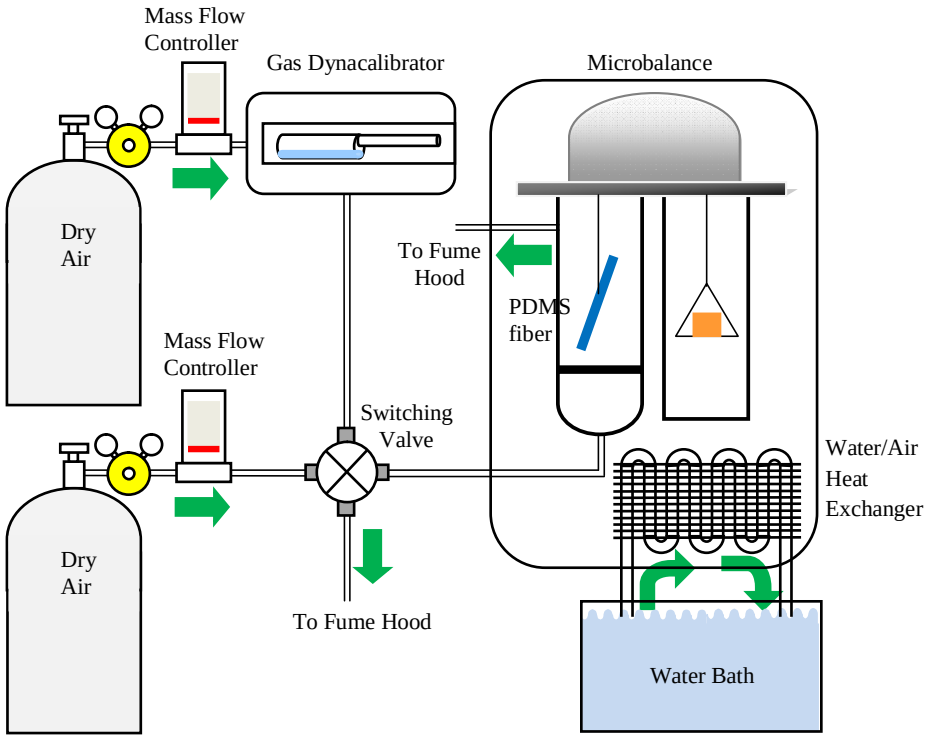

Figure 5.1 Schematic diagram of the microbalance system.

5.3.3 Microbalance sorption test

A high-resolution (0.1 μg) dynamic microbalance (Thermo Cahn D-200, Thermo Fisher Scientific, Waltham, MA) equipped with a PC-based data-acquisition system was used to measure and record the mass gain of SPME fibers during the sorption tests. Figure 5.1 shows the schematic diagram of the microbalance system. The microbalance was placed in an insulated enclosure whose temperature was controlled by a water/air heat exchanger connected to a constant-temperature water bath (Isotemp 1028D, Thermo Fisher Scientific, Waltham, MA). The temperature within the microbalance enclosure was monitored by a resistance temperature detector (RTD PT 100, Omega Engineering Inc., Stamford, CT) with temperature variation of less than ±0.3 ^{o}C from set values. The fiber samples were hung on the measuring arm of the microbalance and the mass was recorded every 5 seconds. Before each sorption test, clean air was passed through the measuring chamber for at least 24 hours until the mass of the test fiber sample became stable. Then air supplied from the gas dynacalibrator was switched into the measuring chamber for the sorption test until the mass of the fiber sample became constant, indicating that sorption equilibrium had been reached between the gas phase and coating phase.

The clean air flow and the air supplied from the gas dynacalibrator were kept at the same flow rate of 255±5 mL/min by mass flow controllers so that they could be switched into the measuring chamber by four-way switching valve alternately without affecting the mass measurement. The microbalance system has been successfully used to investigate the transport of VOCs in vinyl flooring (Cox et al. 2001), polystyrene foam and oriented strand board (Yuan et al., 2007).

5.3.4 Determination of partition and diffusion coefficients

The equilibrium and kinetic parameters, partition coefficient (K) and diffusion coefficient (D), can be determined from the sorption data recorded by the microbalance. Describing the sorption equilibrium for a VOC between the PDMS coating and the air, K is given as

$$K = \frac{C_{equ}}{y_{\infty}} \tag{5.1}$$

where y_{∞} is the gas-phase VOC concentration in the supply air (mg/m^3) and C_{equ} is the corresponding equilibrium concentration in the PDMS coating (mg/m^3), which can be calculated by dividing the microbalance-recorded mass gain of the SPME fiber at the end of the sorption test by the coating volume. K can be regarded as a constant within low gas-phase concentration range so that the amount of a particular VOC extracted by the fiber is linearly proportional to the gas-phase concentration in the air (Vas and Vekey, 2004). In this study, K was obtained from the linear regression of three data sets for the gas-phase and coating-phase concentrations in equilibrium. In addition, for each VOC, sorption tests were carried out at three different temperatures to evaluate the temperature impact on K. Table 5.1 summarizes the sorption test conditions to determine K.

Table 5.1 Microbalance sorption test conditions to determine K. Each VOC was tested at three temperatures and for each temperature, three different gas-phase concentrations (y_{∞}) were used, with nominal values (mg/m^3) listed in the corresponding cells.

		7-µm PDMS fiber	**30-µm PDMS fiber**	**100-µm PDMS fiber**
Benzene	23 ºC	1000 1800 2500	1000 1800 2500	1000 1800 2500
	31.5 ºC	2500 3500 6000	2500 3500 6000	2500 3500 6000
	40 ºC	2500 3500 6000	1000 1800 2500	1000 1800 2500

Toluene	20 ºC	700 1200 1600	700 1200 1600	700 1200 1600
	24 ºC	700 1200 1600	700 1200 1600	700 1200 1600
	29 ºC	700 1200 1600	700 1200 1600	700 1200 1600
p-Xylene	23 ºC	400 600 1000	400 600 1000	400 600 1000
	31.5 ºC	400 600 1000	400 600 1000	400 600 1000
	40 ºC	400 600 1000	400 600 1000	400 600 1000

By investigating the thermodynamic principles of partitioning, Martos and Pawliszyn (1997) developed a simple equation to predict K of VOCs between air and the PDMS coating, which is given by

$$\log K = \left(\frac{\Delta H^V}{2.303R} \right) \times \frac{1}{T} + \left[\log \left(\frac{RT}{\gamma_i p^*} \right) - \frac{\Delta H^V}{2.303RT^*} \right] \quad (5.2)$$

where ΔH^V is the heat of vaporization of the pure VOC, R is the universal gas constant, T is temperature, γ_i is the modified analyte activity coefficient in the PDMS coating, and p^* is the vapor pressure of the pure VOC at a known temperature T^*. For a given VOC, ΔH^V, γ_i, and p^* at a fixed T^* are constant so that K is exclusively dependent on T. Although the term in the square brackets is dependent on T, it has been proven that the dependence is so small that ignoring the dependence leads to little error. Therefore, Equation (5.2) essentially describes the linear dependence of logK on 1/T. The reported values of the slope and intercept for benzene, toluene and p-xylene (Martos and Pawliszyn, 1997) are listed in Table 5.2 and Equation (5.2) can thus be used to predict our experimental results.

Table 5.2 Slope and intercept values in Equation (5.2) (Martos and Pawliszyn, 1997).

	Slope (unit: K)	**Intercept (unit: dimensionless)**
Benzene	2025	-4.304
Toluene	2189	-4.419
p-Xylene	2234	-4.097

The diffusion coefficient was determined by fitting a Fickian diffusion model for the PDMS coating, which is actually a hollow cylinder, to the sorption data. Considering the change of the gas-phase concentration in the measuring chamber and the diffusion within the fiber coating, but

ignoring the external gas-phase mass transfer resistance, the model can predict the coating-phase concentration development and thus the transient mass gain of the fiber during the sorption test. D is the only unknown parameter of the model and therefore the model-predicted transient mass gain can be compared to the experimental sorption data to obtain the best-fitting D value. The development of the Fickian diffusion model is given in Appendix A.

5.3.5 Standard gas calibration

To evaluate the practical measurement using SPME, 1-cm × 100-μm PDMS fibers assembled with fiber holders for manual sampling were used to sample standard gases with various toluene concentrations generated by the gas dynacalibrator. A specially designed glass sampling tube was connected to the outlet of the gas dynacalibrator and three manual samplers were used for sampling. The samplers were conditioned at 250 ^{o}C for ten minutes and exposed to the gas stream for 6 minutes for equilibrium sampling. Then the samplers were thermally desorbed in the injection port of a GC-MS (Shimadzu GCMS-QP-2010, Shimadzu America, Inc., Columbia, MD) directly for analysis. The injection port was held at 250 ^{o}C with a split injection mode and the split ratio was 20:1. The analytes were separated in a 30-m long ZB-5MS capillary column with a film thickness of 1 μm and an internal diameter of 0.25 mm. During the analysis, the column was held at 80 ^{o}C for 4 minutes and the linear velocity was 50 cm/sec. The absorbed mass of toluene (M) recovered by the GC-MS was thereby used to calculate the gas-phase toluene concentration in the standard gas based upon the partition equilibrium between the coating phase and the gas phase, or

$$y = \frac{M}{V_s \cdot K} \tag{5.3}$$

where y is the gas-phase concentration of the standard gas (mg/m^3) to be determined, V_s is the coating volume (m^3) calculated according to the geometric structure of the fiber and K is the partition coefficient of toluene at the sampling temperature, determined in the previous section. The calculated y value was then compared to the real concentration obtained according to the gas dynacalibrator to evaluate the accuracy of the SPME technique.

5.4 Results and discussion

5.4.1 Determination of partition coefficient

As described previously, K was obtained by performing a linear regression on the three data sets for the gas-phase and coating-phase concentrations in equilibrium, fixing the intercept at zero. Figure 5.2 shows an example of the linear regression and K is exactly equal to the slope of the linear model, 884.86 in this case, with the coefficient of determination (R^2) indicating the linearity between the gas-phase concentration and the coating-phase concentration in equilibrium.

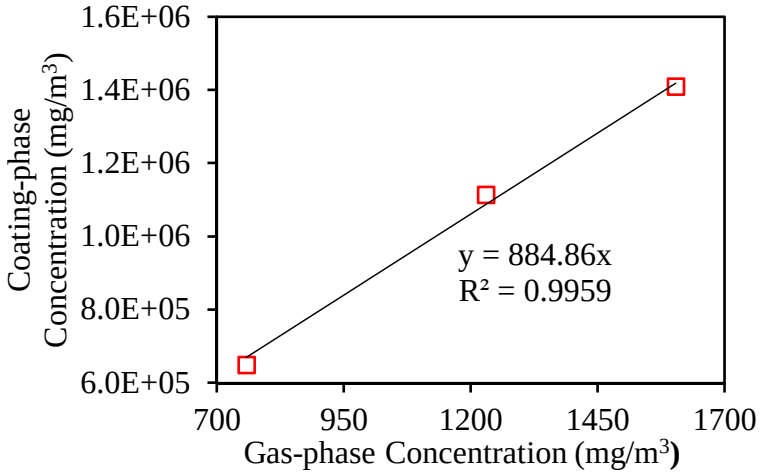

Figure 5.2 An example of determining K by linear regression on the three data sets for the gas-phase and coating-phase concentrations in equilibrium.

Table 5.3 has the same layout as Table 5.1, showing the R^2 values of linear regressions for all the tests. Most R^2 values are larger than 0.99, with a few exceptions, and all the values are larger than 0.96, suggesting good linearity between the gas-phase concentration and equilibrium coating-phase concentration for the three VOCs. As shown in Table 5.1, a fairly large range of gas-phase concentrations was covered and K is indeed constant as long as the gas-phase concentration does not exceed the highest level tested. The SPME can therefore be used for sampling a large range of gas-phase concentrations.

Table 5.3 R^2 of linear regression in determining K. For each VOC, three different gas-phase concentrations were used at each temperature and the corresponding coating-phase concentrations in equilibrium were measured. Linear regressions were performed for gas-phase and coating-phase concentrations in equilibrium at each temperature, with R^2 values of linear regression listed in corresponding cells.

		7 μm	30 μm	100 μm
Benzene	23 ^{o}C	0.9821	0.9983	0.9993
	31.5 ^{o}C	0.9906	0.9975	0.998
	40 ^{o}C	0.9658	0.977	0.9839
Toluene	20 ^{o}C	0.9794	0.9953	0.9946
	24 ^{o}C	0.9937	0.9929	0.9959
	29 ^{o}C	0.9642	0.9749	0.9946
p-Xylene	23 ^{o}C	0.9993	0.9987	0.9968
	31.5 ^{o}C	0.9981	0.998	0.9954
	40 ^{o}C	0.9941	0.9987	0.9996

Figure 5.3 shows the comparisons of predicted K by Equation (5.2) and the values obtained from linear regression based upon the sorption test data for benzene, toluene and p-xylene. For each compound, it is observed that fibers with different coating thicknesses have very close K values and they are all reasonably well predicted by Equations (5.2). At the same temperature, K of the three VOCs increases substantially when molecular weight increases from benzene to p-xylene since with larger molecular weight, vapor pressure of the pure compound is smaller and VOC molecules tend to be present in the coating phase. With the prediction showing a clear trend, K of each VOC decreases greatly when temperature increases, consistent with the fact that vapor pressure increases with temperature. Therefore, in practical applications, SPME fibers with a suitable coating thickness can be selected according to sampling requirements while a single K value can be used for different thicknesses, which can be calculated easily by Equation (5.2). When several analytes are determined simultaneously, the K value for each analyte should still be valid because absorption of each compound onto the PDMS coating is independent of the others (Cho et al., 2003). Due to the strong dependence of K on temperature, it is necessary to specify the temperature at which the sample is taken if K will be used for quantification. When calibration methods (Ouyang and Pawliszyn, 2006) are employed, all the samples should be taken at the same temperature to assure the same partition equilibrium between SPME fibers and air samples.

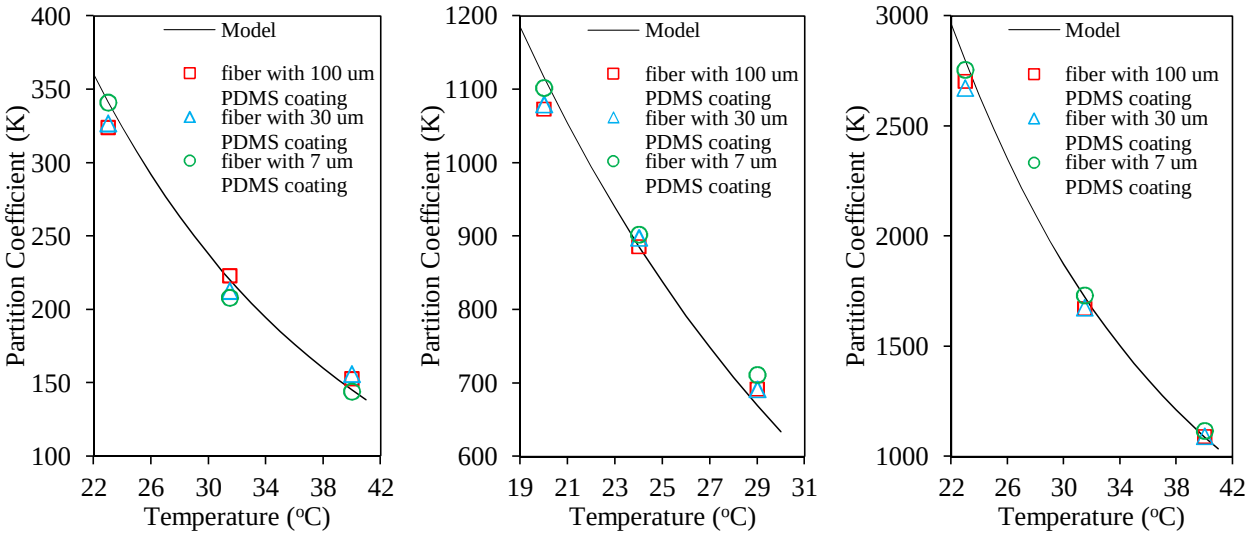

Figure 5.3 Comparison of predicted and experimentally determined K for (a) benzene, (b) toluene, and (c) p-xylene.

5.4.2 Determination of diffusion coefficient

The model considering the gas-phase concentration development over time in the measuring chamber and diffusion of VOCs in the PDMS coating is discussed in detail in Appendix A. Figure 5.4(a) compares the model predicted toluene mass gain in the 100-μm-thick PDMS coating during the sorption period and typical sorption profiles measured in experiments. The toluene mass gain at time t (M_t) is normalized by the total absorbed mass when partition equilibrium is reached (M_∞). D is the only unknown parameter and predictions with different D values are shown in Figure 5.4(a). In addition to model predictions and experiment results, Figure 5.4(a) also shows the chamber gas-phase concentration development, which is normalized by the concentration of VOCs in the incoming air supplied from the gas dynacalibrator (y_∞), and therefore represents exactly the normalized model predicted mass gain in the coating with infinite large D. According to Figure 5.4(a), although the changing gas-phase concentration in the measuring chamber has significant impact on the mass gain profile, the model prediction is still rather sensitive to the D value. From the comparisons, the best-fitting D is 3×10^{-11} m^2/s.

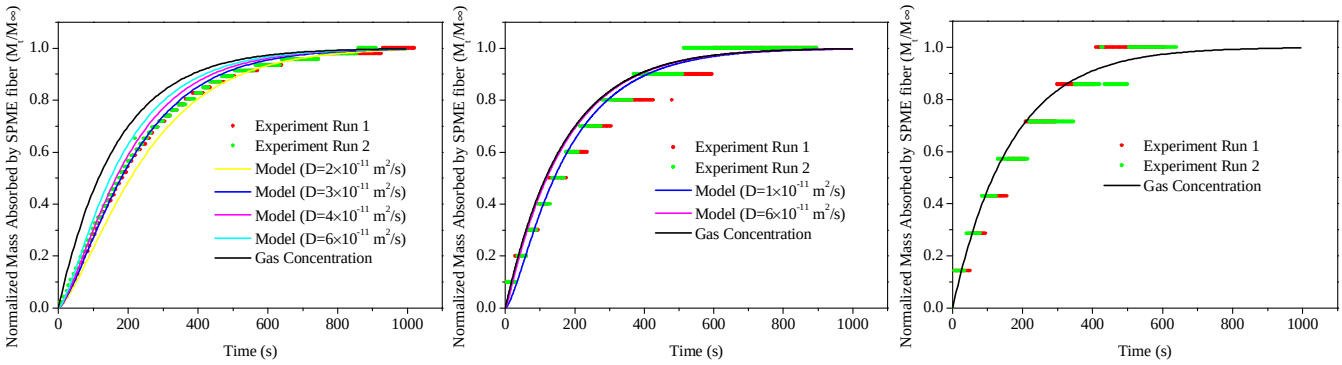

(a) (b) (c)

Figure 5.4 Model predictions with various D and experimental results for fibers with (a)100-µm-thick PDMS coating, (b) 30-µm-thick PDMS coating, and (c) 7-µm-thick PDMS coating.

As to the comparisons of normalized model predictions and experimental data for the fiber with 30-µm-thick coating shown in Figure 5.4(b), the model prediction is not sensitive to D because the coating is so thin that the effect of internal mass transfer resistance due to diffusion is small compared to the effect of the changing gas-phase concentration in the measuring chamber. Furthermore, the normalized gas-phase concentration development in the measuring chamber itself fits the experiment results quite well, implying that the external gas-phase mass transfer resistance is insignificant, as assumed in the model. With even thinner coating, the same phenomenon occurs for the fiber with 7-µm-thick coating, as shown in Figure 5.4(c). Therefore, only the sorption data of the fiber with 100-µm-thick coating are used to determine the best-fitting D for toluene.

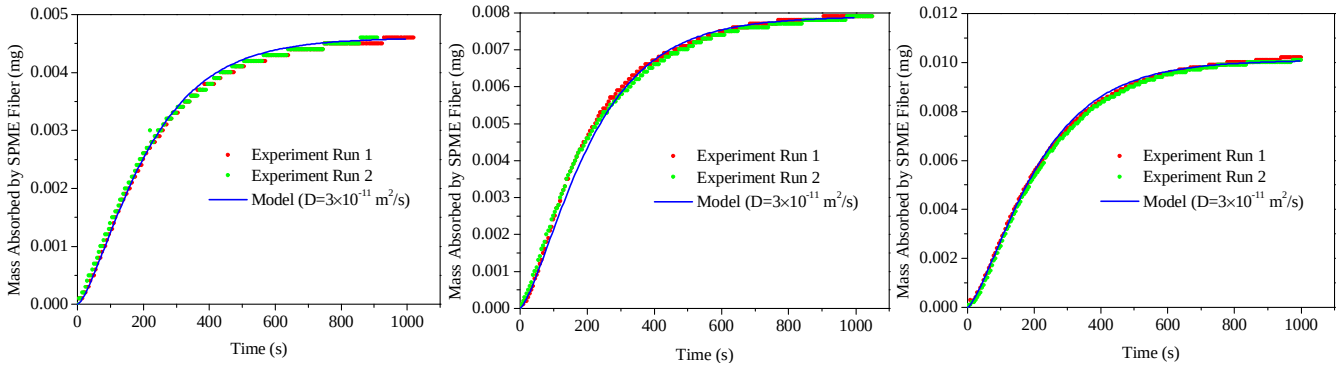

(a) (b) (c)

Figure 5.5 D obtained by model fitting with experimental data of 100- µ m-thick PDMS coating at 24 ºC: (a) y_∞=700 mg/m^3; (b) y_∞=1200 mg/m^3; (c) y_∞=1600 mg/m^3.

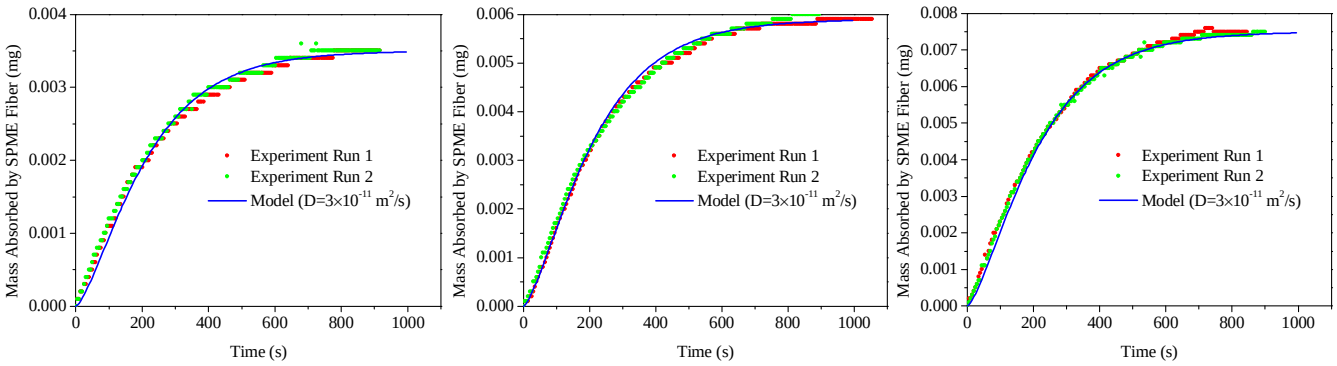

Figure 5.6 D obtained by model fitting with experimental data of 100- μ m-thick PDMS coating at 29 ^{o} C: (a) y_{∞}=700 mg/m^3; (b) y_{∞}=1200 mg/m^3; (c) y_{∞}=1600 mg/m^3.

Figure 5.5 shows the model fitting to the experimental sorption profiles of the fiber with 100-μm-thick coating at 24 ^{o}C with three different nominal gas-phase toluene concentrations (y_{∞}) and Figure 5.6 shows the cases at 29 ^{o}C. All six cases yield the same best-fitting D value of 3×10^{-11} m^2/s. Zee and Graauw (1997) determined D of toluene in a PDMS membrane to be 8×10^{-11} m^2/s based on model fitting to toluene uptake from a stirred liquid solution by a PDMS sheet submerged in the liquid solution. They also found that D has little concentration dependence for toluene in PDMS when toluene weight fraction is less than 5%, which is also illustrated in our results. Janes et al. (2008) measured D of toluene in a cylindrical hollow PDMS membrane using aqueous feed stream solutions and two approximate models resulted in D values of 6.5×10^{-11} and 5.0×10^{-11} m^2/s respectively. Lue et al. (2008) reported D values of toluene vapor in a PDMS membrane ranging from 1.77 to 3.20×10^{-11} m^2/s, according to different fitting strategies. The literature reported values vary due to differences in the structure and composition of the PDMS materials and different testing methods. For example, PDMS membranes in the first two studies were in contact with aqueous solution and were saturated with water. Despite the variability, our D of 3×10^{-11} m^2/s falls within the range of reported values. In addition, it is found that increasing temperature from 24 ^{o}C to 29 ^{o}C does not cause any observable change in D, which is consistent with the conclusion reached by Boscaini et al. (2004) that D of toluene in PDMS does not increase significantly with temperature.

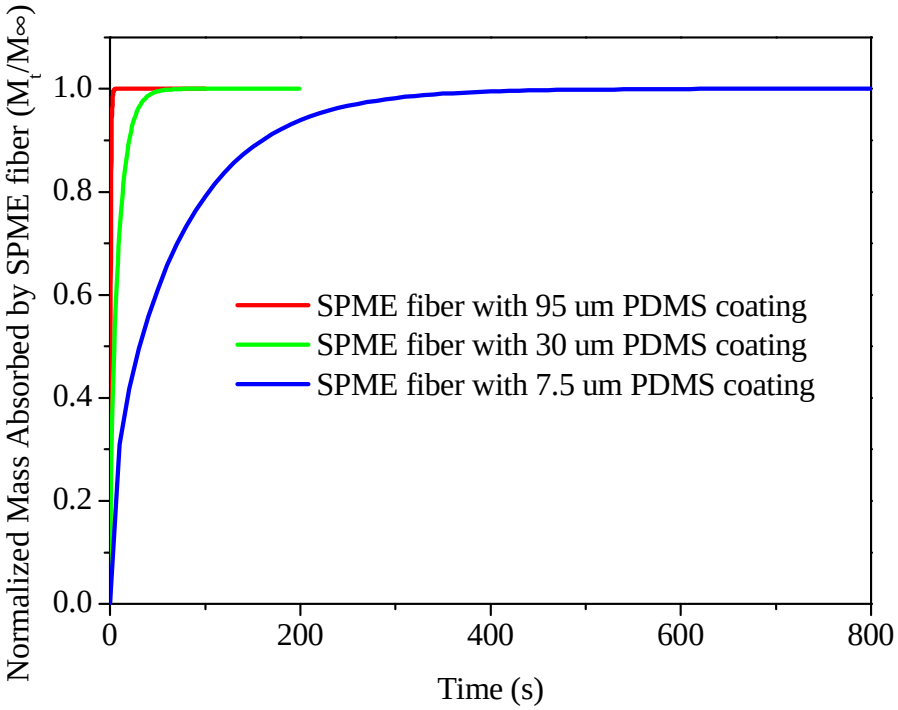

Figure 5.7 Model predicted sorption profiles with a constant gas concentration.

With D of toluene in PDMS obtained above, we can use the mass transfer model developed in Appendix A to predict the sorption profile when a SPME fiber is employed for air sampling. In this case, the concentration of the sampled gas is assumed constant, which is true when the gas sample volume is large or when a continuous gas stream is sampled. Figure 5.7 shows the predicted absorbed mass normalized by the total absorbed mass when partition equilibrium is reached for fibers with 7, 30 and 100 μm thick PDMS coatings. The sorption profiles of the fibers with 7 and 30 μm thick coating indicate that the fibers reach equilibrium with the air sample very rapidly, requiring less than 10 s and 60 s, respectively. This prediction is consistent with the previous discussion concerning Figure 5.4. For the fiber with 100-μm-thick coating, approximately 10 minutes is needed to reach equilibrium. However, after only 5 minutes, the SPME fiber has sorbed more than 98% of the total absorbed mass at equilibrium. In the model prediction, the external mass transfer resistance is ignored, which may increase the time required to reach equilibrium. However, it is reported that at room temperature, the diffusion coefficient of toluene in air is as high as 8×10^{-6} m^2/s (Erbil and Avci, 2002) so that even when gas-phase mass transfer resistance exists, the time required to reach equilibrium should not be much longer than the model prediction. The discussion of Figure 5.4 also suggests that the external gas-phase

mass transfer resistance is not significant when a continuous flow is sampled. Therefore, for practical equilibrium sampling of toluene in air, 6-10 minutes is sufficient for the 100-μm PDMS fiber and the sampling time can be as short as 1-2 minutes for the 7 and 30-μm PDMS fibers. For other analytes, additional care should be taken to guarantee sufficient time for equilibrium sampling.

5.4.3 Standard gas calibration

According to the knowledge acquired above, the sampling strategies for standard gases containing toluene were developed as described in the method section. Figure 5.8 shows the concentrations of eight standard gases measured using SPME, which are correlated with the true concentrations determined according to the gas dynacalibrator. Figure 5.8 shows an excellent linear correlation with slope not significantly different from 1, indicating that measurement using SPME is very accurate. Furthermore, the small deviation of the measurements for each gas concentration level using three SPME fibers implies good reproducibility.

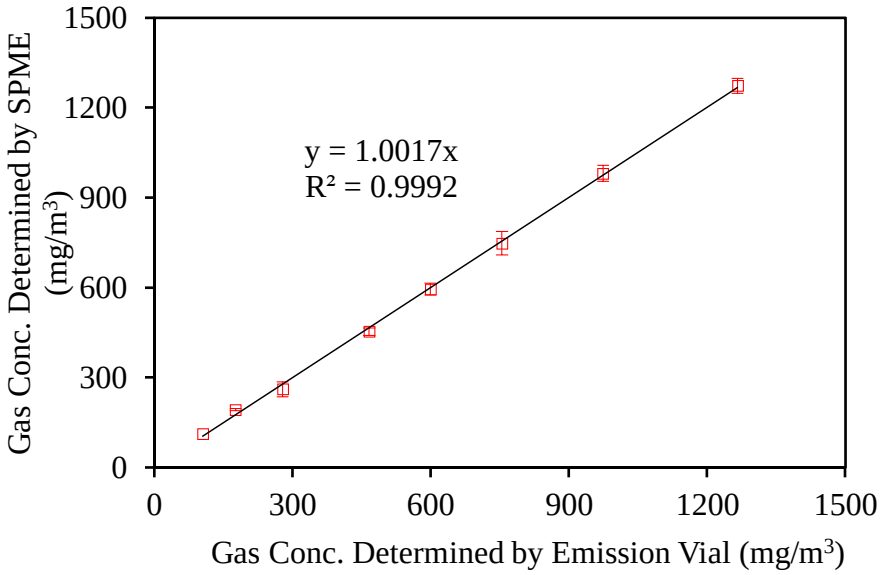

Figure 5.8 Standard gas concentrations measured by SPME.

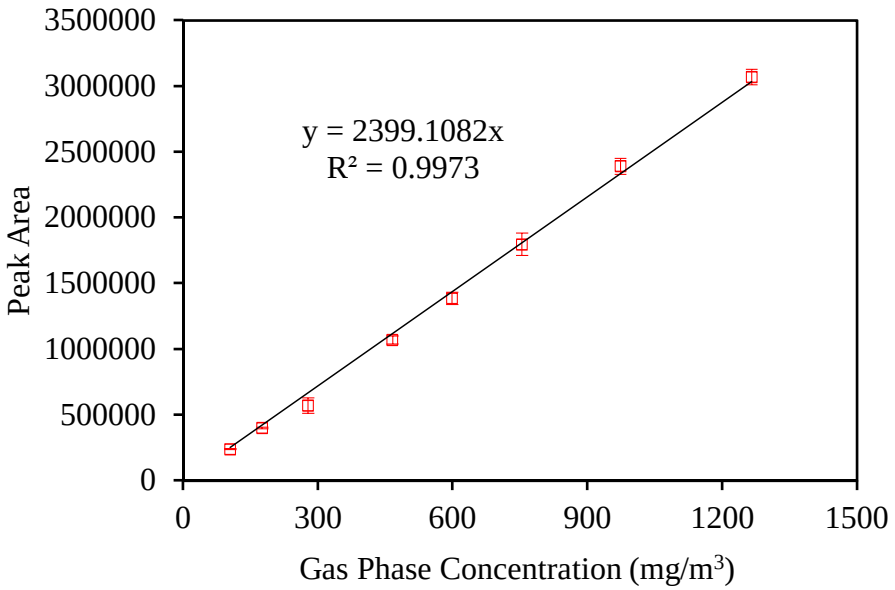

Figure 5.9 Calibration line constructed from standard gas measurements.

Based upon the response of the GC-MS for each standard gas sampled by SPME, a calibration line is constructed as shown in Figure 5.9. A linear relation is fitted describing the correlation between the peak area from the GC-MS and the original toluene concentration of the standard gas. For an unknown gas sample to be measured, the same SPME fibers can be used for sampling at the same temperature as for the standard gases and then analyzed by the GC-MS to obtain the responding peak area. The gas-phase concentration in the sample can therefore be derived directly from the calibration line.

5.5 Conclusions

This paper investigated the mass transfer properties of three VOCs in SPME fibers with PDMS coating employing independent microbalance sorption tests and model analysis. The information obtained provides guidance for applying SPME in indoor VOC measurement. It is shown that SPME is a powerful air sampling/sample preparation technique which can be used to achieve accurate measurement in a simple and time and cost efficient manner. When used in emission chamber tests, SPME fibers can be exposed to the outlet flow from the emission chamber to measure the VOC concentration in the chamber air. Due to the rapid sorption kinetics discussed above, the equilibrium sampling and sample enrichment can be done within a very short time and then the fibers can be thermally desorbed in the GC injection port for direct analysis. While the

VOC reference material can help to identify and resolve the errors and variability within the entire chamber test procedure, SPME can actually eliminate complicated sampling and analytical procedures and thus many root causes of variability in the measurement. Therefore, SPME holds great potential to facilitate emissions testing and improve the quality of testing data. Furthermore, the performance of SPME as a new technique for VOC emissions testing can be also systematically evaluated using the VOC reference material.

5.6 Acknowledgements

Financial support was provided by the National Science Foundation (CMS 0600090). We thank Harold McNair of the Department of Chemistry at Virginia Tech for his help on the analytical procedures.

5.7 References

Aragon, P., Atienza, J. and Climent, M.D. (2000) Analysis of organic compounds in air: A review, *Critical Reviews in Analytical Chemistry*, **30**, 121-151.

Berlardi, R.P. and Pawliszyn, J. (1989) The application of chemically modified fused silica fibers in the extraction of organics from water matrix samples and their rapid transfer to capillary columns, *Water Pollution Research Journal of Canada*, **24**, 179-191.

Boeglin, M.L., Wessels, D. and Henshel, D. (2006) An investigation of the relationship between air emissions of volatile organic compounds and the incidence of cancer in Indiana counties, *Environmental Research*, **100**, 242-254.

Boscaini, E., Alexander, M.L., Prazeller, P. and Mark, T.D. (2004) Investigation of fundamental physical properties of a polydimethylsiloxane (PDMS) membrane using a proton transfer reaction mass spectrometer (PTRMS), *International Journal of Mass Spectrometry*, **239**, 179-186.

Chang, C.C., Sree, U., Lin, Y.S. and Lo, J.G. (2005) An examination of 7:00-9:00 PM ambient air volatile organics in different seasons of Kaohsiung city, southern Taiwan, *Atmospheric Environment*, **39**, 867-884.

Chien, Y.C. and Yin, K.G. (2009) Simultaneous determination of airborne carbonyls and aromatic hydrocarbons using mixed sorbent collection and thermal desorption-gas

chromatography/mass spectrometric analysis, *Journal of Environmental Monitoring*, **11**, 1013-1019.

Cho, H., Baek, K., Lee, H., Lee, S. and Yang, J. (2003) Competitive extraction of multi-component contaminants in water by carboxen-polydimethylsiloxane fiber during solid-phase microextraction, *Journal of Chromatography A*, **988**, 177-184.

Claeson, A.S., Sandstrom, M. and Sunesson, A.L. (2007) Volatile organic compounds (VOCs) emitted from materials collected from buildings affected by microorganisms, *Journal of Environmental Monitoring*, **9**, 240-245.

Claeson, A.S. and Sunesson, A.L. (2005) Identification using versatile sampling and analytical methods of volatile compounds from Streptomyces albidoflavus grown on four humid building materials and one synthetic medium, *Indoor Air*, **15**, 41-47.

Colon, M., Pleil, J.D., Hartlage, T.A., Guardani, M.L. and Martins, M.H. (2001) Survey of volatile organic compounds associated with automotive emissions in the urban airshed of Sao Paulo, Brazil, *Atmospheric Environment*, **35**, 4017-4031.

Cox, S.S., Zhao, D. and Little, J.C. (2001) Measuring partition and diffusion coefficients for volatile organic compounds in vinyl flooring, *Atmospheric Environment*, **35**, 3823-3830.

Demeestere, K., Dewulf, J., Witte, B.D. and Langenhove, H.V. (2007) Sample preparation for the analysis of volatile organic compounds in air and water matrices, *Journal of Chromatography A*, **1153**, 130-144.

Eisert, R. and Levsen, K. (1996) Solid-phase microextraction coupled to gas chromatography: A new method for the analysis of organics in water, *Journal of Chromatography A*, **733**, 143-157.

Erbil, H.Y. and Avci, Y. (2002) Simultaneous determination of toluene diffusion coefficient in air from thin tube evaporation and sessile drop evaporation on a solid surface, *Langmuir*, **18**, 5113-5119.

Hewitt, C.N., Hayward, S. and Tani, A. (2003) The application of proton transfer reaction-mass spectrometry (PTR-MS) to the monitoring and analysis of volatile organic compounds in the atmosphere, *Journal of Environmental Monitoring*, **5**, 1-7.

Hippelein, M. (2006) Analysing selected VVOCs in indoor air with solid phase microextraction (SPME): A case study, *Chemosphere*, **65**, 271-277.

Hippelein, M. (2004) Background concentrations of individual and total volatile organic compounds in residential indoor air of Schleswig-Holstein, Germany, *Journal of Environmental Monitoring*, **6**, 745-752.

Hsieh, L.L., Chang, C.C., Sree, U. and Lo, J.G. (2006) Determination of volatile organic compounds in indoor air of buildings in nuclear power plants, Taiwan, *Water, Air, and Soil Pollution*, **170**, 107-121.

Huang Y., Ho, S.S.H., Ho, K.F., Lee, S.C., Gao, Y., Cheng, Y. and Chan, C.S. (2011) Characterization of biogenic volatile organic compounds (BVOCs) in cleaning reagents and air fresheners in Hong Kong, *Atmospheric Environment*, **45**, 6191-6196.

Huang Y., Ho, S.S.H., Ho, K.F., Lee, S.C., Gao, Y. and Feng, N.S.Y. (2012) Optimization of solid-phase microextraction (SPME) to determine airborne biogenic volatile organic compounds (BVOCs): An application for measurement of household cleaning products, *Analytical Methods*, **4**, 277-283.

Huxham, M. and Thomas, C.L.P. (2000) Sampling procedures for intrinsically valid volatile organic compound measurements, *Analyst*, **125**, 825-832.

Janes, D.W., Durning, C.J., Pel, D.M., Lynch, M.S., Gill, C.G. and Krogh, E.T. (2008) Modeling analyte permeation in cylindrical hollow fiber membrane introduction mass spectrometry, *Journal of Membrane Science*, **325**, 81-91.

Jia, C., Batterman, S. and Godwin, C. (2008) VOCs in industrial, urban and suburban neighborhoods, Part 1: Indoor and outdoor concentrations, variation, and risk drivers, *Atmospheric Environment*, **42**, 2083-2100.

Kataoka, H., Lord, H.L. and Pawliszyn, J. (2000) Applications of solid-phase microextraction in food analysis, *Journal of Chromatography A*, **880**, 35-62.

Klepeis, N.E., Nelson, W.C., Ott, W.R., Robinson, J.P., Tsang, A.M., Switzer, P., Behar, J.V., Hern, S.C., and Englemann, W.H. (2001) The National Human Activity Pattern Survey (NHAPS): a resource for assessing exposure to environmental pollutants, *Journal of Exposure Analysis and Environmental Epidemiology*, **11**, 231-252.

Koziel J.A. and Novak, I. (2002) Sampling and sample-preparation strategies based on solid-phase microextraction for analysis of indoor air, *Trends in Analytical Chemistry*, **21**, 840-850.

Kuster, W.C., Jobson, B.T., Karl, T., Riemer, D., Apel, E., Goldan, P.D. and Fehsenfeld, F.C. (2004) Intercomparison of volatile organic carbon measurement techniques and data at La

Porte during the TexAQS2000 air quality study, *Environmental Science and Technology*, **38**, 221-28.

Lord, H. and Pawliszyn, J. (2000) Microextraction of drugs, *Journal of Chromatography A*, **902**, 17-63.

Lue, S.J., Wang, S.F., Wang, L.D., Chen, W.W., Du, K.M. and Wu, S.Y. (2008) Diffusion of multicomponent vapors in a poly(dimethyl siloxane) membrane, *Desalination*, **233**, 277-285.

Martos, P.A. and Pawliszyn, J. (1997) Calibration of solid phase microextraction for air analyses based on physical chemical properties of the coating, *Analytical Chemistry*, **69**, 206-215.

Mills, G.A. and Walker, V. (2002) Headspace solid-phase microextraction procedures for gas chromatographic analysis of biological fluids and materials, *Journal of Chromatography A*, **902**, 267-287.

Mølhave, L. (1989) The sick buildings and other buildings with indoor climate problems, *Environmental International*, **15**, 65-74.

Namiesnik, J., Zygmunt, B. and Jastrzebska, A. (2000) Application of solid-phase microextraction for determination of organic vapours in gaseous matrices, *Journal of Chromatography A*, **885**, 405-418.

Nicolle, J., Desauziers, V. and Mocho, P. (2008) Solid phase microextraction sampling for a rapid and simple on-site evaluation of volatile organic compounds emitted from building materials, *Journal of Chromatography A*, **1208**, 10-15.

Nicolle, J., Desauziers, V., Mocho, P. and Ramalho, O. (2009) Optimization of FLEC-SPME for field passive sampling of VOCs emitted from solid building materials, *Talanta*, **80**, 730-737.

Ochiai, N., Daishima, S. and Cardin, D.B. (2003) Long-term measurement of volatile organic compounds in ambient air by canister-based one-week sampling method, *Journal of Environmental Monitoring*, **5**, 997-1003.

Ohura, T., Amagai, T., Senga, Y. and Fusaya, M. (2006) Organic air pollutants inside and outside residences in Shimizu, Japan: Levels, sources and risks, *Science of the Total Environment*, **366**, 485-499.

Ouyang, G. and Pawliszyn, J. (2006) Recent developments in SPME for on-site analysis and monitoring, *Trends in Analytical Chemistry*, **25**, 692-703.

Pacenti, M., Dugheri, S., Boccalon, P., Arcangeli, G., Dolara, P. and Cupelli, V. (2010) Air monitoring and assessment of occupational exposure to peracetic acid in a hospital environment, *Industrial Health*, **48**, 217-221.

Pacolay, B.D., Ham, J.E. and Wells, J.R. (2006) Use of solid-phase microextraction to detect and quantify gas-phase dicarbonyls in indoor environments, *Journal of Chromatography A*, **1131**, 275-280.

Rappenglück, B., Apel, E., Bauerfeind, M., Bottenheim, J., Brickell, P., Čavolka, P., Cech, J., Gatti, L., Hakola, H., Honzak, J., Junek, R., Martin, D., Noone, C., Plass-Dülmer, Ch., Travers, D. and Wang D. (2006) The first VOC intercomparison exercise within the Global Atmosphere Watch (GAW), *Atmospheric Environment*, **40**, 7508-7527.

Ras, M.R., Marce, R.M. and Borrul, F. (2008) Solid-phase microextraction - Gas Chromatography to determine volatile organic sulfur compounds in the air at sewage treatment plants, *Talanta*, **77**, 774-778.

Rennix, C.P., Quinn, M.M., Amoroso, P.J., Eisen, E.A. and Wegman, D.H. (2005) Rish of breast cancer among enlisted army women occupationally exposed to volatile organic compounds, *American Journal of Industrial Medicine*, **48**, 157-167.

Salthammer, T. and Bahadir, M. (2009) Occurrence, dynamics and reactions of organic pollutants in the indoor environment, *Clean*, **37**, 417-435.

Salthammer, T. and Mentese, S. (2008) Comparison of analytical techniques for the determination of aldehydes in test chambers, *Chemosphere*, **73**, 1351-1356.

Sax, S.N., Bennett, D.H., Chillrud, S.N., Ross, J., Kinney, P.L. and Spengler, J.D. (2006) A cancer risk assessment of inner-city teenagers living in New York City and Los Angeles, *Environmental Health Perspectives*, **114**, 1558-1566.

Tassi, F., Capecchiacci, F., Buccianti, A. and Vaselli, O. (2012) Sampling and analytical procedures for the determination of VOCs released into air from natural and anthropogenic sources: A comparison between SPME (Solid Phase Micro Extraction) and ST (Solid Trap) methods, *Applied Geochemistry*, **27**, 115-123.

Toscano, P., Gioli, B., Dugheri, S., Salvini, A., Matese, A., Bonacchi, A., Zaldei, A., Cupelli, V. and Miglietta, F. (2011) Locating industrial VOC sources with aircraft observations, *Environmental Pollution*, **159**, 1174-1182.

Tumbiolo, S., Gal, J.F., Maria, P.C. and Zerbinati, O. (2004) Determination of benzene, toluene, ethylbenzene and xylenes in air by solid phase micro-extraction/gas chromatography/mass spectrometry, *Analytical and Bioanalytical Chemistry*, **380**, 824-830.

Ulrich, S. (2000) Solid-phase microextraction in biomedical analysis, *Journal of Chromatography A*, **902**, 167-194.

Vas, G. and Vekey, K. (2004) Solid-phase microextraction: a powerful sample preparation tool prior to mass spectrometric analysis, *Journal of Mass Spectrometry*, **39**, 233-254.

Wang D.K.W. and Austin, C.C. (2006) Determination of complex mixtures of volatile organic compounds in ambient air: an overview, *Analytical and Bioanalytical Chemistry*, **386**, 1089-1098.

Wang, J.L., Chen, S.W. and Chew, C. (1999) Automated gas chromatography with cryogenic/sorbent trap for the measurement of volatile organic compounds in the atmosphere, *Journal of Chromatography A*, **863**, 183-193.

Wang, J.X., Tuduri, L., Mercury, M., Millet, M., Briand, O. and Montury, M. (2009) Sampling atmospheric pesticides with SPME: Laboratory developments and field study, *Environmental Pollution*, **157**: 365-370.

Warneke, C., Gouw, J.A.D., Kuster, W.C., Goldan, P.D. and Fall, R. (2003) Validation of atmospheric VOC measurements by proton-transfer-reaction mass spectrometry using a gas-chromatographic preseparation method, *Environmental Science and Technology*, **37**, 2494-2501.

Weschler, C.J. (2009) Changes in indoor pollutants since the 1950s, *Atmospheric Environment*, **43**, 153-169.

Weschler, C.J., Wisthaler, A., Cowlin, S., Tamas, G., Strom-Tejsen, P., Hodgson, A.T., Destaillats, H., Herrington, J., Zhang, J. and Nazaroff, W. (2007) Ozone-initiated chemistry in an occupied simulated aircraft cabin, *Environmental Science and Technology*, **41**, 6177-6184.

Yuan, H., Little, J.C. and Hodgson, A.T. (2007) Transport of polar and non-polar volatile compounds in polystyrene foam and oriented strand board, *Atmospheric Environment*, **41**, 3241-3250.

Zee, G.V. and Graauw, J.E. (1997) Determination of the diffusivity in elastomer solutions by batch sorption studies from a dilute liquid phase, *Journal of Applied Polymer Science*, **66**, 347-353.

Zhu, J., Newhook, R., Marro, L. and Chan, C.C. (2005) Selected volatile organic compounds in residential air in the city of Ottawa, Canada, *Environmental Science and Technology*, **39**, 3964-3971.

Zuraimi, M.S., Tham, K.W. and Sekhar, S.C. (2004) A study on the identification and quantification of sources of VOCs in 5 air-conditioned Singapore office buildings, *Building and Environment*, **39**, 165-177.

Chapter 6 – Developing a Reference Material for Formaldehyde Emissions Testing: Proof of Concept

Zhe Liu[1], Xiaoyu Liu[2] and John C. Little[1]

[1]Department of Civil and Environmental Engineering, Virginia Tech, Blacksburg, VA 24061

[2]National Risk Management Research Laboratory, Environmental Protection Agency, Research Triangle Park, NC 27711

6.1 Abstract

Due to the serious health effects caused by indoor exposure to formaldehyde gas, there is a need to reduce formaldehyde emissions from indoor materials and products. To demonstrate compliance with low-emission standards, manufacturers generally submit products to independent laboratories for emissions testing. However, different emissions testing methods are specified in available standards for formaldehyde and there is substantial variability within the testing procedures of individual laboratories, both of which can lead to large uncertainties in emissions testing results. There is thus a compelling need for a reference material that can be used as a standard emission source of formaldehyde by individual laboratories. In this paper, a prototype reference material for formaldehyde emissions testing was created by infusing gas-phase formaldehyde into a thin polymer film via a sorption process. It was found that sorption of formaldehyde by the film occurs through both diffusion within the film and formaldehyde polymerization at the film surface, but that desorption of formaldehyde from the film is primarily due to diffusion. A fundamental mass-transfer model based on diffusion was therefore employed to predict formaldehyde emissions from the pre-loaded material. The preliminary results show that the model prediction compares reasonably well to the measured emission profiles in small chambers. With the model prediction serving as the reference emission value, the reference material can be used to validate different emissions testing methods, to evaluate the test performance, and to identify the root causes of variability.

6.2 Introduction

Formaldehyde ($H_2C=O$), the simplest member of the aldehyde family, is a flammable, colorless gas with a pungent odor at room temperature. Since the 1880s, formaldehyde has been produced commercially and in recent years, annual global industrial production of formaldehyde is estimated at more than 20 million tonnes (Bizzari, 2000). One of the primary uses of formaldehyde is for producing synthetic resins such as urea-formaldehyde, phenol-formaldehyde, melamine-formaldehyde and polyacetal resins, which are used as adhesives and impregnating resins in wood products, curable moulding products, and textile, leather, rubber and cement industries (IARC, 2006). These products may emit formaldehyde during the use phase although the emission rate may vary greatly (Kelly et al., 1999; Meyer and Boehme, 1997; Weigl et al., 2009). Due to the ubiquitous presence of formaldehyde emission sources indoors as well as the slow removal rate in the indoor environment (outdoor formaldehyde is readily removed by photolysis and reaction with hydroxyl radicals in the presence of sunlight to produce carbon dioxide), formaldehyde concentration in indoor air is usually much higher than outdoors, ranging from 10 to 4000 $\mu g/m^3$ (IARC, 2006; Salthammer et al., 2010; WHO, 1989). Therefore, although people can be exposed to formaldehyde through other sources such as food, indoor air is the most influential exposure pathway for the general population, while occupational exposures are important for specific populations such as employees in formaldehyde-related industries and sanitary services (Kauppinen et al, 2000). It is well recognized that exposure to formaldehyde can cause irritation of the eye and upper respiratory system and induce allergic contact dermatitis and contact urticaria (Arts et al., 2008; Koss and Tesseraux, 1999; Paustenbach et al., 1997). Because of the cytotoxic and genotoxic effects of chronic formaldehyde exposure, it has been classified as "carcinogenic to humans (Group 1)" by the International Agency for Research on Cancer (IARC, 2006) and described as a "known human carcinogen" by the US National Toxicology Program (NTP, 2011). In addition, several studies have suggested that long-term exposure to formaldehyde may lead to teratogenicity and a variety of neural and vascular disorders (Aslan et al., 2006; Kilburn, 1994; Sakanashi et al., 1996; Yu et al., 2003).

Due to the health risks associated with indoor formaldehyde exposure, various guidelines and recommendations have been established around the world for formaldehyde in indoor air (Salthammer et al., 2010). For example, the Formaldehyde Standards for Composite Wood

Products Act was signed into law by the US President in July 2010. To demonstrate compliance with these standards, manufacturers and independent laboratories often conduct formaldehyde emissions testing in chambers with environmental conditions similar to a real building. Unfortunately, there are substantial unidentified uncertainties involved in these chamber tests, with published inter-laboratory studies for emissions of volatile organic compounds (VOCs) showing coefficients of variation between measured emission rates on the order of 50 % and as large as 300 % (Howard-Reed et al., 2007). For formaldehyde alone, standard emissions testing methods vary substantially in different countries, creating additional variability in the emissions testing results (Risholm-Sundman et al., 2007). Currently, equivalence between emissions testing methods and laboratories is established in inter-laboratory studies. However, inter-laboratory studies can be costly and time-consuming, and may lead to inconclusive results, especially because there is no way to identify which laboratory's results are correct. The creation of a well characterized reference material for formaldehyde emissions testing is therefore a critical prerequisite for validating and calibrating emissions testing procedures and developing low-emission products.

In collaboration with the National Institute of Standards and Technology (NIST), we have developed a prototype reference material for VOCs emissions testing (Cox et al., 2010; Howard-Reed et al., 2011). It consists of a thin polymethylpentene (PMP) film that has been loaded to equilibrium with a carrier gas stream containing a known gas-phase toluene concentration. Extensive chamber tests at NIST and other emissions testing laboratories have shown that the reference material mimics real homogenous building materials with emission profiles that can be accurately predicted by a mechanistic model. The model predicted emission profiles therefore serve as true reference values and can be compared to emissions testing results of individual laboratories. This is of considerable benefit because the model not only provides reference emission values for validating individual laboratories' performance, but also can provide insight into the likely causes of variability and experimental errors. Our recent work also shows that the same approach using PMP is applicable to n-butanol, a polar compound.

In the present work, a similar procedure was employed for creating a reference material for formaldehyde, which involved the following basic steps (Figure 6.1): (1) identifying a suitable

polymer substrate and determining its mass-transfer properties; (2) loading formaldehyde into the polymer film; (3) predicting formaldehyde emissions from the pre-loaded polymer films employing a fundamental emission model; (4) measuring formaldehyde emissions from the pre-loaded films in small environmental chambers; and, (5) comparing the predicted emission profiles with the measured results. It is found that polycarbonate (PC) serves as a promising substrate although the mass transfer of formaldehyde is complicated by its chemical reactivity. Overall, our preliminary results show that the model predicted emission profile from the pre-loaded PC film compared reasonably well to the measurements in chamber tests, demonstrating the feasibility of the proposed approach to create a reference material for formaldehyde emissions testing.

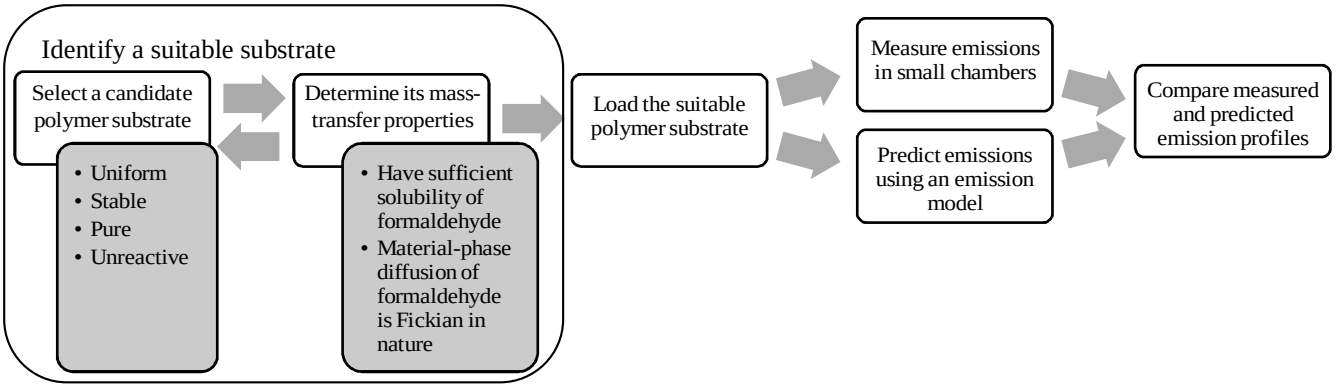

Figure 6.1 Strategy to develop a reference material for formaldehyde emissions testing.

6.3 Materials and methods

6.3.1 Selecting polymer substrates

As outlined in Figure 6.1, identifying a suitable polymer substrate was the first step in creating a viable reference material. An ideal polymer should be uniform and stable so that the material properties do not change. It should neither react with formaldehyde nor contain any reactive or volatile impurities (additives or contaminants) that may confound the mass transfer of formaldehyde within the material. Furthermore, the success of this method depends on two key criteria: firstly, formaldehyde needs to be sufficiently soluble in the polymer substrate so that an adequate amount of formaldehyde can be loaded into and then allowed to emit from the substrate; and secondly, the diffusion of formaldehyde in the polymer substrate needs to be ideal or "Fickian" in nature. Although the encouraging application of PMP for both toluene and n-

butanol suggests that diffusion of formaldehyde within PMP, a non-polar polymer, may be ideal, its solubility is rather low given formaldehyde's small molecular size and low boiling point. It is expected that formaldehyde has higher solubility in polar matrices. For example, the solubility in polycarbonate is reported to be about 150 times higher than in polypropylene (Hennebert, 1988). However, additional attention should be paid when selecting polar polymers because formaldehyde may react with hydroxyl (–OH) or amine ($–NH_2$) groups in polymers by forming a methylol ($–CH_2OH$) group with the active hydrogen (Walker, 1975). Such reactions have been observed in cellulose, paper, nylon, latex and polyester, rendering formaldehyde's transport within these materials non-ideal (Hennebert, 1988). Therefore, we selected a PMP material with a thickness of 0.01 inch and two polycarbonate (PC) materials with thicknesses of 0.01 and 0.02 inch, respectively, as candidates in this study. The three polymeric materials are all commercially available and were purchased directly from manufacturers in large pristine sheets.

6.3.2 Generating gas-phase formaldehyde

As described later, a continuous gas stream with a constant formaldehyde concentration was needed to characterize mass transfer properties of candidate polymers and to load formaldehyde into the polymer substrate. The formaldehyde generating system consisted of a diffusion vial placed in a temperature-controlled oven (Dynacalibrator Model 190, VICI Metronics Inc., Santa Clara, CA) with a purge flow regulated by a mass-flow controller (Model FC-280S, Tylan General, Carson, CA). Solid paraformaldehyde (97%, Alfa Aesar, Ward Hill, MA) contained in the diffusion vial depolymerized to monomeric formaldehyde gas at elevated temperatures (Röck et al., 2010), which then diffused into the purge flow of dry and clean air (UN1002, Airgas Inc., Radnor, PA). Maintaining the purge flow rate constant at 250±5 mL/min, formaldehyde concentration in the generated gas stream was varied by adjusting the oven temperature and using diffusion vials with different diffusion path lengths.

To determine the formaldehyde release rate from the diffusion vial containing paraformaldehyde, it was weighed by a mechanical balance (10 μg) over appropriate time intervals. The linearity between the measured weight and time can be examined to determine whether the formaldehyde release rate was constant. The formaldehyde concentration in the generated gas stream can then be calculated by dividing the formaldehyde release rate by the purge flow rate. The true flow rate

was measured using a bubble flowmeter (mini-Buck Calibrator, A.P. BUCK Inc., Orlando, FL). For comparison, the formaldehyde concentration in the gas stream was also directly measured by visible absorption spectrometry, following NIOSH Analytical Method 3500 (NIOSH, 1994). Briefly, an appropriate volume of the gas stream was passed through two impingers in series containing 20 mL 1% sodium bisulfite solution so that the gas-phase formaldehyde was completely absorbed by the solution, forming $HOCH_2 \cdot SO_3Na$. The backup impinger was used to check collection efficiency. Then aliquots of the impinger solution were transferred to a flask and mixed with 0.1 mL 1% chromotropic acid and 6 mL concentrated sulphuric acid. After heating the sample solution at 95 ^oC for 15 minutes and maintaining it at room temperature for 2 hours so that the chromophore was fully developed, the absorbance at 580 nm was measured using a spectrophotometer (Spectronic 20D+, Thermo Scientific, West Palm Beach, FL). Meanwhile, a blank and six calibration standard solutions prepared from a formaldehyde standard aqueous solution (1000 μg/mL, AccuStandard, New Haven, CT) were also treated with the reagents and analyzed by the spectrophotometer for absorbance at 580 nm. A calibration line (absorbance versus formaldehyde concentration of the calibration standard) was constructed and the formaldehyde concentration in the tested solution sample was obtained from the calibration line. Finally, formaldehyde concentration in the gas stream was calculated using an appropriate aliquot factor and the gas sample volume.

6.3.3 Determining mass-transfer properties of selected polymers

As well documented in the literature, the key mass-transfer parameters of a given polymeric material which control its formaldehyde emissions include diffusion coefficient of formaldehyde in the material (D) and partition coefficient of formaldehyde between the material and air (K) (Cox et al., 2010; Xiong et al., 2011a; Xiong et al., 2011b). To determine D and K, a microbalance sorption/desorption method was employed (Cox et al., 2001). As shown in Figure 6.2(a), a polymer film sample was continuously weighed by a high-resolution (0.1 μg) dynamic microbalance (Thermo Cahn D-200, Thermo Fisher Scientific, Waltham, MA). During the sorption test when air containing a known concentration of formaldehyde was passed across the film, formaldehyde was sorbed by the material and the mass gain of the film was recorded, generating a sorption curve. Once the film had reached sorption equilibrium with the gas stream, clean air was passed through the film causing desorption, with a desorption curve generated by

measuring the mass loss from the film over time. When Fickian diffusion controls the sorption and desorption process, D can be determined by fitting a Fickian diffusion model to the sorption and desorption curves. Under the experimental configuration, the mass change caused by Fickian diffusion of formaldehyde inside the film is given by (Crank, 1975):

$$\frac{M_t}{M_\infty} = 1 - \sum_{n=0}^{\infty} \frac{8}{(2n+1)^2 \pi^2} \cdot \exp\left\{\frac{-D(2n+1)^2 \pi^2 t}{4H^2}\right\} \tag{6.1}$$

where M_t is the total formaldehyde mass that has entered or left the film via diffusion in time t, M_∞ is the formaldehyde mass in the film when partition equilibrium is reached between the film and the air, and 2H is the film thickness. Furthermore, K can be derived by dividing M_∞ by the volume of the film sample and the gas-phase formaldehyde concentration.

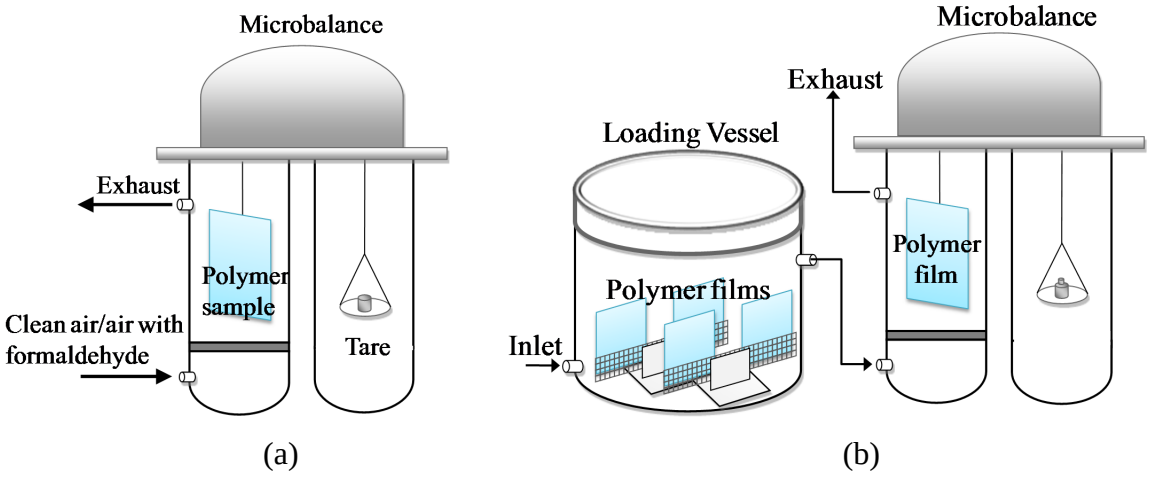

Figure 6.2 (a) Microbalance sorption/desorption test: air with a constant formaldehyde concentration is swept across the film for the sorption test and clean air is swept across the sample for the desorption test; (b) the microbalance and loading vessel system.

6.3.4 Loading the identified polymer substrate with formaldehyde

After a suitable polymer substrate was identified, reference materials were created by loading precisely-cut film samples with formaldehyde. As shown in Figure 6.2(b), formaldehyde was infused into the films by passing a continuous air stream with a constant formaldehyde concentration through a stainless steel loading vessel containing several films and allowing material-phase/gas-phase sorption equilibrium to be reached. The effluent from the loading vessel was passed across an addition film whose mass gain was continuously monitored by a

microbalance during the loading process. Because the film on the microbalance went through the same mass transfer process as those in the loading vessel, the microbalance data were used to determine when material-phase/gas-phase equilibrium was reached. Furthermore, the material-phase concentration in the loaded films, C_0, can be obtained from the microbalance data, by dividing the final measured mass of formaldehyde infused into the film by the film sample volume.

6.3.5 Measuring formaldehyde emissions from pre-loaded films in small chambers

After material-phase/gas-phase sorption equilibrium had been reached in the loading vessel, films were removed from the loading vessel rapidly, wrapped in aluminum foil, sealed in zip-loc bags, and placed in coolers containing dry ice. The coolers were then shipped via overnight mail to the US Environmental Protection Agency (EPA) for emissions testing. Once received, the films were retained in the original package and stored at -12 ^{o}C prior to being tested in small chambers. Formaldehyde emission from each film was measured at 23 ºC in a 53-L stainless steel chamber with an air change rate of 1 h^{-1}, following the guidelines of ASTM International *Standard Guide for Small-scale Environmental Chamber Determinations of Organic Emissions from Indoor Materials/Products* (ASTM Standard D5116-2010) (ASTM 2010). Both sides of the film were fully exposed to the chamber air by using a specially-designed sample holder. The chamber air was sampled at appropriate time intervals to measure the gas-phase formaldehyde concentration development in the chamber, according to EPA standard method *Determination of Formaldehyde and Other Aldehydes in Indoor Air Using a Solid Adsorbent Cartridge* (EPA method IP-6A) (US EPA, 1990). Briefly, the chamber air was pulled through a cartridge containing silica gel coated with 2,4-dinitrophenylhydrazine (DNPH) so that the gas-phase formaldehyde was collected on the cartridge by forming hydrazones with DNPH. After sampling, the cartridge was eluted with acetonitrile to extract the hydrazones, which were then analyzed by high performance liquid chromatography (HPLC) and ultraviolet (UV) spectroscopy.

6.3.6 Predicting formaldehyde emissions from pre-loaded films

Figure 6.3 shows the mechanisms governing the emission of formaldehyde from a homogeneous solid material slab in a test chamber. If we assume that external convective mass-transfer rate is

much faster than internal diffusion, then a simple fundamental model can predict the emission profile. The following derivation applies to emissions from a single-sided source, but the solution can easily be adjusted and applied to a double-sided source. The transient diffusion equation in the material slab is given by Fick's second law:

$$\frac{\partial C}{\partial t} = D\frac{\partial^2 C}{\partial x^2} \tag{6.2}$$

where t is time, x is the distance from the base of the slab, and C is the material-phase concentration of formaldehyde as a function of t and x. The initial condition assumes a uniform material-phase concentration of formaldehyde in the slab, C_0. The boundary condition at the base of the slab assumes there is no mass flux through the bottom surface. The boundary condition at the exposed surface is imposed via a mass balance on formaldehyde in the chamber air, or

$$\frac{dy}{dt}\cdot V = Q\cdot y_{in} - A\cdot D\cdot \left.\frac{\partial C}{\partial x}\right|_{x=L} - Q\cdot y \tag{6.3}$$

where y_{in} and y are the gas-phase formaldehyde concentration in the influent air and the bulk chamber air respectively, Q is the volumetric air flow rate, V is the well-mixed chamber volume, A is the exposed surface area of the slab, and L is the thickness of the slab. A linear and instantaneously reversible equilibrium relationship is assumed between the slab surface and the chamber air, or

$$K = \left.C\right|_{x=L} / y \tag{6.4}$$

Equation (6.4) implies that the convective mass-transfer resistance through the boundary layer at the exposed surface is negligible compared to internal diffusion, which is common for compounds with small D (Cox et al., 2010). Assuming y_{in} and the initial chamber concentration are zero, an analytical solution to these equations was given by Little et al. (1994):

$$C(x,t) = 2C_0\sum_{n=1}^{\infty}\left\{\frac{\exp\left(-Dq_n^2 t\right)\left(h - kq_n^2\right)\cos\left(q_n x\right)}{\left[L\left(h - kq_n^2\right)^2 + q_n^2\left(L + k\right) + h\right]\cos\left(q_n L\right)}\right\} \tag{6.5}$$

where

$$h = Q/(ADK) \tag{6.6}$$

$$k = V/(AK) \tag{6.7}$$

and the q_ns are the positive roots of

$$q_n \tan\left(q_n L\right) = h - kq_n^2 \tag{6.8}$$

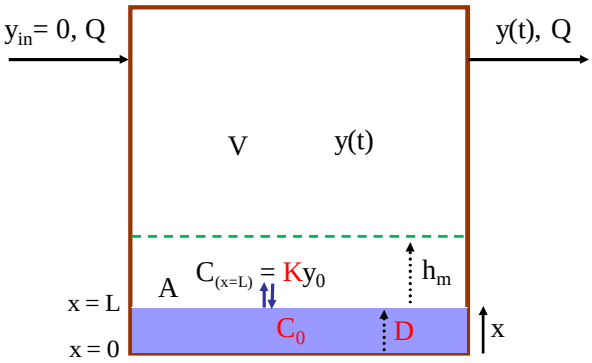

Figure 6.3 Schematic representation of a solid formaldehyde source in a test chamber showing mechanisms controlling the emission rate.

When key model parameters, D, K and C_0 are determined as described above and other parameters (V, Q, L, and A) are obtained from the chamber test configuration, C can be obtained using Equation (6.5) and y can be then simply calculated using Equation (6.4). In addition, when the model is used to predict the emission from a pre-loaded film with both sides exposed to the chamber air, L should be half of the film thickness and A should be the total surface area of both sides.

6.4 Results and discussion

6.4.1 Generating gas-phase formaldehyde

By weighing the diffusion vial containing paraformaldehyde at certain time intervals, the formaldehyde release rate could be determined. Figure 6.4 shows the measured weight change of diffusion vials (Vial 1, 2 and 3) containing paraformaldehyde maintained at different temperatures (85, 95, 100, and 105 ºC). It is found that the weight decrease in all cases followed a linear pattern: when linear regression is performed between weight and time in each case, coefficients of determination (R^2) for all six cases are larger than 0.9995. Therefore, the formaldehyde release rate in each case, derived from the slope of the corresponding linear regression, was constant over time. The difference in diffusion vials (Vial 1, 2, and 3) is that Vial 1 has the longest diffusion path, Vial 3 has the shortest diffusion path, and Vial 2 lies somewhere between the two extremes. As shown in Figure 6.4, at a fixed temperature, the formaldehyde release rate and thus the concentration in the generated gas stream increases when the diffusion path length decreases (from Vial 1 to 3). Moreover, the formaldehyde release rate from a

diffusion vial increases with temperature, which is due to the faster depolymerization rate of solid paraformaldehyde at higher temperatures.

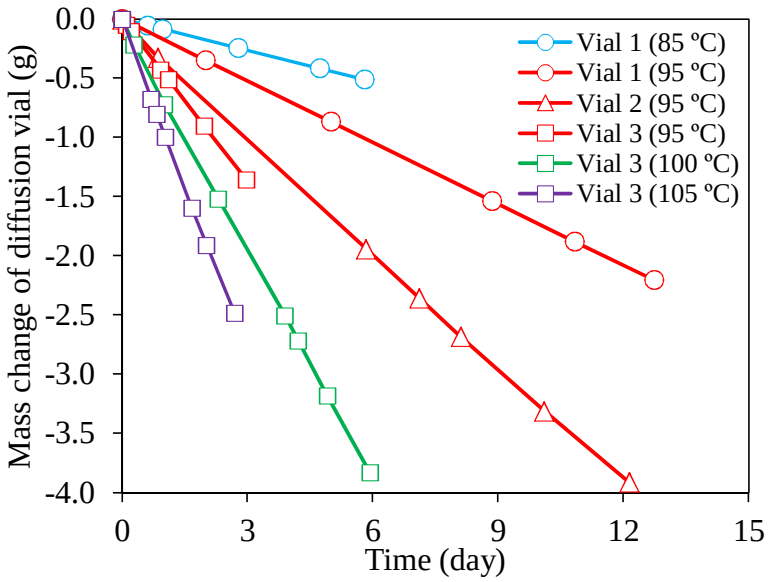

Figure 6.4 Measured weight decrease of diffusion vials over time: marker color indicates temperature and marker shape indicates emission vials with different diffusion path length.

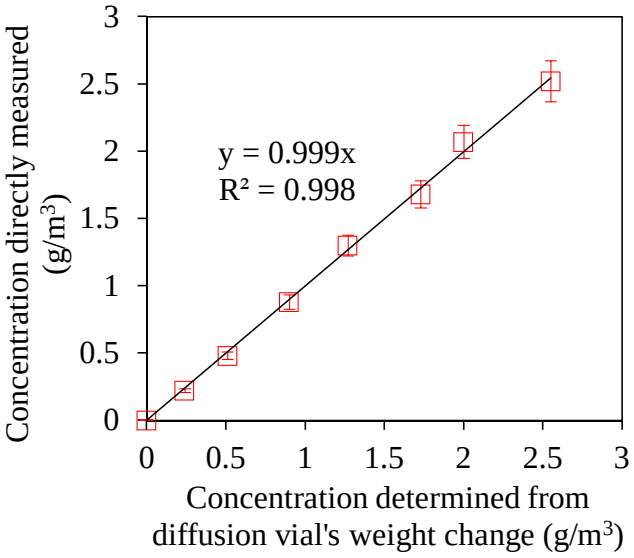

Figure 6.5 Comparison of directly measured formaldehyde concentration with that calculated from diffusion vial's weight change.

Figure 6.5 compares the directly measured formaldehyde concentration in the generated gas stream using visible absorption spectrometry with that determined from the corresponding diffusion vial's weight change. It is found that the gas-phase formaldehyde concentrations obtained by these two approaches match well (a paired t test yields a P value of 0.66), suggesting that either approach is able to determine the concentration accurately. Overall, the results shown in Figure 6.4 and 6.5 prove that a gas stream with a constant formaldehyde concentration at different levels can be achieved using the generating system.

6.4.2 Determining mass-transfer properties of selected polymers

Considering the criteria in Figure 6.1, one PMP film with a thickness of 0.01 inch and two different PC films with thicknesses of 0.01 and 0.02 inch, respectively, were chosen as candidate substrates. To determine their mass-transfer properties, small film samples were cut from the original large sheets for the microbalance sorption/desorption tests. The measured mass gain of a 0.01 inch thick PMP sample (3.6 cm × 3.6 cm) during a sorption/desorption test is shown as blue circles in Figure 6.6(a). The gas-phase formaldehyde concentration for the sorption test was 1.73 g/m^3. If simple Fickian diffusion governs the sorption process, the mass would level off when reaching sorption equilibrium, as demonstrated for toluene/PMP and phenol/vinyl flooring (Cox et al., 2001; Cox et al., 2010). But in contrast to what would be expected for simple Fickian diffusion, the mass of the PMP film continued to increase linearly as shown in Figure 6.6(a). Meanwhile, the mass desorbed from the PMP film during the desorption period (~0.025 mg) was much less than the mass sorbed by the film during the sorption period (~0.07 mg). Given that PMP should not react with formaldehyde, a possible explanation is that formaldehyde adsorption and polymerization occurred at the film surface, with overall mass gain during the sorption cycle due to both Fickian diffusion inside the film (absorption) and surface polymerization (adsorption). It has been shown that surfaces such as glass and stainless steel readily adsorb formaldehyde, with the amount being dependent on the nature of the surface, relative humidity, gas-phase formaldehyde concentration, and exposure time (Braswell et al., 1970). It should be noted that while dry air was used for the purge flow, the gas stream still contained a little water vapor, as a result of the depolymerization of paraformaldehyde in the diffusion vial. As demonstrated in the work of Braswell et al. (1970), surface polymerization may occur even at very low humidity levels because a trace amount of water induces polymerization, building

polyoxymethylene on surfaces (Walker, 1975). Moreover, the linear mass increase due to polymerization implies that the surface polymerization rate was constant throughout the sorption period. As shown in Figure 6.6(b), the linear mass gain due to polymerization (purple line) can be subtracted from the total mass gain (blue line), yielding the net mass gain due to diffusion (green line) which can be very well described by the Fickian diffusion model given in Equation (6.1). Assuming that polymerization at the film surface and Fickian diffusion inside the film are completely independent and using the method described above, D and K can be determined to be $(3.5\pm0.2)\times10^{-14}$ m^2/s and 40±5. K of formaldehyde between PMP and air is much smaller than that of toluene, which is 500±30 (Howard-Reed et al., 2011), indicating that formaldehyde has rather low solubility in PMP. During the desorption period, the mass decrease should be due to Fickian diffusion within the film and depolymerization of polyoxymethylene at the film surface. However, as shown in Figure 6.6(a), it is found that the Fickian diffusion model (Equation (6.1)) with D and K obtained from the sorption test predicts the overall mass decrease well. It appears that depolymerization occurred very slowly and contributed little to the total mass decrease.

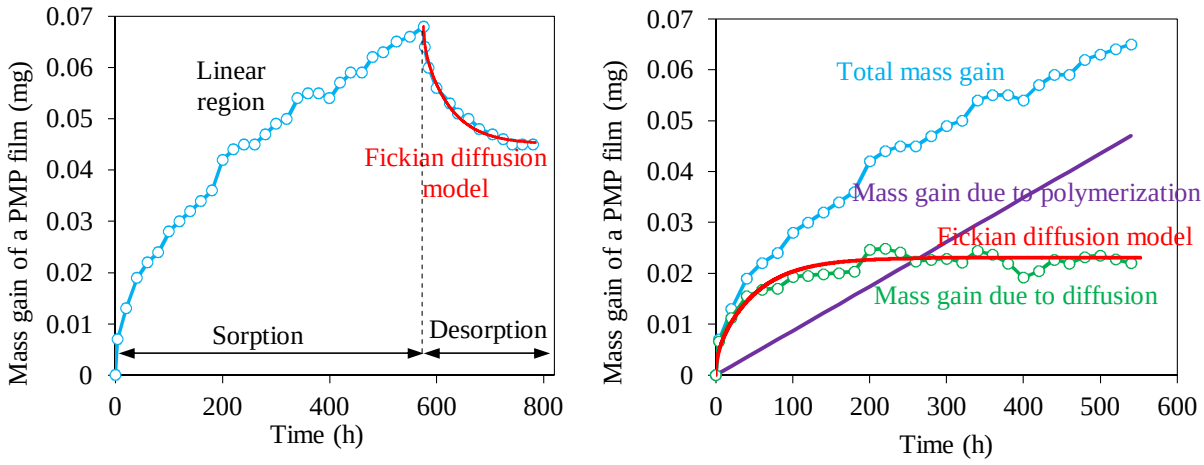

Figure 6.6 Sorption/desorption data and analysis for the 0.01 inch thick PMP.

Figure 6.7 and 6.8 show the microbalance sorption/desorption results for a 0.01 inch thick PC sample (3.6 cm × 3.6 cm) and a 0.02 inch thick PC sample (3.6 cm × 3.6 cm). The gas-phase formaldehyde concentration for these sorption tests was 0.86 g/m^3. The mass increases of these two films during the sorption period followed a similar trend to PMP, as a result of the combined effect of polymerization at the film surface and Fickian diffusion inside the film. Based on the

net mass gain due to diffusion during the sorption period (green lines in Figure 6.7 and 6.8), we can also determine D and K for the two PC films. D and K were found to be $(1.9\pm0.3)\times10^{-13}$ m^2/s and 233±40 for the 0.01 inch thick PC, and $(3.9\pm0.2)\times10^{-13}$ m^2/s and 170±20 for the 0.02 inch thick PC, respectively. Therefore, these two PC films are slightly different in nature, but both of them have much greater solubility than PMP. In addition, the desorption curves of these two film samples can also be well predicted using the Fickian diffusion model with D and K obtained from the sorption tests.

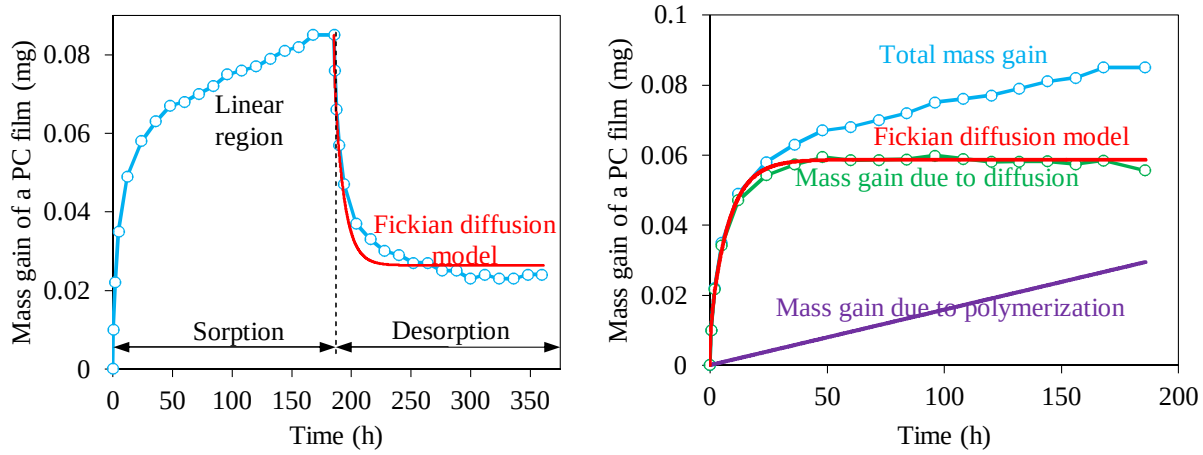

Figure 6.7 Sorption/desorption data and analysis for the 0.01 inch thick PC.

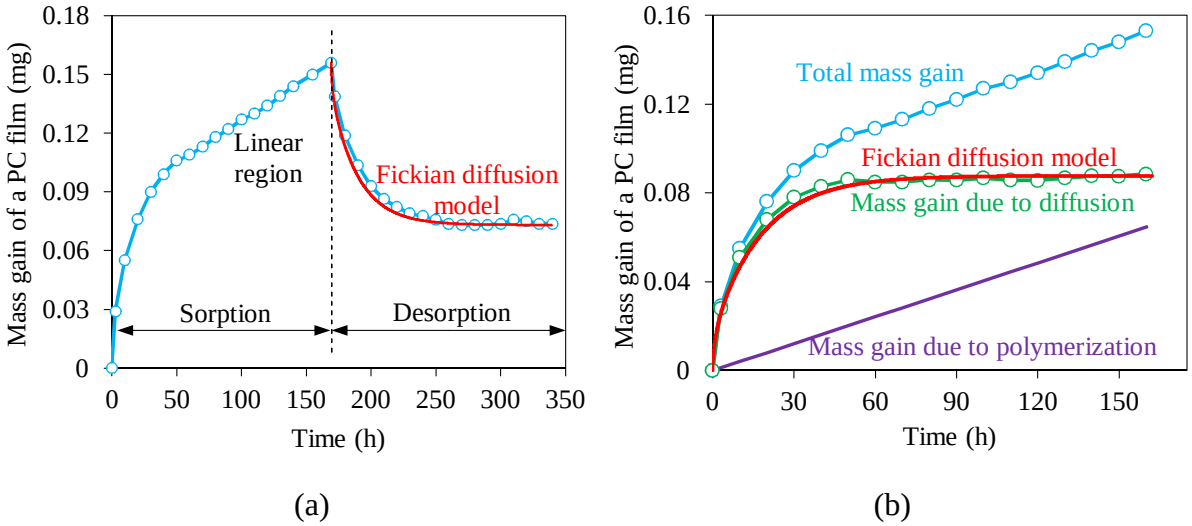

Figure 6.8 Sorption/desorption data and analysis for the 0.02 inch thick PC.

In summary, the sorption/desorption tests of the three polymer candidates suggest that the gross mass uptake during the sorption period was a combined result of constant-rate polymerization of formaldehyde at the film surface (forming polyoxymethylene) and Fickian diffusion inside the film. The depolymerization of polyoxymethylene during the desorption period was very slow and therefore the mass of formaldehyde emitted from the film can be predicted solely based on Fickian diffusion. Finally, the 0.01 inch thick PC was selected as the substrate to create the formaldehyde reference materials.

6.4.3 Measuring and predicting formaldehyde emissions from pre-loaded PC films in small chambers

Three 10 cm × 10 cm films were cut from the 0.01 inch thick PC sheet and loaded in a single batch using a gas stream containing ~0.9 g/m^3 formaldehyde. The loading process lasted for 5 days, long enough for the films to reach sorption equilibrium with the gas stream although the mass never became stable due to formaldehyde polymerization at the film surface. Using the same analysis as in Figure 6.7(b), the net uptake of formaldehyde into the films through diffusion can be obtained and the formaldehyde concentration in the films was determined to be 190±27 g/m^3. The films were then shipped to EPA and tested in small chambers. Figure 6.9 shows the chamber test results of the three pre-loaded films as well as the test conditions (shelf-life and humidity level). The emission profiles are very close, although the age effect and different humidity conditions may explain some of the difference.

Because the desorbed (emitted) mass of formaldehyde from the PC films are primarily due to diffusion instead of polyoxymethylene depolymerization, the emission model based on diffusion introduced earlier is still applicable for formaldehyde and D and K values have been determined to be $(1.9\pm0.3)\times10^{-13}$ m^2/s and 233±40 from the net mass gain due to diffusion during the sorption period. C_0 has been determined based on the net uptake of formaldehyde into pre-loaded films through diffusion, which is 190±27 g/m^3. Therefore, Equation (6.4) and (6.5) can be used to predict the formaldehyde concentration profile in the chamber air during the emission tests. To further estimate the uncertainties of model predicted concentrations associated with the uncertainties of D, K and C_0, the Monte Carlo method (Kim et al., 2004) was employed. 10,000 repeated model simulations were carried out with D, K and C_0 randomly sampled from their

distributions, while the other parameters (L, A, Q, and V) were fixed for each individual run. The results of the 10,000 model predictions were then pooled to assess the expected variation in y as a function of time. Figure 6.9 shows the model prediction, with the black solid line indicating the mean of the transient gas-phase formaldehyde concentration in the chamber air and the shaded area indicting the range of mean ± standard deviation of the transient gas-phase concentration. Compared with the measured results, the model overestimates emissions during the first 20 hours. Possible reasons include: (1) formaldehyde escaped from the pre-loaded films during packaging, shipping, and storage (shelf-life) period, especially when they were removed from the loading vessel and were wrapped; and, (2) the chamber tests were carried out at 23 ºC while the D and K used in the model prediction were obtained from sorption/desorption tests performed at 25 ºC. Higher temperature may tend to increase D and reduce K and thus accelerating emissions (Deng et al., 2009; Zhang et al., 2007). The longer-term predicted concentrations nevertheless compare well with the measured results.

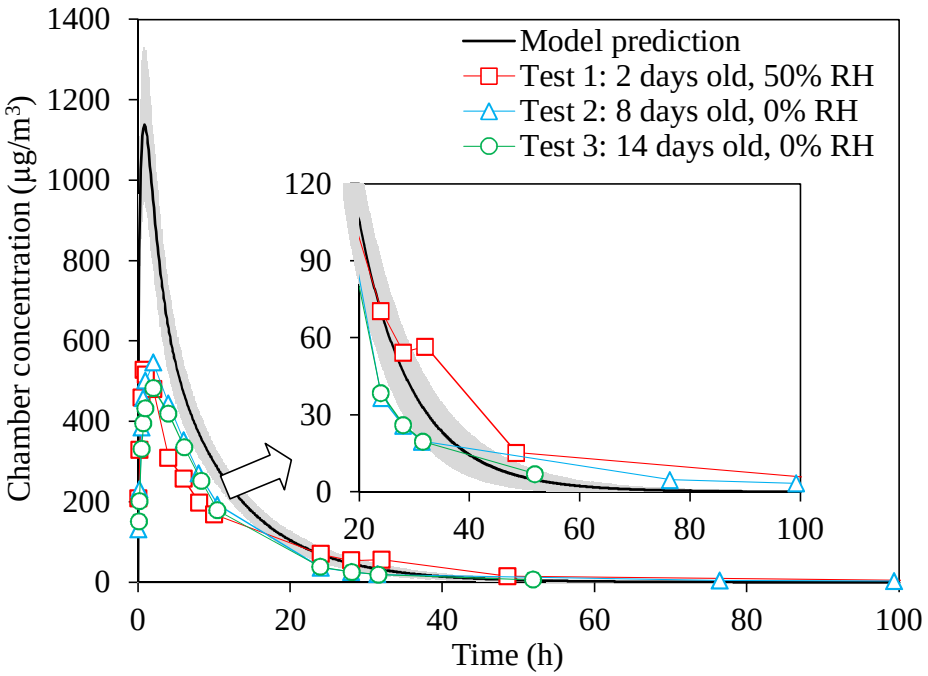

Figure 6.9 Comparison of the measured formaldehyde emission profiles in chamber tests and the model prediction.

6.5 Conclusions

In the present research, we investigated the feasibility of creating a reference material for formaldehyde emissions testing by loading formaldehyde into a suitable polymer substrate and predicting the emissions from pre-loaded films. In the microbalance sorption/desorption tests for a PMP material and two types of PC material, it is found that the formaldehyde sorption process is complicated with Fickian diffusion inside the polymer and polymerization on the polymer surface occurring simultaneously. Fortunately, Fickian diffusion alone dominates desorption and emissions, rendering the emission profiles predictable using a diffusion-based emission model. Prototype reference materials were then created using 0.01 inch thick PC films and the model predicted emission profiles agree reasonably well with the emission chamber measurements. Therefore, when such materials are tested in small chambers by different laboratories, the reference emission profiles predicted by the model can be compared to the observed emission profiles to validate different emissions testing methods, to evaluate the test performance of individual laboratories, and to identify the root causes of variability. While further refinement and testing is needed, our preliminary results suggest that it is indeed possible to create a reference material for formaldehyde emissions testing using the proposed approach.

6.6 Acknowledgements

Financial support from the US EPA under contract EP-11-C-00135 is acknowledged.

6.7 References

Arts, J.H.E., Muijser, H., Kuper, C.F. and Woutersen, R.A. (2008) Setting an indoor air exposure limit for formaldehyde: Factors of concern, *Regulatory Toxicology and Pharmacology*, **52**, 189-194.

Aslan, H., Songur, A., Tunc, A.T., Ozen, O.A., Bas, O., Yagmurca, M., Turgut, M., Sarsilmaz, M. and Kaplan, S. (2006) Effects of formaldehyde exposure on granule cell number and volume of dentate gyrus: A histopathological and stereological study, *Brain Research*, **1122**, 191-200.

ASTM (2010) *ASTM D5116-10, Standard Guide for Small-scale Environmental Chamber Determinations of Organic Emissions from Indoor Materials/Products*, ASTM International, West Conshohocken, PA.

Bizzari, S.N. (2000) *CEH Marketing Research Report: Formaldehyde*, SRI International, Palo Alto, CA.

Braswell, J.R., Spiner, D.R. and Hoffman, R.K. (1970) Adsorption of formaldehyde by various surfaces during gaseous decontamination, *Applied Microbiology*, **20**, 765-769.

Cox, S.S., Liu, Z., Little, J.C., Howard-Reed, C., Nabinger, S.J. and Persily, A. (2010) Diffusion-controlled reference material for VOC emissions testing: proof of concept, *Indoor Air*, **20**, 424-433.

Cox, S.S., Zhao, D. and Little, J.C. (2001) Measuring partition and diffusion coefficients for volatile organic compounds in vinyl flooring, *Atmospheric Environment*, **35**, 3823-3830.

Crank, J. (1975) *The Mathematics of Diffusion, Second Edition*, Clarendon Press, Oxford, England.

Deng, Q., Yang, X. and Zhang, J.S. (2009). Study on a new correlation between diffusion coefficient and temperature in porous building materials, *Atmospheric Environment*, **43**, 2080-2083.

Hennebert, P. (1988) Solubility and diffusion coefficients of gaseous formaldehyde in polymers, *Biomaterials*, **9**, 162-167.

Howard-Reed, C., Little, J.C., Marand, E., Cox, S.S., Nabinger, S.J. and Persily, A. (2007) 'Improving the reliability of VOC emissions testing of building products' In: *Proceedings of ASHRAE IAQ 2007*, Baltimore, MD, American Society of Heating, Refrigerating and Air-Conditioning Engineers (ASHRAE)' conference.

Howard-Reed, C., Liu, Z., Benning, J., Cox, S.S., Samarov, D., Leber, D., Hodgson, A.T., Mason, S., Won, D. and Little, J.C. (2011) Diffusion-controlled reference material for volatile organic compound emissions testing: pilot inter-laboratory study, *Building and Environment*, **46**, 1504-1511.

IARC (2006) *IARC monographs on the evaluation of carcinogenic risks to humans. Vol 88. Formaldehyde, 2-Butoxyethanol and 1-tert-Butoxypropan-2-ol*, International Agency for Research on Cancer, Lyon, France.

Kauppinen, T., Toikkanen, J., Pedersen, D., Young, R., Ahrens, W., Boffetta, P., Hansen, J., Kromhout, H., Maqueda, B.J., Mirabelli, D., de la Orden-Rivera, V., Pannett, B., Plato, N., Savela, A., Vincent, R. and Kogevinas, M. (2000) Occupational exposure to carcinogens in the European Union, *Occupational and Environmental Medicine*, **57**, 10-18.

Kelly, T.K., Smith, D.L. and Satola, J. (1999) Emission rates of formaldehyde from materials and consumer products found in California homes, *Environmental Science and Technology*, **33**, 81-88.

Kiburn, K.H. (1994) Neurobehavioral impairment and seizures from formaldehyde, *Archives of Environmental Health*, **49**, 37-44.

Kim, E., Little, J.C. and Chiu, N. (2004) Estimating exposure to chemical contaminants in drinking water, *Environmental Science and Technology*, **38**, 1799-1806.

Koss, G. and Tesseraux, I. (1999) Hydrocarbons, In: Marquardt, H., Schafer, S.G., McClellan, R. and Welsch, F., eds, *Toxicology*, Academic Press, New York.

Little, J.C., Hodgson, A.T. and Gadgil, A.J. (1994) Modeling emissions of volatile organic compounds from new carpets, *Atmospheric Environment*, **28**, 227-234.

Meyer, B. and Boehme, C. (1997) Formaldehyde emission from solid wood, *Forest Products Journal*, **47**, 45-48.

NIOSH (1994) Formaldehyde by VIS 3500. In: *NIOSH Manual of Analytical Methods (NMAM), Fourth Edition*, NIOSH, Washington, DC.

NTP (2011) *Report on Carcinogens, Twelfth Edition*, U.S. Department of Health and Human Services, National Toxicology Program.

Paustenbach, D., Alarie, Y., Kulle, T., Schachter, N., Smith, R., Swenberg, J., Witschi, H. and Horowitz, S.B. (1997) A recommended occupational exposure limit for formaldehyde based on irritation, *Journal of Toxicology and Environmental Health*, **50**, 217-263.

Risholm-Sundman, M., Larsen, A., Vestin, E. and Weibull, A. (2007) Formaldehyde emission-comparison of different standard methods, *Atmospheric Environment*, **41**, 3193-3202.

Röck, F., Barsan, N. and Weimar, U. (2010) System for dosing formaldehyde vapor at the ppb level, *Measurement Science and Technology*, **21**, 115201-115207.

Sakanashi, T.M., Rogers, J.M., Fu, S.S., Connelly, L.E. and Keen, C.L. (1996) Influence of maternal folate status on the developmental toxicity of methanol in the CD-1 mouse, *Teratology*, **54**, 198-206.

Salthammer, T., Mentese, S. and Marutzky, R. (2010) Formaldehyde in the indoor environment, *Chemical Reviews*, **110**, 2536-2572.

US EPA (1990) *Compendium method IP-6A, Determination of Formaldehyde and Other Aldehydes in Indoor Air Using a Solid Adsorbent Cartridge*, US Environmental Protection Agency, Research Triangle Park, NC.

Walker J.F. (1975) *Formaldehyde, Third Edition*, Robert E. Krieger Publishing Company, Huntington, New York.

Weigl, M., Wimmer, R., Sykacek, E. and Steinwender, M. (2009) Wood-borne formaldehyde varying with species, wood grade, and cambial age, *Forest Products Journal*, **59**, 88-92.

WHO (1989) *Formaldehyde (Environmental Health Criteria, No. 89)*, World Health Organization, Geneva, Switzerland.

Xiong, J., Yan, W. and Zhang Y. (2011a) Variable volume loading method: A convenient and rapid method for measuring the initial emittable concentration and partition coefficient of formaldehyde and other aldehydes in building materials, *Environmental Science and Technology*, **45**, 10111-10116.

Xiong, J., Yao, Y. and Zhang, Y. (2011b) C-history method: rapid measurement of the initial emittable concentration, diffusion and partition coefficients for formaldehyde and VOCs in building materials, *Environmental Science and Technology*, **45**, 3584-3590.

Yu, P.H., Wright, S., Fan, E.H., Lun, Z.R. and Gubisne-Harberele, D. (2003) Physiological and pathological implications of semicarbazide-sensitive amino oxidase, *Biochimica et Biophysica Acta*, **1647**, 193-199.

Zhang, Y., Luo, X., Wang, X., Qian, K. and Zhao, R. (2007) Influence of temperature on formaldehyde emission parameters of dry building materials, *Atmospheric Environment*, **41**, 3203-3216.

Chapter 7 – Measuring and Predicting Phthalate Emissions in a Specially-Designed Chamber: Implications for SVOC Emission Chamber Tests and Reference Material Development

Zhe Liu[1], Ying Xu[2], Jennifer L. Benning[3] and John C. Little[1]

[1]Department of Civil and Environmental Engineering, Virginia Tech, Blacksburg, VA 24061

[2]Department of Civil, Architectural and Environmental Engineering, University of Texas at Austin, Austin, TX 78712

[3]Department of Civil and Environmental Engineering, South Dakota School of Mines and Technology, Rapid City, SD 57701

7.1 Abstract

With the growing concerns about health effects associated with exposure to semi-volatile organic compounds (SVOCs) emitted from indoor materials, characterizing SVOC emissions and understanding the emission mechanisms has become an important need. In the present paper, di(2-ethylhexyl) phthalate (DEHP) emissions from vinyl flooring and the sorption behavior of the chamber wall were investigated in a specially-designed stainless steel chamber developed in previous studies using improved experimental approaches. Furthermore, an improved mechanistic model that predicts SVOC emissions was developed and validated using the chamber test results. Finally, based on the knowledge we have gained about the emission mechanisms, proper procedures to perform SVOCs emission chamber tests and the feasibility of developing reference materials for SVOC emissions testing are discussed. The results demonstrate that although measuring SVOC emissions in chambers is very challenging, it is indeed possible when proper testing procedures are used with due understanding about the emission mechanisms. The mechanistic model can predict the externally controlled SVOC emissions well and based on the model, simple reference materials for SVOC emissions testing can be created.

7.2 Introduction

Since the 1930s, phthalates have been used as plasticizers to enhance the flexibility of rigid polyvinyl chloride (PVC) products (Latini et al., 2004) and current global phthalate production is estimated at about 6 million tonnes per year (Rudel and Perovich, 2009). For example, di(2-ethylhexyl)phthalate (DEHP), one of the most important members of the phthalate family, has been extensively used in building products (such as flooring, pavements, roof coverings, wallpaper, polymeric coatings, tubes, containers, and wire and cable insulation), car products (such as vinyl upholstery, car seats, underbody coating, and trim), clothing (such as footware and raincoats), food packaging, children's products (such as toys and crib bumpers), and medical devices (Kavlock et al., 2002). In some PVC products such as vinyl flooring, DEHP is present at concentrations of 10-60% (w/w) (Rudel and Perovich, 2009). Other major phthalates include dibutyl phthalate (DBP), benzyl butyl phthalate (BBP), di-isononyl phthalate (DINP), and di-isodecyl phthalate (DIDP), which are present in a vast array of building materials and consumer products (Wormuth et al., 2006). Because phthalate plasticizers are not chemically bound to the polymer matrices, they slowly emit from these products to air and then migrate to interior surfaces, leading to common phthalate contamination in indoor air (Fromme et al., 2004; Rudel et al., 2003; Rudel et al., 2010; Rudel and Perovich, 2009; Weschler, 1984; Weschler and Fong, 1986; Wilson et al., 2001) and dust (Bornehag et al., 2004; Bornehag et al., 2005; Clausen et al., 2003; Øie et al., 1997; Rudel et al., 2003; Weschler and Nazaroff, 2008; Weschler and Nazaroff, 2010; Wilkins et al., 1993). Substantial exposure to phthalate plasticizers may occur via inhalation of phthalate vapor and airborne particles, ingestion of dust, and dermal sorption (Xu et al., 2009; Xu et al., 2010). Observed correlations between levels of urinary metabolites of some phthalates and indoor air concentrations have suggested that indoor air is a significant route of exposure to phthalates, or a proxy for other routes such as dermal sorption (Adibi et al., 2003; Adibi et al., 2008). The ubiquitous exposure to phthalates is of concern because several studies suggest that exposure to phthalates may cause various adverse reproductive impacts such as increases in prenatal mortality, reduced growth and birth weight, and skeletal, visceral, and external malformations (Duty et al., 2004; Gray et al., 2000; Kavlock et al., 2002; Lottrup et al., 2006; Matsumoto et al., 2008; McKee et al., 2004; Ritter and Arbuckle, 2007; Sharpe and Irvine, 2004) and phthalates are categorized as endocrine disrupting chemicals (EDCs) (Rudel and Perovich, 2009). In addition, epidemiological studies have suggested an association between

exposure to phthalate plasticizers and increased risk of asthma and allergies (Bornehag and Nanberg, 2010; Jaakkola et al., 2004; Jaakkola et al., 2006; Kolarik et al., 2008).

To identify exposure sources, characterize exposure pathways, and assess exposure and risk, knowledge about the mechanisms governing phthalate emissions from PVC products and subsequent transport in the indoor environment is needed. However, the mechanisms are still not fully understood and only a few chamber studies investigating emission characteristics of phthalates are available (Afshari et al., 2004; Clausen et al., 2004; Clausen et al., 2007; Clausen et al., 2010; Clausen et al., 2012; Fujii et al., 2003; Schripp et al., 2010; Uhde et al., 2001; Xu et al., 2008). Uhde et al. (2001) measured the phthalate concentrations emitted from fourteen PVC-coated wall coverings in regular emission chambers for 14 days and suggested that the chamber concentration of phthalates with lower boiling point tends to be higher than those with higher boiling point. Afshari et al. (2004) tested DBP and DEHP emissions from several materials such as wallpaper, PVC flooring and electric wire in the Chamber for Laboratory Investigations of Materials, Pollution and Air Quality (CLIMPAQ) and the Field and Laboratory Emission Cell (FLEC). They found that the chamber concentration of DEHP reached steady state after about 150 days and that sorption by chamber surfaces had a strong impact on chamber concentrations. Fujii et al. (2003) developed a passive-type sampler to measure the emission rate of phthalates from synthetic leather, wallpaper and vinyl flooring and found that emission rates of several phthalates increased significantly at higher temperatures. Schripp et al. (2010) tested wall paints and pure liquid of DEHP and DBP in two different chambers and measured the DEHP and DBP concentrations in the chamber air and in the dust placed in the chamber. Clausen et al. (2004; 2007; 2010; 2012) performed a series of tests on emissions of DEHP from vinyl flooring in the FLEC. Their work suggested that the emission rate of DEHP is limited by gas-phase mass transfer; the strong sorption of DEHP onto the FLEC chamber surface could result in a very long time period to reach steady state; relative humidity has no impact on the emission; increasing the air change rate of the chamber can enhance the emission rate but lower the chamber concentration due to dilution; and DEHP in vinyl flooring behaves the same as pure DEHP liquid whose emission rate is enhanced significantly at elevated temperatures. Overall, these studies have provided valuable information about the emission characteristics of phthalates from PVC materials and revealed the great difficulties of chamber tests of phthalates due to the very low

gas-phase concentration, strong sorption onto surfaces, and ubiquitous contamination in laboratory facilities.

Based on existing chamber studies, Xu and Little (2006) developed a mechanistic mass transfer model to predict emissions of semi-volatile organic compounds (SVOCs) such as DEHP from polymeric materials. According to the model, SVOC emissions from polymeric materials (such as DEHP from vinyl flooring) are subject to external control, including partition at the material/air interface, external convective mass transfer near the interface, and sorption onto interior surfaces. However, the model assumed an instantaneous partition equilibrium between the bulk air and interior surfaces and ignored the external convective mass-transfer resistance.

Recently, a stainless steel chamber was designed specifically for SVOCs to substantially shorten the time required for emissions testing and stainless steel rods were introduced to examine the sorption properties of the chamber surface (Xu et al., 2008). However, it was assumed that the rods reached partition equilibrium with the chamber air fairly quickly. Furthermore, the fittings and tubing upstream from the sampling tubes may cause deviations between the measured gas-phase concentration and the real chamber concentration since a substantial amount of DEHP may deposit in the fittings and tubing, as suggest by a recent FLEC study (Clausen et al., 2010). The objective of this study is to overcome the drawbacks of the previous chamber study (Xu et al., 2008), further the understanding of the emissions of DEHP from vinyl flooring, and extend the knowledge to other SVOCs emitted from solid materials. The emission profiles of DEHP from vinyl flooring were measured in the same specially-designed stainless steel chamber as in the previous study (Xu et al., 2008) with an improved configuration of sampling tubes. A new rod sorption test was developed to investigate the sorption behavior of DEHP on the stainless steel chamber surface by measuring rods periodically inserted into the chamber. Furthermore, an improved mechanistic model that predicts SVOC emissions was developed and validated using independently obtained model parameters. Finally, based on the integrated knowledge we have learned about the emission mechanisms, proper procedures to perform SVOC emission chamber tests and the feasibility of developing reference materials for SVOC emissions testing are discussed.

7.3 Experimental materials and methods

7.3.1 Chemicals

For calibration and identification purpose, DEHP was purchased from Absolute Standards Inc. (Hamden, CT). Methanol (anhydrous, 99.9%) used for cleaning and as solvent in the standard solutions was purchased from VWR International Inc. (Radnor, PA).

7.3.2 Test specimen

The test material was vinyl flooring (homogeneous polyurethane reinforced PVC flooring) with a thickness of 2.0 mm, exactly the same as those tested previously in the literature (Clausen et al., 2004; Clausen et al., 2007; Clausen et al., 2010; Clausen et al., 2012). The vinyl flooring contains about 15% (w/w) DEHP as the only plasticizer and other phthalates were detected only in trace amounts by gas chromatography and mass spectrometry. The vinyl flooring was delivered as a roll wrapped in plastic foil from a merchant in Denmark. After received, it was cut into 0.45 m×0.45 m square sheets, which were then placed in the specially-designed stainless steel chamber. Pristine Teflon sheets were purchased from Fluoro-Plastics Inc. (Philadelphia, PA) and used in blank chambers instead of the vinyl flooring.

7.3.3 Emission chamber test

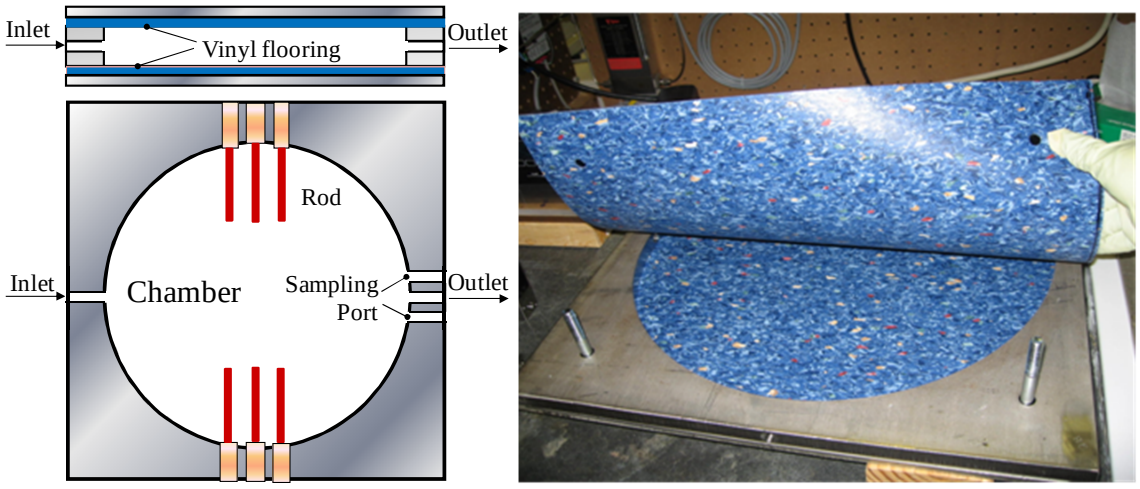

(a) (b)

Figure 7.1 Configuration of the emission chamber: (a) side and top view; (b) photo.

Figure 7.1 shows the configuration of the specially-designed stainless steel chamber (Xu et al., 2008). The chamber was made by cutting a large cylindrical cavity (0.4 m in diameter) through a 1.6 cm thick type-304 stainless steel plate and placing the plate between two vinyl flooring sheets, forming a short cylindrical chamber. The internal surface of the cavity was electro-polished and served as the chamber wall. Therefore, the surface area of the chamber wall, which would adsorb DEHP, was minimized while the emission surface area of the vinyl flooring was maximized. Two additional stainless steel plates were placed outside the vinyl flooring sheets and the layered structure was tightened together with bolts and heavy-duty clamps. The flexible vinyl flooring sheets also acted as sealing gaskets. For blank chambers, two Teflon sheets were used instead of the vinyl flooring sheets. High purity cylinder air was passed into the chamber with the influent flow rate regulated by a mass flow controller. The leakage of the chamber was estimated by measuring the difference between the effluent and influent flow rate, which was determined to be less than 3% of the influent flow rate. During the emission tests and blank chamber tests, Tenax-TA sorbent tubes were used to sample the chamber air for determining the gas-phase DEHP concentration. To eliminate loss of DEHP due to sorption onto any stainless steel tubing and fittings, two sampling ports were drilled next to the chamber outlet and the sorbent tubes were directly inserted into the chamber through the sampling ports with fixtures. The sampling flow rates were controlled through the sampling pumps connected to the sorbent tubes. During the entire test period, the sampling flow rate ranged from 60 mL/min to 150 mL/min and the sampling time was adjusted between 12 h and 24 h based on estimated chamber concentrations. In pilot emission tests, backup tubes were connected after the sampling tubes to check for breakthrough and no backup tubes were found to have DEHP over the detection limit. Therefore backup tubes were spared later. Before each emission test, the stainless steel plates were cleaned with an alkali detergent, tap water and distilled water, and finally rinsed several times with methanol. A blank chamber was then assembled using the cleaned stainless steel plates and two Teflon sheets to check the background DEHP concentration for several days. The blank chamber concentration of DEHP turned out to be less than 0.03 $\mu g/m^3$ and much lower than the emission chamber concentrations as shown later, and then the Teflon sheets were replaced by vinyl flooring sheets for emissions testing. Two independent emission tests were performed as duplicates, both of which lasted for about 80 days. The chamber geometry and emission test conditions are summarized in Table 7.1. Although dry air was used in the present

study, it is expected that humidity has no significant impact on the emission chamber tests (Clausen et al., 2007).

Table 7.1 Chamber geometry and emission test conditions.

Parameters	Values
Chamber diameter (m)	0.4
Chamber height (m)	0.016
Chamber volume (m^3)	0.002
Vinyl flooring emission surface area (m^2)	2×0.126
Stainless steel chamber wall surface area (m^2)	0.02
Chamber air flow rate (mL/min)	850±30
Temperature (^oC)	23±0.5
Relative humidity (%)	0

7.3.4 Rod sorption test

After the measured chamber concentration of DEHP in the second emission test became stable, indicating the chamber had reached steady state, several precision-ground type-304 stainless steel rods (3 mm in diameter and 3 cm in length) were inserted into the chamber through six rod ports (Figure 7.1) and removed periodically and put in empty tubes for analysis. By exposing the rods in the chamber for different time periods and measuring the DEHP concentration on the rods, the surface concentration development on the rods can be investigated. Since the rods have the same finish as the stainless steel chamber wall, they provide a surrogate to study the sorption behavior of DEHP onto the chamber wall. Before inserting into the chamber, all the rods were cleaned with an alkali detergent, tap water and distilled water, and finally sonicated in methanol bath for 20 minutes. Randomly selected rods were analyzed to check the background surface concentration and none of them had DEHP over the detection limit. There is concern that the thermal desorption involved in the analytical procedure may change the stainless steel surface properties (due to thermal oxidation, for example) and the sorption behavior (Clausen et al., 2012; Hamadou et al., 2010; Hirabayashi et al., 1990), and therefore each rod was only used once.

7.3.5 Analysis of DEHP samples

A thermal desorber (TD) (Perkin Elmer ATD 400, Perkin Elmer Inc., Waltham, MA) was connected to a gas chromatograph (GC) (HP Agilent 6890 GC, Agilent Technologies, Santa Clara, CA) with a flame ionization detector (FID) to analyze DEHP samples. The sorbent tubes containing gas samples and empty tubes containing rods were desorbed for 30 min at 300 ^{o}C, with a helium flow of 50 mL/min and a cold trap temperature of -20 ^{o}C. The cold trap which refocused the analytes was narrow bore (low flow trap tube) packed with a small piece of silylated glass wool. Flash heating of the cold trap to 350 ^{o}C transferred the analytes through the valves at 225 ^{o}C and the transfer line at 225 ^{o}C to the GC. The GC-FID had a constant pressure of carrier gas helium, resulting in a flow of about 10 mL/min at 120 ^{o}C and was equipped with a 30 m × 0.53 mm i.d. Restek RTX-1 column. The temperature program was 120 ^{o}C, held for 2 min, then increased to 300 ^{o}C at 15 ^{o}C/min, held for 8 min, and finally increased to 325 ^{o}C at 20 ^{o}C/min and held for 4 min. The FID heater temperature was 275 ^{o}C. The analytical detection limit was estimated to be 0.01 μg/tube (Clausen et al., 2004). Each tube was analyzed by two successive desorptions to test for complete desorption of both the tube and the TD system. In all cases, the second desorption of the tubes resulted in a recovered mass below the detection limit at which the tubes were considered clean. Standard solutions of DEHP in methanol were made at seven different concentration levels with each level having eight replicates. The standard solutions were injected into clean sorbent tubes and analyzed by the TD-GC-FID system to construct the calibration curve. The intercept of the calibration curve is not significantly different from zero and the coefficient of determination (R^2) is larger than 0.996. All the tubes were conditioned at 300 ^{o}C for two hours with high purified nitrogen gas passing through at a flow rate of 80 mL/min, and the background level of DEHP of the tubes were then checked before use.

7.4. Emission model development

Figure 7.2 shows the schematic representation of a new model that predicts the emissions of SVOCs (such as DEHP) from a solid slab in a chamber. Based on a previous developed model (Xu and Little, 2006), the new model ignores the presence of particles and incorporates the sorption behavior of the chamber wall in a more realistic way. According to Figure 7.2, the transient diffusion within the material can be described by Fick's second law, or

$$\frac{\partial C(x,t)}{\partial t} = D\frac{\partial^2 C(x,t)}{\partial x^2} \tag{7.1}$$

where C(x,t) is the material-phase concentration of the SVOC in the slab, x is the distance from the bottom of the slab, t is time, and D is the diffusion coefficient of the SVOC in the material, which may be concentration-dependent due to the high SVOC concentration in the material. The initial condition assumes that the SVOC is uniformly distributed throughout the material, or

$$C(x,t) = C_0 \quad \text{for} \quad t = 0,\ 0 \le x \le L \tag{7.2}$$

where L is the thickness of the material and C_0 is the initial material-phase SVOC concentration. Because the slab is resting on an impermeable surface, the lower boundary condition is

$$\frac{\partial C(x,t)}{\partial x} = 0 \quad \text{for} \quad x = 0,\ t \ge 0 \tag{7.3}$$

The boundary condition imposed at the upper surface is

$$-D\frac{\partial C(x,t)}{\partial x} = h_m\left(y_0(t) - y(t)\right) \quad \text{for} \quad x = L,\ t > 0 \tag{7.4}$$

where h_m is the convective mass-transfer coefficient through the boundary layer near the emission surface, $y_0(t)$ is the SVOC concentration in the air immediately adjacent to the surface, and y(t) is the gas-phase SVOC concentration in the well-mixed bulk chamber air. An instantaneous equilibrium is assumed to exist between the surface of the material and the air immediately adjacent to the surface, or

$$C(x,t) = Ky_0(t) \qquad \text{for} \quad x = L,\ t > 0 \tag{7.5}$$

where K is the material/air partition coefficient for the SVOC, which may be concentration-dependent due to the high concentration in the material. Equation (7.4) actually provides the expression of the emission rate, E(t), or

$$E(t) = h_m\left(y_0(t) - y(t)\right) \tag{7.6}$$

Corresponding to the extremely low vapor pressures of SVOCs, K for SVOCs are huge (on the order of 10^{11} for DEHP in vinyl flooring, for example) so that $y_0(t)$ would be many orders of magnitudes lower than the material-phase concentration. With $y_0(t)$ practically driving the emission into air, E(t) is therefore very small compared to the total mass in the material. As discussed by Xu and Little (2006), only a tiny fraction of the total DEHP in the vinyl flooring is emitted during years. The material-phase concentration as well as y_0 is therefore virtually constant over a long time span. As a result, Equations (7.1) - (7.6) can be simplified into

$$E(t) = h_m(y_0 - y(t)) \tag{7.7}$$

In this way, the internal diffusion within the material is ignored and a single and constant parameter, y_0, represents all the emission properties of the given source, implying that the emissions of SVOCs are externally controlled.

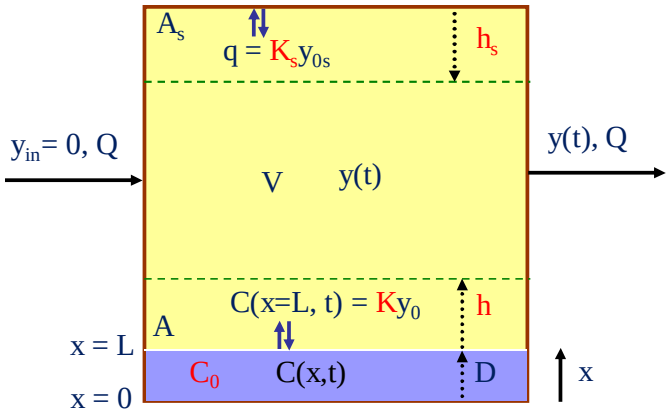

Figure 7.2 Schematic representation of SVOC emission from a solid material in a chamber.

In the previous model (Xu and Little, 2006), a nonlinear instantaneously reversible Freundlich equilibrium relationship was assumed to exist between the chamber wall and the bulk chamber air. In the new model, sorption of the SVOC onto the chamber wall is modeled by considering the convective mass transfer through the boundary layer near the chamber wall, or

$$\frac{dq(t)}{dt} = h_s(y(t) - y_{0s}(t)) \tag{7.8}$$

where q is the surface concentration of the SVOC on the chamber wall, h_s is the convective mass-transfer coefficient through the boundary layer near the chamber wall, and $y_{0s}(t)$ is the SVOC concentration in the air immediately adjacent to the sorption surface, which is analogous to y_0. A instantaneous linear equilibrium is assumed to exist between the surface and the air immediately adjacent to the chamber wall, or

$$q(t) = K_s y_{0s}(t) \tag{7.9}$$

where K_s is the partition coefficient between the chamber wall and air. Defining the sorption rate, S(t), which is comparable to the emission rate E(t), Equations (7.8) and (7.9) can be rearrange into

$$S(t)=\frac{dq(t)}{dt}=h_s\left(y(t)-\frac{q(t)}{K_s}\right) \tag{7.10}$$

Assuming the SVOC concentration in the influent air is zero, the mass balance on the SVOC in the chamber air is given by

$$\frac{dy(t)}{dt}\cdot V=E(t)\cdot A-S(t)\cdot A_s-y(t)\cdot Q \tag{7.11}$$

where V is the well-mixed chamber volume, A and A_s are areas of the emission and sorption surface respectively, and Q is the air flow rate. Given that y and q are both zero initially, the SVOC emission model is obtained by combining Equations (7.7), (7.10) and (7.11) to calculate y(t), q(t), E(t) and S(t). The model parameters include h_m, h_s, K_s and y_0 together with other parameters readily measurable (V, Q, A, and A_s). A full analytical solution to the model is available, which is however awkward to use. Therefore, the model is solved numerically using a finite difference method instead (Yuan et al., 2007).

7.5 Results and discussion

7.5.1 Emission of DEHP into air

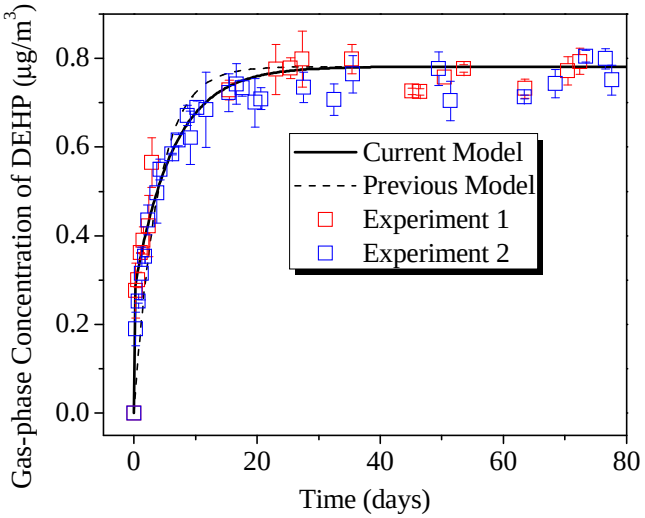

Figure 7.3 Measured and predicted DEHP concentration profiles in the chamber air.

As shown in Figure 7.3, measured transient concentrations (mean ± standard deviation) of the chamber air in the two emission tests agree very well and the measured gas-phase concentrations are much higher than the background concentrations measured in blank chambers (less than 0.03

$\mu g/m^3$). The profiles show that the chamber concentration reached steady state at 0.78 $\mu g/m^3$ after about 20 days, much faster than the emission tests using the same vinyl flooring in FLECs and CLIMPAQs (Clausen et al., 2004) where it took about 150 days to reach steady state. The results validate the design of the emission chamber by maximizing the vinyl flooring surface area while minimizing the chamber wall surface area to reduce time to reach steady state. In the previous study (Xu et al., 2008), a large amount of DEHP deposited on the fittings and tubing before the sampling tubes and therefore, it took longer for the measured gas-phase concentration to reach steady state (about 40 days) although the steady-state chamber concentration was roughly the same. The stainless steel rods were inserted into the chamber after about 20 days when the steady state had been reached in the second test. The additional sorption surface area (about 8% of the chamber wall surface area) due to the introduction of rods did not change the chamber concentration significantly, which had been stable at the steady-state concentration until the end of the test. The concentration fluctuations in the two tests at steady state were probably caused by temperature fluctuations in the laboratory.

7.5.2 Rod sorption test

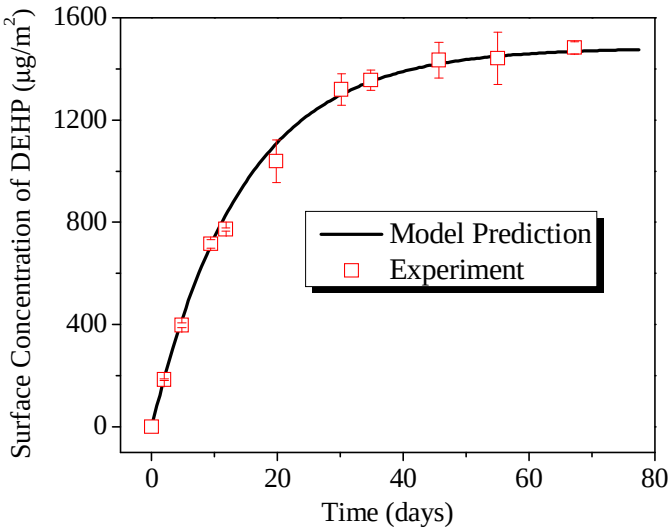

Figure 7.4 Measured and predicted surface concentrations of DEHP on rods.

Figure 7.4 shows the surface concentration (mean ± standard deviation) of DEHP on the rods versus time exposed in the chamber. It is obvious that the surface concentration of DEHP increased when the rods were positioned in the chamber longer, but when the exposure time

exceeded about 50 days, the surface concentration became constant. That is because DEHP adsorbed continuously onto the rods until the chamber air and the rod surface reached sorption equilibrium after about 50 days. K_s can be calculated by dividing the surface concentration on the rods at equilibrium by the steady-state gas-phase concentration of 0.78 μg/m^3, yielding 1900 m. The previous study obtained a K_s value of 1400 m by thermal desorption, much lower than the value obtained here (Xu et al., 2008). The deviation arises because in the previous study, the rods were exposed to the chamber air for much less time and partition equilibrium was not reached between the rods and the chamber air. Equation (7.10) can be also used to investigate the sorption behavior of the rods and by substituting y(t) with the constant steady-state gas-phase concentration ($y_{steady\text{-}state}$), it yields

$$\frac{dq_{rod}(t)}{dt} = h_{rod}\left(y_{steady-state} - \frac{q_{rod}(t)}{K_s} \right) \tag{7.12}$$

where q_{rod} is the surface concentration on the rods and h_{rod} is the convective mass-transfer coefficient through the boundary layer near the rod surface. It can be solved by separation of variables and the solution is

$$q_{rod}(t) = y_{steady-state} K_s \left(1 - e^{-\frac{h_{rod}}{K_s} t} \right) \tag{7.13}$$

The only unknown parameter is h_{rod}. Figure 7.4 shows the comparison of the prediction based upon Equation (7.13) and the measured surface concentrations of DEHP on the rods, with fitted h_{rod} of 0.002 m/s. The prediction matches the experimental results very well, suggesting that it is reasonable to model sorption behavior using Equation (7.10).

7.5.3 Emission model predictions

The newly developed emission model can be used to predict the chamber concentration profiles, with model parameters of V, Q, A, and A_s summarized in Table 7.1. K_s has been found to be 1900 m from the rod sorption test and y_0 was estimated as 0.9 μg/m^3 by computational fluid dynamic (CFD) analysis on emissions testing data in FLECs (Clausen et al., 2010; Clausen et al., 2012). At steady state, the transient terms in the model go to zero and Equations (7.7), (7.10) and (7.11) give rise to

$$h_m = \frac{y_{steady-state} \cdot Q}{(y_0 - y_{steady-state}) \cdot A} \quad (7.14)$$

Therefore, h_m can be calculated to be 0.0004 m/s based on Equation (7.14), close to the value obtained based on the mean flow velocity over the emission surface (Xu et al., 2008). Since only one parameter, h_s, is unknown, the model can be fitted to the measured emission profiles as in Figure 7.3 (solid black line) with the best-fitting h_s of 0.01 m/s. h_s is much larger than h_m, implying the convective mass transfer near the chamber surface was rather intense. The strongly enhanced mass transfer is reasonable considering that the depth of the chamber cavity is so small that the sorption surface is practically surrounded by the boundary layer of the emission surface. The model calculation matches the measured profiles very well, confirming its predictive capability. For comparison, the prediction of the previous model (Xu and Little, 2006) which ignores the convective mass-transfer resistance at the chamber wall is also shown in Figure 7.3 as the dashed line. Considering whether or not the convective mass-transfer resistance at the chamber wall has notable impact on the model predicted concentration profile, the deviation between the two models' predictions will become greater when h_s is smaller or when there is a larger internal sorption surface area.

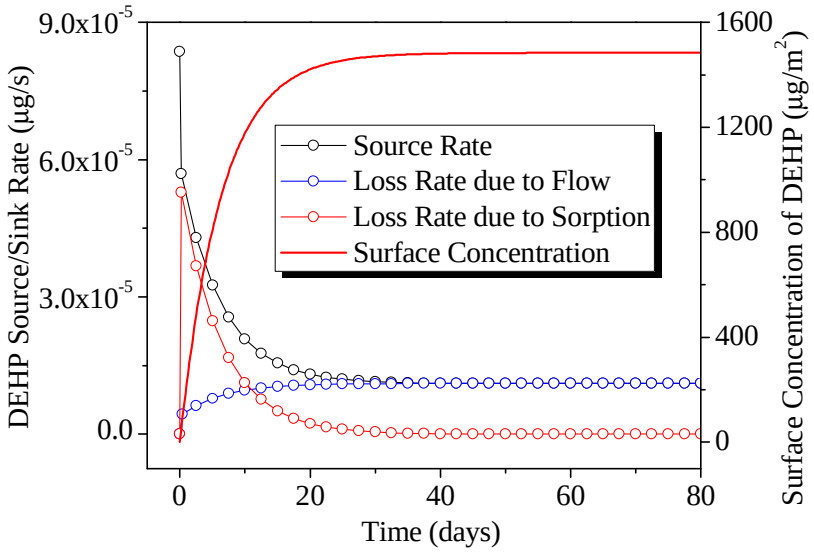

Figure 7.5 Model predicted chamber surface concentration and emission/loss rates.

Figure 7.5 shows the predicted surface concentration of DEHP on the chamber wall and DEHP source and loss rates in the chamber, which correspond to the three terms on the right-hand side

of Equation (7.11). As shown in the figure, the source rate or emission rate decreased over time because the gas-phase concentration increased over time so that the driving force for emission, y_0-y, decreased. When steady state had been reached, the source rate remained constant and equal to the loss rate due to ventilation. During the early period of emission, most emitted mass of DEHP was adsorbed onto the chamber wall but the sorption rate decreased over time and finally reduced to zero after reaching steady state. At the end of the test (80 days), it can be calculated that the total emitted DEHP was about 100 μg, total loss due to ventilation was about 70 μg, total sorbed mass on the chamber wall was about 30 μg while the DHEP present in the chamber air was less than 0.002 μg, far below the amount on the chamber surface. Therefore, sorption onto the chamber wall has significant impact on the emission before steady state, which is consistent with the analysis for emissions testing in FLECs (Clausen et al., 2010). The emitted mass during the tests is only a tiny fraction of the total DEHP in the vinyl flooring, therefore validating the assumption to derive Equation (7.7).

The emission model should also be applicable for other SVOCs from various solid materials (such as brominated flame retardants in office equipment and biocides in wood products) and can be adapted to other chambers (Xu and Little, 2006) or real indoor environments (Xu et al., 2009; Xu et al., 2010). In addition, rearranging Equation (7.14) into an explicit expression of $y_{steady\text{-}state}$ shows that the steady-state gas-phase concentration exclusively depends on y_0, h_m, A, and Q and it can be used as a quick estimation of gas-phase concentration for rapid exposure assessment (Little et al., 2012). Although relatively hard to obtain in the specially-designed chamber due to the complexity in geometry, h_m and h_s are rather easy to estimate in regular chambers or in indoor environments by measuring air flow velocities over the emission and sorption surfaces and employing correlations for convective mass-transfer coefficient over flat surfaces (Axley, 1991). K_s for different surfaces can be experimentally measured or estimated by correlations based on vapor pressure (Xu et al., 2009; Xu et al., 2010). As a simple but integrated emission parameter, y_0 is expected to depend on the material properties and the SVOC concentration in the material and can be estimated from emission chamber studies (Clausen et al., 2010; Clausen et al., 2012; Xu and Little, 2006). The simple linear partition relationship between the material and air that is commonly invoked for volatile organic compounds (VOCs) (Deng and Kim, 2004; Kumar and Little, 2003; Xu and Zhang, 2003) may be inappropriate to estimate y_0 since the

concentration of SVOC additives in polymeric materials is generally very high (Xu and Little, 2006). A recent study has demonstrated that y_0 of DEHP in vinyl flooring is equal to the vapor pressure of pure DEHP, suggesting that it behaves as a pure liquid (Clausen et al., 2012). Indeed, Ekelund et al. (2010) demonstrated the presence of a thin DEHP film on the outer surface of the PVC products and several other studies have also suggested that SVOCs may exist in a thermodynamically separated phase with liquid-like properties (Burks and Harmon, 2001; Cappa et al., 2008; Goldfarb and Suuberg, 2008). It is thus possible to use vapor pressure as an easy estimation of y_0 in some circumstances. However, this may not be true for all the SVOC additives in solid materials. Further development of methods to measure and/or estimate y_0 for SVOCs in materials and products is needed.

7.5.4 Implications for SVOC emission chamber tests

Although a few chamber studies have been performed as briefly reviewed in the introduction, and a standard SVOC emissions testing method has been specified in ISO standard 16000-25 (ISO, 2011), most tests simply follow the conventional procedures of VOC emissions testing without taking into account the substantial differences between SVOCs and VOCs, which may cause a number of problems in the testing procedures and undermine the quality of the results. A clear understanding of SVOC emission mechanisms is required to successfully conduct SVOCs emission chamber tests.

First, chamber design and operation is one of the key issues for SVOCs emission chamber tests. As suggested by Equation (7.14), the steady-state chamber concentration increases with A and h_m but decreases with Q. h_m depends on the flow velocity over the emission surface and generally depends on the chamber flow rate and chamber geometry if a chamber mixing fan is not used. Therefore, appropriate chamber size, chamber flow rate and test specimen size are desirable to achieve sufficiently high chamber concentrations which can be measured accurately. As shown in Equations (7.10) and (7.11), the transient chamber concentration depends not only on the emission rate but also on the sorption rate and therefore, chamber surface area and surface property have significant impact on the chamber concentration development. It is meaningless to compare the concentration profiles obtained from different chambers without specifying the sorption behavior of their chamber surfaces. Therefore, it is also necessary to study the sorption

behavior of the chamber surface (especially K_s) as supplementary information to evaluate the chamber concentration development. Due to strong sorption onto the chamber surface, it may take a long time period for the chamber to reach steady state. Although the time required to reach steady state depends on several factors including Q, V, A, A_s, K_s, h_m and h_s and the dependence is complicated, generally the time decreases when A_s and K_s decrease or A increases. For example, it was found that the emission test of DEHP from vinyl flooring in a FLEC took 150 days to reach steady state because A_s is roughly equal to A and K_s was 7500 m (Clausen et al., 2004; Clausen et al., 2010). When K_s decreased to less than 1000 m due to heating during cleaning procedures, the same test only took about 20 days (Clausen et al., 2012). The specially-designed chamber in the present study maximized A and minimized A_s and reduced the time required to reach steady state. Therefore, three strategies can be employed in chamber design and operation to reduce the time required to reach steady state: (1) maximize A and minimize A_s; (2) minimize K_s, which may be achieved by selecting specific chamber materials or surface treatments (for example, heating); and (3) run the chamber test at an elevated temperature because K_s decreases significantly at higher temperature (Clausen et al., 2012). The last option is especially promising because traditional small-scale environmental chambers can then be used directly for SVOCs and chamber concentration also significantly increases with increasing temperature due to enhanced emission (Clausen et al., 2012), which greatly facilitates the concentration measurement.

Second, proper sampling configuration is also crucial. Because SVOCs adsorb onto any interior surfaces, even a small additional surface area introduced by fittings or tubing before sampling tubes will reduce the gas-phase concentration so that the measured concentration is smaller than the real chamber concentration before steady state is reached. Therefore, eliminating additional surface area before sampling tubes is a necessity to measure the real chamber concentration and the approach used in the present study provides a feasible option. Meanwhile, the sampling time and sampling flow rate should be optimized to collect sufficient analyte mass for analytical instruments and also to catch the transient development of the chamber concentration.

Finally, the entire experimental approach is vulnerable to background contamination and therefore, extra efforts are required for cleaning and checking background concentration. But

additional care should be taken when heating is involved to prevent any uncertainties caused by potential changes in surface properties.

7.5.5 Implications for developing SVOC reference materials

With the growing concerns about various health effects due to SVOCs exposure and the desire to control SVOC emissions in the indoor environment, measuring SVOC emissions has become an urgent need and many laboratories around the world are starting this practice. However, measuring SVOC emissions in chambers is still an extremely challenging task with many errors and uncertainties. As suggested by the performance of a prototype reference material for VOC emissions testing (Cox et al., 2010; Howard-Reed et al., 2011), SVOC reference materials would be of important help in validating chamber test results, calibrating testing procedures, and instilling consensus and confidence in SVOC emissions testing.

The prototype reference material for VOC emissions testing is diffusion controlled and mimics real building materials which emit VOCs (Cox et al., 2010; Howard-Reed et al., 2011). In contrast, SVOC emissions from solid materials, such as DEHP from vinyl flooring, are controlled by external mass-transfer processes including partition at the material/air interface, external convective mass transfer near the interface, and sorption onto interior surfaces. As shown in the present paper, such an SVOC source is virtually constant and can be represented by an integrated and constant parameter, y_0. Therefore, the approach for creating VOC reference materials is not applicable to SVOCs. Instead, a SVOC reference material or standard emission source can be simply a Petri dish containing pure SVOC liquid/solid with a known vapor pressure. Such a standard source can mimic the real emissions of SVOCs from solid materials well and can be used to validate several aspects of the chamber tests. As suggested by the results of the present study, a feasible way to employ the SVOC reference material could include: (1) placing the reference material with a known vapor pressure in the chamber and measuring the chamber concentration until reaching steady state; (2) measuring the flow velocity over the emission surface and chamber wall to estimate h_m and h_s; (3) measuring the SVOC concentration on the chamber wall at steady state to determine K_s; (4) predicting the true emission profile of the reference material by the mechanistic model, with y_0 equal to the vapor pressure; and finally (5) comparing the predicted and measured steady-state chamber concentration and also

comparing the predicted and measured transient chamber concentration development profiles to validate the testing performance or identify errors and variability. Through this validation procedure, chamber configuration and operation, analytical procedure for measuring chamber concentration and surface concentration, and flow velocity measurement can all be carefully checked.

7.6 Acknowledgements

Financial support was provided by the National Science Foundation (CBET 0504167 and CBET-1066642).

7.7 References

Adibi, J.J., Perera, F.P., Jedrychowski, W., Camann, D.E., Barr, D., Jacek, R. and Whyatt, R.M. (2003) Prenatal exposures to phthalates among women in New York City and Krakow, Poland, *Environmental Health Perspectives*, **111**, 1719-1722.

Adibi, J.J., Whyatt, R.M., Williams, P.L., Calafat, A.M., Camann, D., Herrick, R., Nelson, H., Bhat, H.K., Perera, F.P., Silva, M.J. and Hauser, R. (2008) Characterization of phthalate exposure among pregnant women assessed by repeat air and urine samples, *Environmental Health Perspectives*, **116**, 467-473.

Afshari, A., Gunnarsen, L., Clausen, P.A. and Hansen, V. (2004) Emission of phthalates from PVC and other materials, *Indoor Air*, **14**, 120-128.

Axley, J.W. (1991) Adsorption modeling for building contaminant dispersal analysis, *Indoor Air*, **1**, 147-171.

Bornehag, C.-G., Lundgren, B., Weschler, C.J., Sigsgaard, T., Hagerhed-Engman, L. and Sundell, J. (2005) Phthalates in indoor dust and their association with building characteristics, *Environmental Health Perspectives*, **113**, 1399-1404.

Bornehag, C.-G. and Nanberg, E. (2010) Phthalate exposure and asthma in children, *International Journal of Andrology*, **33**, 333-345.

Bornehag, C.-G., Sundell, J., Weschler, C.J., Sigsgaard, T., Lundgren, B., Hasselgren, M. and Hägerhed-Engman, L. (2004) The association between asthma and allergic symptoms in children and phthalates in house dust: A nested case-control study, *Environmental Health Perspectives*, **112**, 1393-1397.

Burks, G.A. and Harmon, T.C. (2001) Volatilization of solid-phase polycyclic aromatic hydrocarbons from model mixtures and lampblack-contaminated soils, *Journal of Chemical and Engineering Data*, **46**, 944-949.

Cappa, C.D., Lovejoy, E.R. and Ravishankara, A.R. (2008) Evidence for liquid-like and nonideal behavior of a mixture of organic aerosol components, *Proceedings of the National Academy of Sciences*, **105**, 18687-18691.

Clausen, P.A., Bille, R.L.L., Nilsson, T., Hansen, V., Svensmark, B. and Bøwadt, S. (2003) Simultaneous extraction of di(2-ethylhexyl) phthalate and nonionic surfactants from house dust: Concentrations in floor dust from 15 Danish schools, *Journal of Chromatography A*, **986**, 179-190.

Clausen, P.A., Hansen, V., Gunnarsen, L., Afshari, A. and Wolkoff, P. (2004) Emission of Di-2-ethylhexyl phthalate from PVC flooring into air and uptake in dust: Emission and sorption experiments in FLEC and CLIMPAQ, *Environmental Science and Technology*, **38**, 2531-2537.

Clausen, P.A., Liu, Z., Kofoed-Sørensen, V., Little, J.C. and Wolkoff, P. (2012) Influence of temperature on the emission of di-(2-ethylhexyl)phthalate (DEHP) from PVC flooring in the emission cell FLEC, *Environmental Science and Technology*, **46**, 909-915.

Clausen, P.A., Liu, Z., Xu, Y., Kofoed-Sørensen, V. and Little, J.C. (2010) Influence of air flow rate on emission of DEHP from vinyl flooring in the emission cell FLEC: Measurements and CFD simulation, *Atmospheric Environment*, **44**, 2760-2766.

Clausen, P.A., Xu, Y., Kofoed-Sørensen, V., Little, J.C. and Wolkoff, P. (2007) The influence of humidity on the emission of di-(2-ethylhexyl) phthalate (DEHP) from vinyl flooring in the emission cell FLEC, *Atmospheric Environment*, **41**, 3217-3224.

Cox, S.S., Liu, Z., Little, J.C., Howard-Reed, C., Nabinger, S.J. and Persily, A. (2010) Diffusion controlled reference material for VOC emissions testing: proof of concept, *Indoor Air*, **20**, 424-433.

Deng, B. and Kim, C.N. (2004) An analytical model for VOCs emission from dry building materials, *Atmospheric Environment*, **38**, 1173-1180.

Duty, S.M., Calafat, A.M., Silva, M.J., Ryan, L. and Hauser, R. (2004) Phthalate exposure and reproductive hormones in adult men, *Human Reproduction*, **20**, 604-610.

Ekelund, M., Azhdar, B. and Gedde, U.W. (2010) Evaporative loss kinetics of di(2-ethylhexyl) phthalate (DEHP) from pristine DEHP and plasticized PVC, *Polymer Degradation and Stability*, **95**, 1789-1793.

Fromme, H., Lahrz, T., Piloty, M., Gebhart, H., Oddoy, A. and Rüden, H. (2004) Occurrence of phthalates and musk fragrances in indoor air and dust from apartments and kindergartens in Berlin (Germany), *Indoor Air*, **14**, 188-195.

Fujii, M., Shinohara, N., Lim, A., Otake, T., Kumagai, K. and Yanagisawa, Y. (2003) A study on emission of phthalate esters from plastic materials using a passive flux sampler, *Atmospheric Environment*, **37**, 5495-5504.

Gray, L.E., Ostby, J., Furr, J., Price, M., Veeramachaneni, D.N.R. and Parks, L. (2000) Perinatal exposure to the phthalates DEHP, BBP, and DINP, but not DEP, DMP, or DOTP, alters sexual differentiation of the male rat, *Toxicological Sciences*, **58**, 350-365.

Hamadou, L., Kadri, A. and Benbrahim, N. (2010) Impedance investigation of thermally formed oxide films on AISI 304L stainless steel, *Corrosion Science*, **52**, 859-864.

Hirabayashi, T., Sung, K.-W., Sasaki, T.A. and Saeki, M. (1990) Change in tritium-sorption property of stainless steel by thermal surface oxidation, *Journal of Nuclear Materials*, **175**, 78-83.

Howard-Reed, C., Liu, Z., Benning, J., Cox, S.S., Samarov, D., Leber, D., Hodgson, A.T., Mason, S., Won, D. and Little, J.C. (2011) Diffusion-controlled reference material for volatile organic compound emissions testing: pilot inter-laboratory study, *Building and Environment*, **46**, 1504-1511.

ISO (2011) *ISO 16000-25, Determination of the Emission of Semi-volatile Organic Compounds by Building Products – Micro-chamber Method*, International Organization for Standardization, Geneva, Switzerland.

Jaakkola, J.J.K., Ieromnimon, A. and Jaakkola, M.S. (2006) Interior surface materials and asthma in adults: A population-based incident case-control study, *American Journal of Epidemiology*, **164**, 742-749.

Jaakkola, J.J.K., Parise, H., Kislitsin, V., Lebedeva, N.I. and Spengler, J.D. (2004) Asthma, wheezing, and allergies in Russian schoolchildren in relation to new surface materials in the home, *American Journal of Public Health*, **94**, 560-562.

Kavlock, R., Boekelheide, K., Chapin, R., Cunningham, M., Faustman, E., Foster, P., Golub, M., Henderson, R., Hinberg, I., Little, R., Seed, J., Shea, K., Tabacova, S., Tyl, R., Williams, P. and Zacharewski, T. (2002) NTP Center for the Evaluation of Risks to Human Reproduction: phthalates expert panel report on the reproductive and developmental toxicity of di(2-ethylhexyl) phthalate, *Reproductive Toxicology*, **16**, 529-653.

Kolarik, B., Naydenov, K., Larsson, M., Bornehag, C.-G. and Sundell, J. (2008) The association between phthalates in dust and allergic diseases among Bulgarian children, *Environmental Health Perspectives*, **116**, 98-103.

Kumar, D. and Little, J.C. (2003) Single-layer model to predict the source/sink behavior of diffusion-controlled building materials, *Environmental Science and Technology*, **37**, 3821-3827.

Latini, G., Felice, C.D. and Verrotti, A. (2004) Plasticizers, infant nutrition and reproductive health, *Reproductive Toxicology*, **19**, 27-33

Little, J.C., Weschler, C.J., Liu, Z. and Cohen Hubal, E.A. (2012) Rapid methods to estimate potential exposure to semivolatile organic compounds in the indoor environment, *Submitted to Environmental Science and Technology*.

Lottrup, G., Andersson, A.-M., Leffers, H., Mortensen, G.K., Toppari, J., Skakkebæk, N.E. and Main, K.M. (2006) Possible impact of phthalates on infant reproductive health, *International Journal of Andrology*, **29**, 172-180.

Matsumoto, M., Hirata-Koizumi, M. and Ema, M. (2008) Potential adverse effects of phthalic acid esters on human health: A review of recent studies on reproduction , *Regulatory Toxicology and Pharmacology*, **50**, 37-49.

Mckee, R.H., Butala, J.H., David, R.M. and Gans, G. (2004) NTP center for the evaluation of risks to human reproduction reports on phthalates: addressing the data gaps , *Reproductive Toxicology*, **18**, 1-22.

Øie, L., Hersoug, L.-G. and Madsen, J.Ø. (1997) Residential exposure to plasticizers and its possible role in the pathogenesis of asthma, *Environmental Health Perspectives*, **105**, 972-978.

Ritter, L. and Arbuckle, T.E. (2007) Can exposure characterization explain concurrence or discordance between toxicology and epidemiology? *Toxicological Sciences*, **97**, 241-252.

Rudel, R.A., Camann, D.E., Spengler, J.D., Korn, L.R. and Brody, J.G. (2003) Phthalates, alkylphenols, pesticides, polybrominated diphenyl ethers, and other endocrine-disrupting compounds in indoor air and dust, *Environmental Science and Technology*, **37**, 4543-4553.

Rudel, R.A., Dodson, R.E., Perovich, L.J., Morello-Frosch, R., Camann, D.E., Zuniga, M.M., Yau, A.Y., Just, A.C. and Brody, J.G. (2010) Semivolatile endocrine-discrupting compounds in paired indoor and outdoor air in two northern California communities, *Environmental Science and Technology*, **44**, 6583-6590.

Rudel, R.A. and Perovich, L.J. (2009) Endocrine disrupting chemicals in indoor and outdoor air, *Atmospheric Environment*, **43**, 170-181.

Schripp, T., Fauck, C. and Salthammer, T. (2010) Chamber studies on mass-transfer of di(2-ethylhexyl)phthalate (DEHP) and di-n-butylphthalate (DnBP) from emission sources into house dust, *Atmospheric Environment*, **44**, 2840-2845.

Sharpe, R.M. and Irvine, D.S. (2004) How strong is the evidence of a link between environmental chemicals and adverse effects on human reproductive health? *British Medical Journal (Clinical Research Edition)*, **328**, 447-451.

Uhde, E., Bednarek, M., Fuhrmann, F. and Salthammer, T. (2001) Phthalic esters in the indoor environment - Test chamber studies on PVC-coated wallcoverings, *Indoor Air*, **11**, 150-155.

Weschler, C.J. (1984) Indoor-outdoor relationships for nonpolar organic constituents or aerosol particles, *Environmental Science and Technology*, **18**, 648-652.

Weschler, C.J. and Fong, K.L. (1986) Characterization of organic species associated with indoor aerosol particles, *Environment International*, **12**, 93-97.

Weschler, C.J. and Nazaroff, W.W. (2008) Semivolatile organic compounds in indoor environments, *Atmospheric Environment*, **42**, 9018-9040.

Weschler, C.J. and Nazaroff, W.W. (2010) SVOC partitioning between the gas phase and settled dust indoors, *Atmospheric Environment*, **44**, 3609-3620.

Wilkins, C.K., Wolkoff, P., Gyntelberg, F., Skov, P. and Valbjørn, O. (1993) Characterization of office dust by VOCs and TVOC release: Identification of potential irritant VOCs by partial least squares analysis, *Indoor Air*, **3**, 283-290.

Wilson, N.K., Chuang, J.C. and Lyu, C. (2001) Levels of persistent organic pollutants in several child day care centers, *Journal of Exposure Analysis and Environmental Epidemiology*, **11**, 449-458.

Wormuth, M., Scheringer, M., Vollenweider, M. and Hungerbühler, K. (2006) What are the sources of exposure to eight frequently used phthalic acid esters in Europeans? *Risk Analysis*, **26**, 803-824.

Xu, Y., Cohen Hubal, E.A, Clausen, P.A. and Little, J.C. (2009) Predicting residential exposure to phthalate plasticizer emitted from vinyl flooring: A mechanistic analysis, *Environmental Science and Technology*, **43**, 2374-2380.

Xu, Y., Cohen Hubal, E.A and Little, J.C. (2010) Predicting residential exposure to phthalate plasticizer emitted from vinyl flooring: Sensitivity, uncertainty, and implications for biomonitoring, *Environmental Health Perspectives*, **118**, 253-258.

Xu, Y. and Little, J.C. (2006) Predicting emissions of SVOCs from polymeric materials and their interaction with airborne particles, *Environmental Science and Technology*, **40**, 456-461.

Xu, Y., Park, J., Kofoed-Sørensen, V., Clausen, P.A. and Little, J.C. (2008) Characterizing emissions of phthalate plasticizer from vinyl flooring in a specially-designed chamber, *Epidemiology*, **19**, S294-S295.

Xu, Y. and Zhang, Y. (2003) An improved mass transfer based model for analyzing VOC emissions from building materials, *Atmospheric Environment*, **37**, 2497-2505.

Yuan, H., Little, J.C., Marand, E. and Liu, Z. (2007) Using fugacity to predict volatile emissions from layered materials with a clay/polymer diffusion barrier, *Atmospheric Environment*, **41**, 9300-9308.

Appendix A – Supplementary Material for Chapter 5: Developing a Fickian Diffusion Model for PDMS Fibers

Assuming the measuring chamber of the microbalance behaves as a continuous stirred-tank reactor (CSTR), the mass balance on a particular VOC within a short time interval Δt is given as

$$\Delta y \cdot V + \Delta M_s = y_\infty \cdot Q \cdot \Delta t - y \cdot Q \cdot \Delta t \quad \text{(A1)}$$

where y is the gas-phase VOC concentration in the measuring chamber, y_∞ is the gas-phase VOC concentration in the air supplied from the gas dynacalibrator, V is the volume of the measuring chamber and Q is the air flow rate through the measuring chamber. Δy denotes the gas-phase concentration change in the measuring chamber within Δt and ΔM_s denotes the mass of the VOC absorbed into the PDMS coating within Δt. If the entire PDMS coating were to reach equilibrium with the air instantaneously, the mass of the absorbed VOC within Δt should be $\Delta y \cdot K \cdot V_s$, where V_s is the volume of the PDMS coating, and therefore,

$$\Delta M_s < \Delta y \cdot K \cdot V_s \quad \text{(A2)}$$

V is 7×10^{-4} m^3 and V_s is 1.1×10^{-9}, 1.6×10^{-9}, and 7.1×10^{-9} m^3 for the 39.3-cm × 7-μm, 11.9-cm × 30-μm and 11.6-cm × 100-μm fiber samples, respectively. Therefore for most VOCs with K less than 10000, it is always valid that

$$\Delta M_s < \Delta y \cdot K \cdot V_s << \Delta y \cdot V \quad \text{(A3)}$$

The mass balance expressed by Equation (A1) can thereby be simplified to

$$\Delta y \cdot V = y_\infty \cdot Q \cdot \Delta t - y \cdot Q \cdot \Delta t \quad \text{(A4)}$$

whose differential form is

$$\frac{dy}{dt} V = Q(y_\infty - y) \quad \text{(A5)}$$

Considering that y is zero at the beginning of the sorption test (t=0), the solution of Equation (A5) is (t is in units of second):

$$y = y_\infty \left(1 - e^{-\frac{Q}{V}t}\right) = y_\infty \left(1 - e^{-0.006t}\right) \quad \text{(A6)}$$

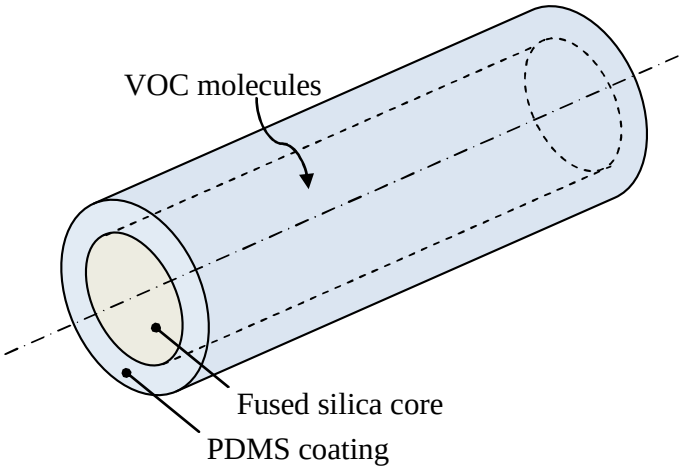

Figure A1 Configuration of a PDMS-coated SPME fiber.

Figure A1 shows the configuration of the SPME fibers. The interior grey cylinder is a fused silica core which is impermeable and the blue outer part is the PDMS coating. Different SPME fibers may have different coating thicknesses but the same core size. It is assumed that the external gas-phase mass transfer resistance can be ignored so that the outer surface of the PDMS coating is always in reversible equilibrium with the air in the measuring chamber, which is expressed by Equation (A6). The transient mass transfer process can therefore be described by Fick's second law in a cylindrical coordinate system:

$$\frac{\partial C}{\partial t} = D\frac{1}{r}\frac{\partial}{\partial r}\left(r\frac{\partial C}{\partial r}\right) \tag{A7}$$

which is subject to the auxiliary conditions:

$$\left.\frac{\partial C}{\partial r}\right|_{r=r_{in}} = 0 \tag{A8}$$

$$C\big|_{r=r_{out}} = y_{\infty}\left(1 - e^{-0.006\,t}\right)K \tag{A9}$$

$$C\big|_{t=0} = 0 \tag{A10}$$

where r is the radial distance from the center of the fused silica core, C is the VOC concentration in the PDMS coating as a function of r and t, and r_{in} and r_{out} are the radius of the fused silica core and the entire SPME fiber, respectively. The mass of VOC absorbed by the PDMS coating at time t, M_t, is given as

$$M_t = \int_{r_{in}}^{r_{out}} C(r,t) \cdot L \cdot 2\pi r \cdot dr \qquad \text{(A11)}$$

where L is the length of the SPME fiber.

A finite difference method is used to obtain a numerical solution for C(r,t) based upon Equations (A7) to (A10) and then Equation (A11) is solved by numerical integration. The partition coefficient K was obtained from the microbalance sorption test leaving D as the only unknown parameter. MATLAB (R2007a, MathWorks, Inc.) was used for the numerical calculations.